Probing gravity-matter systems

by

Mustafa Saeed

Bachelor of Science, Lahore University of Management Sciences, 2015
Master of Science, University of New Brunswick, 2019

A THESIS SUBMITTED IN PARTIAL FULFILLMENT OF THE REQUIREMENTS FOR THE DEGREE OF

Doctor of Philosophy

In the Graduate Academic Unit of Physics

Supervisor:	Viqar Husain, PhD, Mathematics and Statistics
Examining Board:	Ben Newling, PhD, Physics
	Sanjeev Seahra, PhD, Mathematics and Statistics
	Edward Wilson-Ewing, PhD, Mathematics and Statistics
External Examiner:	Bianca Dittrich, PhD, Research Faculty, Perimeter Institute for Theoretical Physics

This thesis is accepted by the
Dean of Graduate Studies

THE UNIVERSITY OF NEW BRUNSWICK

August, 2023

Abstract

This thesis explores gravity-matter systems within the context of cosmology and black holes. Two different studies are presented.

First we study cosmological perturbation theory (CPT) with scalar field and pressureless dust in the Hamiltonian formulation, with the dust field chosen as a clock. The corresponding canonical action describes the dynamics of the scalar field and metric degrees of freedom with a non-vanishing physical Hamiltonian and spatial diffeomorphism constraint. We construct a momentum space Hamiltonian that describes linear perturbations, and show that the constraints to this order form a first class system. We then write the Hamiltonian as a function of certain gauge invariant canonical variables and show that it takes the form of an oscillator with time dependent mass and frequency coupled to an ultralocal field. We compare our analysis with other Hamiltonian approaches to CPT that do not use dust-time.

Next we construct and study spin models on Euclidean black hole backgrounds. These resemble the Ising model, but are inhomogeneous with two parameters, the black hole mass M and the cosmological constant Λ. We use Monte-Carlo methods to study macroscopic properties of these systems for Schwarzschild and anti-deSitter black holes in four and five dimensions for spin-1/2 and spin-1. We find in every case that increasing M causes the spins to undergo a second order phase transition from disorder to order and that the phase transition occurs at sub-Planckian M.

Dedication

For Charlie, my favorite Saeed.

Acknowledgements

I will begin by acknowledging the patience with which my supervisor Dr. Viqar Husain guided me through the MS and PhD degrees. He was generous with his time, kind in addressing my concerns, encouraging of my creative endeavours (both in physics and in fiction), reassuring during my job applications and accommodating in aligning the conclusion of the degree with the commencement of my job. I also appreciate his boldness in addressing the important problems in the field, dedication to quality of research and advocacy of explaining said research clearly.

Undoubtedly the graduate students and post-docs of the gravity group were sounding boards and quality controls. They and their significant others were also people with whom I was happy to break bread. In particular Moeez and Doyeon were like elder siblings, Muzammil brought out the joyful nature of the group, Nomaan was a fellow explorer of Fredericton's trails and Jarod a fellow swimmer in the St. John river (not recommended).

During my PhD, Drs. Sanjeev and Jay trusted me with multiple teaching assignments, namely Math 1003, Phys 1081, Astr 1013, Math 0863 and Phys 1052. Dr. Ben's assistance for the physics courses was invaluable. Dr. Igor was a professional, easy-to-work-with and fun co-professor for Phys 1052. I am thankful to these gentlemen for my development as an instructor.

Through the courses I taught I met students who fiercely owned the learning

process. This made teaching a rewarding experience. More importantly it was a useful reminder for me to own my learning also.

A highlight of my final year as a graduate student was the fiction class taught by Dr. David Huebert. He and the graduate students in English were receptive of my foray into creative writing and supportive of the story I wanted to tell.

Having never wrestled prior, I chose to do so at UNB. Which is why I must effusively thank Don Ryan for trusting a walk-on. My time in the Den was characterized by a drive for excellence, preparation and accountability. These wonderful lessons in life I learned with a pack of Black Bears, of whom I have fond memories. Additionally I am grateful to CJ and Tom for being mentors and friends.

For my first three days in Fredericton I stayed as an airbnb guest at the beautiful home of Francis Perry and Greg Moffitt. Since then they've festively celebrated my achievements and built up my strength at my low points. They've showed up, always. They're my Canadian family.

My parents Drs. Afzal and Shaista Saeed were uncertain of my choice to pursue a higher education in physics; they stood by me with unwavering dedication nevertheless. My sister Dr. Amna Saeed cheered me on the loudest. My uncle Iqbal Sayeed and cousin Sanaullah Chabra propped me up in my early days in Fredericton and continue to do so till the day of writing.

I'll end by thanking the Almighty for giving me the strength and the requisite circumstances to make fruitful and meaningful my time as a graduate student.

Alhumdullillah.

Table of Contents

Abstract ii

Dedication iii

Acknowledgements iv

Table of Contents vi

List of Tables ix

List of Figures x

Abbreviations xii

1 Introduction 1

2 Cosmological perturbation theory with matter-time 12

2.1 Introduction 12

2.2 Hamiltonian gravity with dust 15

2.2.1 Dust-time gauge 16

2.3 Cosmological perturbation theory 18

2.3.1 Linearized theory 21

2.3.2 Linearized theory in momentum space 22

2.3.3 Canonical action in momentum space 25

2.3.4 Partial gauge fixing: removal of vector modes 27

2.3.5 Graviton equation 29
2.4 Scalar modes 30
2.4.1 Diffeomorphism invariant observables 31
2.5 Comparison with perturbation theory without dust 37
2.5.1 Gauge invariant variables 40
2.5.2 Gauge fixed action 42
2.6 Summary and discussion 44

3 Ising-like models on Euclidean black holes **46**
3.1 Introduction 46
3.2 Background 48
3.2.1 Monte-Carlo scheme 48
3.2.2 Euclidean time periodicity and temperature 50
3.3 Euclidean black holes 52
3.4 Spin models on black holes 57
3.4.1 Discretization 58
3.5 Simulation details and results 61
3.5.1 Numerical results 65
3.5.2 Correlation lengths at criticality 74
3.6 Discussion 75

4 Reflections **78**

Bibliography **83**

A Cosmological perturbation theory with matter-time **92**
A.1 Derivation of second order Hamiltonian 92
A.2 Derivation of graviton equation 94
A.3 Diffeomorphism constraint is first class 95

B Ising-like models on Euclidean black holes **97**

B.1 Unique, positive solution for $r(\rho)$ for the AdS black holes 97

B.2 Spins on Euclidean Rindler background 98

C Publication rights **105**

Vita

List of Tables

3.1 Table of critical masses and critical temperatures for spin 1/2 and spin 1 models on the Euclidean black hole backgrounds considered. . 70

List of Figures

3.1 Temperature-Mass relation for 4d Euclidean AdS-Schwarzschild for $L = 0.3, 0.4, 0.5, 0.6$ (top to bottom). 57

3.2 Spins on Euclidean Schwarzschild background with $M = 0.025$ are thermalized at around the 50^{th} MC sweep. 63

3.3 Plots of thermodynamic quantities for spin 1/2 models on Euclidean black holes with respect to $\frac{M}{M_c}$. The critical masses for Schwarzschild, and 4d and 5d Schwarzschild AdS ($\Lambda = -4$) are 0.070, 0.072 and 0.023 respectively in Planck units. 66

3.4 Plots of thermodynamic quantities for spin 1/2 models on Euclidean black holes with respect to $\frac{T}{T_c}$. The critical temperatures for Schwarzschild, 4d Schwarzschild AdS and 5d Schwarzschild AdS are 0.57, 0.61 and 0.80 respectively. For the AdS cases the point circled blue represents the black hole that corresponds to T_{min}, the black diamonds correspond to the large black holes, and the red dots correspond to the small black holes. 67

3.5 Plots of thermodynamic quantities for spin 1 models on Euclidean black holes with respect to $\frac{M}{M_c}$. The critical masses for Schwarzschild, 4d Schwarzschild AdS and 5d Schwarzschild AdS are 0.14, 0.17 and 0.065 respectively. 68

3.6 Plots of thermodynamic quantities for spin 1 models on Euclidean black holes with respect to $\frac{T}{T_c}$. The critical temperatures for Schwarzschild, 4d Schwarzschild AdS and 5d Schwarzschild AdS are 0.28, 0.36 and 0.53 respectively. For the AdS cases the point circled blue represents the black hole that corresponds to T_{min}, the black diamonds correspond to the large black holes, and the red dots correspond to the small black holes. 69

3.7 Estimating critical exponents of thermodynamic quantities for spin 1/2 models on Euclidean black holes. The horizontal axis is $\ln(t)$ and the vertical axis is the ln of the thermodynamic variable in the corresponding row. 72

3.8 Estimating critical exponents of thermodynamic quantities for spin 1 models on Euclidean black holes. The horizontal axis is $\ln(t)$ and the vertical axis is the ln of the thermodynamic variable in the corresponding row. 73

3.9 Thermalized Ising-like models on Euclidean Schwarzschild background at and close to criticality. 74

B.1 Alignment as a function of metric parameter a for spin 1/2 and spin 1 models on a Euclidean Rindler background. 102

B.2 A group of aligned spins. 103

B.3 For a spin 1 model on a Euclidean background, this graph shows $p_{1\to 0}$ as a function of column number n for different a values. 104

List of Symbols, Nomenclature or Abbreviations

ADM	Arnowitt, Deser and Misner
AdS	Anti deSitter
CPT	Cosmological perturbation theory
DOF	Degree(s) of freedom
dS	deSitter
EOM	Equation(s) of motion
$FLRW$	Friedmann-Lemaître-Robertson-Walker
FRG	Functional renormalization group
GR	General relativity
KS	Kruskal-Szekeres
L	AdS scale
M_c	Critical mass
MC	Monte-Carlo
MS	Mukhanov-Sasaki
QFT	Quantum field theory
$QFTCS$	Quantum field theory on curved spacetime
r_0	Horizon radius
RG	Renormalization group
SVT	Scalar, vector, tensor
T_c	Critical temperature
TFT	Thermal field theory
β	Compactification circumference of Euclidean time
Λ	Cosmological constant

Chapter 1

Introduction

General relativity (GR) classically describes how spacetime and matter interact [1, 2]. According to GR, gravity is the curvature of spacetime and - as best summarized by John Wheeler - "spacetime tells matter how to move; matter tells spacetime how to curve." This tenet is captured in Einstein's equations:

$$G_{ab}\,(\,g_{ab}\,)\;+\;\Lambda\,g_{ab}\;=8\pi G\,T_{ab}\,(\,g_{ab}\,,\,\Phi\,) \tag{1.1}$$

where g_{ab} is the spacetime metric, G_{ab} is the Einstein tensor which represents the curvature of spacetime, Φ is the matter field, T_{ab} is the stress-energy tensor which encodes the energy and momentum representing quantities of Φ, Λ is the cosmological constant and G is Newton's constant [1]. Solutions to these equations give all matter and spacetime geometry.

One can intuit two such solutions using (1.1). In vacuum, i.e the absence of Φ and Λ, $G_{ab} = 0$. In this case the simplest solution of Einstein's equations is flat spacetime

[1]Hereafter natural units will be used, whereby Newton's constant G, speed of light c and Planck's constant $\hbar$ are set equal to one.

aka the Minkowski metric:

$$ds^2 = -dt^2 + dr^2 + r^2 d{\Omega_2}^2. \tag{1.2}$$

Here t is time, r is the radial coordinate and $d{\Omega_2}^2$ is the metric on the unit two sphere. The Minkowski metric is physically meaningful because it represents an absence of curvature.

In the absence of matter but not Λ, Einstein's equations yield a spacetime with constant curvature. Two immediate cases are $\Lambda > 0$ and $\Lambda < 0$ respectively. The solution of the former case is the de Sitter metric:

$$ds^2 = -\left(1 - \frac{r^2}{l^2}\right) dt^2 + \left(1 - \frac{r^2}{l^2}\right)^{-1} dr^2 + r^2 d{\Omega_2}^2, \quad l = \sqrt{\frac{3}{\Lambda}} \tag{1.3}$$

where l is called the de Sitter scale. This metric is not discussed further in this thesis. The solution for the $\Lambda < 0$ case is called the Anti-de Sitter (AdS) spacetime:

$$ds^2 = -\left(1 + \frac{r^2}{L^2}\right) dt^2 + \left(1 + \frac{r^2}{L^2}\right)^{-1} dr^2 + r^2 d{\Omega_2}^2, \quad L = \sqrt{-\frac{3}{\Lambda}} \tag{1.4}$$

where L is called the AdS scale. The AdS spacetime has interesting applications (which will be discussed later) even if it does not have observational support.

Other interesting solutions of GR are obtained by imposing a simplifying symmetry on the spacetime and matter. This is advantageous for two reasons. Firstly, these symmetries reduce the number of degrees of freedom required to describe the theory and therefore lead to simpler calculations. This is why such models are called symmetry reduced models. Secondly, these models are idealizations of some physical systems found in nature. Two such systems are described next.

It has been assumed since the time of Copernicus that the large scale universe is homogeneous (same at every point) and isotropic (same in every direction). The

biggest indicator of the latter is the cosmic microwave background (CMB) – a bath of radiation at a temperature $T = 2.7\,K$ in all directions. The homogeneous and isotropic universe is called the Friedman-Lemaître-Robertson-Walker (FLRW) universe; it is described by the metric

$$ds^2 = -dt^2 + a(t)^2 \left(dr^2 + r^2 d{\Omega_2}^2\right) \tag{1.5}$$

where the scale factor $a(t)$ denotes the universe's expansion [2]. The matter distribution of the universe is also assumed to be homogeneous and isotropic. Studying the FLRW spacetime and matter using GR explained Hubble's observations regarding the expansion of the universe.

Consider now a spherically symmetric, non-moving body of mass M (such as the Earth, Sun, star, etc.) surrounded by vacuum. The exterior gravitational field of this body is called the Schwarzschild spacetime [3]:

$$ds^2 = -\left(1 - \frac{2M}{r}\right) dt^2 + \left(1 - \frac{2M}{r}\right)^{-1} dr^2 + r^2 d{\Omega_2}^2. \tag{1.6}$$

In the absence of the body (i.e for $M = 0$) the metric becomes flat (1.2) as expected. The Scwarzschild metric is ill-defined at $r = 2M$ and $r = 0$; such points are called singularities. The first of these is due to the coordinate system being used and can be removed under appropriate coordinate transformations (as will be shown later); therefore $r = 2M$ is called a coordinate singularity. The $r = 0$ singularity however cannot be removed by coordinate transformations. Since some curvature scalars also become infinite in the limit $r \to 0$ (unlike the $r = 2M$ case), this is called a curvature singularity. If one wants to study the Earth, Sun or stars then one need not worry about these points since the Schwarzschild solution is only valid for the vacuum exterior, which for these bodies corresponds to $r > 2M$. However the same cannot

[2] Only the spatially flat case is considered in this thesis.

be said for black holes: astrophysical bodies that have gravitationally collapsed to a point whereby the Schwarzschild solution is valid for all r.

It is reasonable to expect that the gravitational field weakens as one goes far away from a black hole. This expectation is satisfied by Schwarzschild spacetime as it is asymptotically flat. This means that for distances far from the black hole, the Schwarzschild metric resembles the Minkowski metric (1.2). Likewise a black hole that is asymptotically AdS is described by the Scwarzchild AdS metric:

$$ds^2 = -\left(1 - \frac{2M}{r} + \frac{r^2}{L^2}\right) dt^2 + \left(1 - \frac{2M}{r} + \frac{r^2}{L^2}\right)^{-1} dr^2 + r^2 d{\Omega_2}^2. \tag{1.7}$$

Investigating Schwarzschild spacetime accounted for the perihelion shift of Mercury's orbit and led to novel predictions such as the bending of light by a massive object. This prediction was later verified experimentally. Another notable finding by Bardeen, Carter and Hawking [4] was that the gravitational field of a black hole with mass M and area A satisfies

$$dM = \left(\frac{1}{8\pi M}\right)\left(\frac{dA}{4}\right). \tag{1.8}$$

This resembles the first law of thermodynamics

$$dE = T\, dS \tag{1.9}$$

where E, T and S are energy, temperature and entropy respectively. This resemblance indicated a correspondence between M and T and between A and S. It was shown later using different methods that a black hole radiates as if it was a blackbody with temperature $T = (8\pi M)^{-1}$ [5]. This indicated that the temperature-mass relationship as obvious from (1.8) and (1.9) was more than just a correspondence. This point will be revisited soon.

All the aforementioned spacetimes - Minkowski, AdS, FLRW, Schwarzschild and Schwarzschild AdS - represent ideal physical systems. It is reasonable to expect that there exist perturbations on them. For example, it is known that there exist temperature fluctuations δT in the CMB satisfying $\delta T/T \sim 10^{-4}$. The study of perturbations on the solutions of GR is called perturbation theory and it consists of the following steps:

1. Expressing the metric and matter fields in terms of backgrounds and perturbations:

$$g_{ab} = \bar{g}_{ab} + \delta g_{ab}, \quad \Phi = \bar{\phi} + \delta\phi; \tag{1.10}$$

   here (g_{ab}, Φ) are the metric and matter fields, $(\bar{g}_{ab}, \bar{\phi})$ are the background quantities and $(\delta g_{ab}, \delta\phi)$ are the perturbations,

2. Finding the equations of motion (EOM) for the background,

3. Finding the EOM for the perturbations on the background solutions.

Perturbation theory on a flat background, which involves perturbing the gravity sector only, led to the discovery of gravitational waves. These were experimentally observed nearly a century later. Cosmological perturbation theory (CPT) involves perturbing both the gravity and matter sectors [6]. An important result of CPT is the cosmological gravitional wave equation. Another prominent result was published in [7]. To understand this result, recall that in GR there is a gauge-freedom. This means that there is a freedom to perform gauge transformations, which in the context of CPT are chosen to be infinitesimal coordinate transformations (since more general coordinate transformations may yield a background metric that does not reflect the symmetries of the spacetime). In general, the values of the degrees of freedom (DOF) change due to these gauge transformations. However one can construct combinations

of the DOF such that the value of that combination is unchanged under the gauge transformation. Such combinations of the DOF are called gauge-invariant variables. In [7] the author constructed a gauge-invariant perturbation from the metric and scalar field perturbations. This was called the Mukhanov-Sasaki (MS) variable and its EOM resembled that of an oscillator.

Let's now briefly discuss the canonical description of gravity which was introduced by Arnowitt, Deser and Misner (ADM) in 1959 [8]. In this description it was found that the Hamiltonian for gravity was a sum of the Hamiltonian constraint and the diffeormorphism constraint [3]. The former is due to the time reparametrization invariance of GR: that in GR coordinate time is irrelevant and has no physical significance. Similarly the diffeomorphism constraint is due to the space reparametrization invariance of GR. These phase space constraints are manifestations of the general covariance of GR. Arriving at a physical Hamiltonian requires using functions of the phase space as time and space references; this is called fixing a gauge and the algebraic form of the physical Hamiltonian depends on what variables one chooses to fix the gauge [10]. For now let's consider fixing a time gauge only.

For a system of gravity and matter one may also use the matter DOF as the clock. In addition to resulting in a physical Hamiltonian, this choice is also reasonable from an observational standpoint: recall that one observes gravity-matter systems from one's trajectory on spacetime; hence one's proper time is what one uses to make observations; this is why using the proper time of a matter field as the time in the theory is a reasonable choice. Examples of matter that has been used as a clock include a scalar field [11], Brown Kuchař dust [12] and pressureless dust [13].

[3] A constraint is an independent relationship between the phase space variables [9]. Consider a particle moving on a unit two-sphere whereby it satisfies the following constraint

$$x^2 + y^2 + z^2 - 1 = 0 \tag{1.11}$$

for its position. The Hamiltonian and diffeomorphism constraints are generalizations of this since they are independent relationships of the phase space variables.

Using the latter to fix the time gauge has the unique outcomes that the physical Hamiltonian has the same algebraic form as the Hamiltonian constraint and the diffeomorphism constraint is untouched.

The Hamiltonian theory of a system consisting of the metric and scalar field has been used to study CPT. The first such analysis was done by Langlois [14] and others that develop CPT in the canonical framework have appeared in the last two decades [15, 16, 17, 18, 19, 20]. Some of the references mentioned use additional matter fields as clocks; all of them use gauge-invariant perturbations. Brief descriptions of these studies are provided later.

The preceding discussion is focused on the classical interactions of spacetime and matter. A widely held belief since the early 20^{th} century is that the quantum description is closer to nature and hence more fundamental.

Quantum field theory (QFT) describes the quantum behaviour of matter on classical, fixed Minkowski spacetime [21, 22]. Determining how field values at different spacetime points are correlated is an important calculation in QFT. These correlators - which are also known as Lorentzian Wightman functions - are used to explain most interactions of elementary particles that are observed in particle accelerators. A procedure used to make this calculation easier is Wick rotation: it is the replacement of real time by imaginary - or Euclidean - time. This causes the action of a field in 1 time and d space dimensions to resemble the Hamiltonian of a field in $d+1$ space dimensions and for the path integral to resemble a partition function [23, 24]. As an additional step one may compactify Euclidean time by introducing an upper limit on the Euclidean time coordinate and enforcing periodic boundary conditions for the field in Euclidean time. The resultant theory is called Euclidean QFT [25, 26, 27, 28] and it has a useful correspondence with statistical mechanics whereby the compactification circumference β - the upper limit of the Euclidean time coordinate - is inverse temperature. This is why Euclidean QFT is interpreted as

the study of a quantum field in contact with an external, fixed heat bath. It is also worth noting that the Euclidean correlation functions can be used to define unique Lorentzian Wightmann distributions [29].

However this correspondence does not extend to curved backgrounds and is applicable only when the background spacetime is Minkowski. For curved backgrounds Wick rotation can also become problematic, a possible issue being that the procedure results in complex metric components whereby one obtains a theory of quantum fields on classical, complex background. For example Wick rotating a cosmological spacetime (1.5) yields a complex scale factor whereby the space-space components of the metric become complex. Another example is the Kerr metric [30] that has non-zero time-space components; upon Wick rotation these become complex also [31, 32].

Euclidean QFT has two main branches: zero temperature Euclidean QFT in which $\beta \to \infty$, and thermal field theory (TFT) in which β is kept finite. TFT is used to study interactions in which temperatures are large such as the heavy ion collisions which lead to the production of the quark gluon plasma, the early universe and neutron stars.

Generalizations of QFT include QFT on curved spacetime (QFTCS) which is the study of quantum matter on classical, fixed, curved spacetime [33, 34]. Using QFTCS it was shown that the expansion of the universe creates quantum particles and that a black hole emits particles as if it is a thermal body with a temperature related to the inverse of its mass [5]. This was the same relationship between the mass and temperature of a black hole that was discovered via GR [4]. That this relationship was obtained separately from GR and QFTCS motivated Gibbons and Hawking to seek a statistical mechanics description for the thermodynamic properties of a black hole. They succeeded by using Euclidean Schwarzschild geometry [35] and their calculation involved Wick rotation and compactification of Euclidean time. The

resultant Euclidean Schwarzschild geometry had a temperature $T = (8\pi M)^{-1}$; this will be covered in detail in a later section. It is worth noting that the Schwarzschild metric does not become complex due to Wick rotation.

Later, Hawking and Page used this approach to study the gravitational field of a black hole in AdS space (the Schwarzschild AdS metric also does not become complex upon Wick rotation) [36]. They found that an asymptotically AdS black hole has a characteristic temperature and entropy and that for a fixed value of the cosmological constant, black holes less than a certain mass are unstable and decay into AdS space. Hawking and Page's work - which was originally in 4d - was generalized to study asymptotically AdS black holes in 5d. This was later applied to the hypothesis that the gravitational theory of a 5d AdS black hole is dual to a strongly coupled gauge theory at finite temperature in 4d such as quantum chromodynamics (QCD). This proposal is called the finite temperature AdS/CFT conjecture (where CFT stands for conformal field theory) [37, 38]. It claims that a strongly coupled gauge theory at finite temperature in 4d - which is not easy to analyze - can be understood via a dual theory: the gravitational theory of a 5d AdS black hole.

This thesis probes gravity-matter systems within the context of cosmology and black holes. Brief descriptions of each study are provided next.

Chapter 2 is related to the author's MSc thesis [39] which was motivated the question: how does CPT with a dust clock complement the known results and what new information does it provide? In [39] a system of gravity and pressureless dust was considered; this system had local gravitational and scalar dust DOF. The canonical description was derived and the dust was fixed as a clock [13, 40]; a consequence of this choice was that the gravity sector acquired an additional scalar DOF. One goal of this work was to study the nature of the additional scalar DOF that corresponded to pressureless dust within the context of CPT. The canonical action was used to derive the equations of motion; the perturbed cosmological spatial metric and its conjugate

momentum were substituted in the equations of motion, which were then expanded to linear order in the perturbations; the perturbations were expressed in terms of spatial Fourier modes and then classified based on their properties under rotations in spatial Fourier space. The salient results were the cosmological graviton equation and an additional ultralocal scalar DOF in the metric that represented presureless dust. That a propagating scalar DOF was not discovered was due to the fact that the dust (which was used to fix the time gauge) was pressureless. That a MS-like equation was not found was unsurprising since the MS variable mixes perturbations from the gravity and scalar field sectors; this was not possible here since the starting system consisted of gravity and dust only.

Motivated by this, chapter 2 generalizes [39] by considering a system of gravity, pressureless dust and scalar field. This is a valid generalization of [39] since the universe consists of multiple matter fields. Now the starting system has local gravitational, scalar field and dust DOF. After fixing the dust-time gauge the metric acquires an additional scalar DOF that corresponds to dust. The perturbed phase space variables for the FLRW spacetime and scalar field are substituted in the canonical action. The action is expanded to second order in the perturbations which are then expressed in terms of spatial Fourier modes. These modes are next classified based on their properties under rotations in spatial Fourier space. Finally the equations of motion for the perturbations are derived using the second order action: the main results are the cosmological graviton equation, the MS equation with a source term and another equation for an ultralocal DOF which represents dust. This work is different from other CPTs, most importantly because it uses gravity, scalar field and pressureless dust with the latter being used to fix a time gauge. This uniqueness is manifested in the MS equation being generalized to include a source term and the additional ultralocal DOF.

Chapter 3 is motivated by the question: since Euclidean Schwarzschild background

has a temperature [2, 35] to what extent does it behave like a heat bath for a quantum field that lives on it? To answer this a procedure is defined that allows one to study the thermodynamic properties of the field for different M using Monte-Carlo (MC) simulations. This is Euclidean QFT on black hole space which is different from standard QFTCS in several ways. Firstly, the proposed method uses the Euclicdean black hole background whereas QFTCS uses the Lorentzian background. Secondly, in the proposed method the compactification of Euclidean time results in a correspondence with statistical mechanics. There is no such correspondence between QFTCS and statistical mechanics. This work is also different from TFT since it uses Euclidean black hole backgrounds and TFT uses flat Euclidean space. The remaining differences require technical background and therefore will be discussed after Euclidean black holes are introduced.

To ensure a simple model and reasonable computation times the excitations of the field are restricted. One restriction is that the field can take values $\pm$ 1 whereby one has an Ising-like model [41] on black hole space. It is found that for small M the spins are disordered, for large M the spins are ordered, the phase transition is second order and it occurs at sub-Planckian M. Ising-like models on AdS black holes in four and five dimensions are also studied. Then the allowed excitations of the field are extended to 0 and $\pm$ 1; this is like the Blume Capel model [42, 43] (which is a generalization of the Ising model) on the three backgrounds mentioned. Second order phase transitions that occur at sub-Planckian M are discovered for all spin models studied. This research will be sent for publication soon.

The fourth chapter summarizes the thesis and discusses future extensions and applications of the works presented. The appendices contain supplementary calculations, additional details and the reuse and permission license for the research presented in Chapter 2.

Chapter 2

Cosmological perturbation theory with matter-time

2.1 Introduction

The diffeomorphism symmetry of general relativity (GR) is manifested in its canonical formulation through the presence of phase space constraints that generate a closed Poisson algebra. The Hamiltonian is a linear combination of these constraints, and so vanishes on shell [44, 45]. The path to a physical non-vanishing Hamiltonian requires selecting a function on the phase space as a choice of time; the negative of the phase space variable conjugate to the time choice provides this Hamiltonian [10]. It is clear that there are numerous choices for physical Hamiltonians, and the classical dynamics generated using these, for given ansätze, lead ultimately to the same solutions, but in different charts, and covering different regions of the spacetime manifold.

In early work on general relativity, time choices were divided into "intrinsic," where time is a function of the spatial metric, and "extrinsic," where time is a function of the extrinsic curvature (or the momentum conjugate to the spatial metric). Two fre-

quently studied examples of such choices are 3-volume, and the trace of the extrinsic curvature (York time) [46].

For GR with matter fields, there is also the possibility of using matter phase space functions as clocks. Examples of such clocks date back to early studies of cosmological models, where a scalar field was used as a clock [47]. More generally Brown and Kuchař [12] gave a prescription for using a 4-component fluid field coupled to GR as a matter reference system for time and space. This idea, along with the older one of scalar field time, has subsequently been used in many works with the aim of building models for quantum gravity [13, 48, 49, 50].

There are two closely related approaches in which geometric or matter reference systems may be used for classical and quantum models. One of these is to fix the gauge and solve the corresponding constraint strongly and thereby obtain a partially or fully gauge fixed (or "deparametrized") system. The other is to use "relational" observables [51] without deparametrizing, where the evolution of one variable is observed relative to that of the chosen clock variable. This latter procedure generates gauge invariant (Dirac) observables through eliminating the arbitrary time parameter t by inverting the evolution of a clock phase space variable T: one inverts $T(t) \to t(T)$ in some domain, and then substitutes $t(T)$ into any other observables $\mathcal{O}(t)$ of interest, $\mathcal{O}(t) \to \mathcal{O}(t(T))$.

In this chapter we apply a specific matter-time gauge (dust-time) to cosmological perturbation theory in the Hamiltonian formulation. The principal advantage of this gauge is that the physical Hamiltonian takes a simple form: it is exactly the same algebraic expression as the Hamiltonian constraint without the dust contribution. At this first stage we do not fix the spatial diffeomorphism symmetry, which remains as a decoupled gauge symmetry until we proceed to a second order expansion of the canonical action. In the diffeomorphism constraint also the dust contribution is now absent. We emphasize that the process we follow applies to GR coupled to

dust and any other matter fields, including additional scalars, fermions or gauge fields; in the dust-time gauge the physical Hamiltonian is always the same algebraic expression as the Hamiltonian constraint without the dust contribution, and the spatial diffeomorphism decouples in the same way as for the case of a single scalar field we develop here.

Our work is not the first to construct a Hamiltonian perturbation theory for cosmology. The first such analysis was given in [14]; others using the relational approach have appeared recently [19, 20]. However our approach differs from both in several respects, the primary one being that we use only a clock field, and fix a matter-time gauge strongly at the outset before proceeding to cosmology [13]. This step simplifies the analysis significantly by removing the Hamiltonian constraint at the outset. Another important difference is that the theory we consider, GR, with dust and a scalar field, has four local physical degrees of freedom, two gravitational, one scalar and one dust. Therefore, after selecting the dust-time gauge, the metric acquires an additional degree of freedom. In these aspects our work complements these earlier works, with little overlap. The approach we follow was used by one of the authors for studying perturbations on Minkowski space [40]; the work presented here may be considered an extension of this to cosmological perturbation theory. It may be generalized to include additional matter fields.

In the next section we review the use of the dust-time gauge in the ADM canonical framework [12, 13]. In Sec. 2.3 we develop the linearized perturbation theory by expanding the Hamiltonian and diffeormorphism constraints about an arbitrary FLRW-scalar solution. We show from the canonical perspective that the graviton equations turn out to be exactly those derived in the standard covariant perturbation theory without dust (see e.g. [6]), and that the vector modes may be gauged away. In Sec. 2.4 we introduce diffeormorphism invariant phase space variables to study the scalar field and curvature degrees of freedom (which are independent degrees of

freedom in the dust-time gauge). In Sec. 2.5 we give a detailed comparison with standard perturbation theory. We conclude in Sec. 2.6 with a summary and possible future directions. Several appendices provide details of our calculations: Appendix A.1 gives details of the Hamiltonian perturbation expansion, Appendix A.2 gives a derivation of the graviton equation, and Appendix A.3 provides a proof that the linearized constraints are first class.

2.2 Hamiltonian gravity with dust

We consider GR coupled to dust and a scalar field. The action is

$$S = -\frac{1}{2\pi}\int d^4x\sqrt{-g}R + \frac{1}{4\pi}\int d^4x\sqrt{-g}\; m(g^{ab}\partial_a T\partial_b T + 1) + \int d^4x\; \mathcal{L}(\Phi). \quad (2.1)$$

The second term is the dust action, and the last term is the minimally coupled scalar field with an arbitrary potential $V(\Phi)$. With $u^a = g^{ab}\partial_b T$, the dust energy-momentum tensor is

$$T^{ab}_D = mu^a u^b + \frac{m}{2}g^{ab}\left(g_{cd}u^c u^d + 1\right). \quad (2.2)$$

Thus on shell, m is interpreted as the dust energy density.

The ADM canonical theory obtained from this action is

$$S = \int dt\; d^3x\left(\pi^{ab}\dot{q}_{ab} + p_\Phi\dot{\Phi} + p_T\dot{T} - N\mathcal{H} - N^a\mathcal{C}_a\right), \quad (2.3)$$

where the pairs (q_{ab}, π^{ab}), (Φ, p_Φ) and (T, p_T) are respectively the phase space variables of gravity, scalar field and dust. The lapse and shift functions, N and N^a are the coefficients of the Hamiltonian and diffeomorphism constraints

$$\mathcal{H} = \mathcal{H}^G + \mathcal{H}^D + \mathcal{H}^\Phi, \quad (2.4)$$

$$\begin{aligned}\mathcal{C}_a =& \mathcal{C}_a^G + \mathcal{C}_a^D + \mathcal{C}_a^\Phi \\ =& -2D_b\pi_a^b + p_T\partial_a T + p_\Phi\partial_a\Phi,\end{aligned} \tag{2.5}$$

where

$$\mathcal{H}^G = \frac{1}{\sqrt{q}}\left(\pi^{ab}\pi_{ab} - \frac{1}{2}\pi^2\right) - \sqrt{q}R^{(3)} \tag{2.6}$$

$$\mathcal{H}^D = \frac{1}{2}\left[\frac{p_T^2}{m\sqrt{q}} + m\sqrt{q}\left(q^{ab}\partial_a T\partial_b T + 1\right)\right] \tag{2.7}$$

$$\mathcal{H}^\Phi = \frac{1}{2}\left(\frac{p_\Phi^2}{\sqrt{q}} + \sqrt{q}q^{ab}\partial_a\Phi\partial_b\Phi\right), \tag{2.8}$$

∂_a, D_a are the spatial partial and covariant derivatives, and $R^{(3)}$ is the spatial Ricci scalar. The field m appears only in $\mathcal{H}^D$ as an auxiliary field. We can therefore solve its EOM for m and substitute the result back into $\mathcal{H}^D$:

$$m = \pm\frac{p_T}{\sqrt{q(q^{ab}\partial_a T\partial_b T + 1)}}, \tag{2.9}$$

$$\mathcal{H}^D = \mathrm{sgn}(m)\ p_T\sqrt{q^{ab}\partial_a T\partial_b T + 1}, \tag{2.10}$$

where $\mathrm{sgn}(m)$ is the sign convention chosen in (2.9). With this expression for $\mathcal{H}^D$, the final canonical action retains the form (2.3), but now with no dependence on m except for its sign.

2.2.1 Dust-time gauge

We now introduce a partial gauge fixing by setting a time gauge to obtain a physical Hamiltonian; this fixes the time-reparmetrization invariance, while the spatial diffeomorphisms remain as a full gauge symmetry. We use the dust-time gauge [13, 52] which equates the physical time with the dust field, i.e., the spatial hyper-

surfaces are level surfaces of the dust field,

$$\lambda \equiv T - \epsilon t \approx 0, \quad \epsilon = \pm 1. \tag{2.11}$$

This is a special case of the Brown-Kuchař matter reference frame system which is designed to fix all four coordinate conditions. The condition (2.11) has a nonzero Poisson bracket with the Hamiltonian constraint, so this pair of conditions constitute a second class set. According to the Dirac criteria, a gauge condition is considered suitable if the matrix of second class constraints is invertible at all points [45]. In the present case this matrix is

$$C = \begin{bmatrix} 0 & \{\lambda, \mathcal{H}\} \\ \{\mathcal{H}, \lambda\} & 0 \end{bmatrix} = \mathrm{sgn}(m) \begin{bmatrix} 0 & 1 \\ -1 & 0 \end{bmatrix}. \tag{2.12}$$

This matrix is invertible everywhere on the manifold (since $\mathrm{sgn}(m)$ is merely a sign convention selected in (2.9)). Therefore the dust-time gauge does not breakdown at any point and is therefore a robust choice. The second condition on a canonical gauge is that it be preserved in time. This gives an equation for the lapse function:

$$\epsilon = \dot{T} = \left\{ T, \int d^3x \left(N\mathcal{H} + N^a \mathcal{C}_a \right) \right\} \Big|_{T=t} = \mathrm{sgn}(m) N \ . \tag{2.13}$$

Solving the Hamiltonian constraint for p_T and substituting the gauge condition back into (2.3) gives the gauge fixed action

$$S_{GF} = \int dt \ d^3x \left[\pi^{ab} \dot{q}_{ab} + p_\Phi \dot{\Phi} - \epsilon \ \mathrm{sgn}(m) \left(\mathcal{H}^G + \mathcal{H}^\Phi \right) - N^a \mathcal{C}_a \right], \tag{2.14}$$

This identifies the physical Hamiltonian density

$$\mathcal{H}_P = \epsilon \ \mathrm{sgn}(m) \left(\mathcal{H}^G + \mathcal{H}^\Phi \right) = \mathrm{sgn}(N) \left(\mathcal{H}^G + \mathcal{H}^\Phi \right), \tag{2.15}$$

where the last equality follows from (2.13). Thus the physical Hamiltonian is determined up to an overall sign of the lapse function. Since we are free to choose the lapse up to sign, we will work with $N = 1$. The corresponding spacetime metric is

$$ds^2 = -dt^2 + (dx^a + N^a dt)(dx^b + N^b dt)q_{ab}. \tag{2.16}$$

In the following we apply the dust-time canonical action (2.14) to flat FLRW cosmology and construct the linearized perturbation theory. At this stage we note the central difference with standard perturbation theory: we have a physical Hamiltonian not a Hamiltonian constraint, therefore the gauge invariant observables we work with are those that are invariant under the spatial diffeomorphisms. Furthermore, the physical Hamiltonian (2.15) is what would be the Hamiltonian constraint for the gravity-scalar system. As a result, per point we have three physical degrees of freedom in the metric, and one in the scalar field; the presence of the third degree of freedom in the metric is due ultimately to the fact that our starting action had a dust field. As we will show, these can be rearranged into two graviton modes, a curvature perturbation, and the scalar field, with a relatively simple coupled dynamics.

2.3 Cosmological perturbation theory

Our starting point for developing a canonical perturbation theory for flat FLRW models is the selection of a background solution starting with the action (2.14). This starting point is distinct from all standard treatments of the subject, both canonical and covariant, with the key difference being that the Hamiltonian constraint is no longer a constraint, but is instead the physical Hamiltonian. This has several consequences, the main one being that the additional local degree of freedom that came from the dust emerges in the metric perturbation.

Let us take the following parametrization for the ADM variables for the background

solution:

$$q_{ab}^{(0)} = \bar{a}^2(t)\ e_{ab}, \quad \pi^{ab(0)} = \left(\frac{\bar{p}(t)}{6\bar{a}(t)}\right) e^{ab}, \tag{2.17}$$

$$\Phi^{(0)} = \bar{\phi}(t), \qquad p_{\Phi}^{(0)} = \bar{p}_{\phi}(t), \tag{2.18}$$

$$N^{a(0)} = 0 \tag{2.19}$$

where e_{ab} is the Euclidean metric, $(\bar{a}(t), \bar{p}(t))$ and $(\bar{\phi}(t), \bar{p}_{\phi}(t))$ are the scale factor and scalar field and their conjugate momenta. Substituting these into the dust-time gauge fixed canonical action (2.14) gives the reduced action for the background

$$S = \int dt \left[\dot{\bar{a}}\bar{p} + \dot{\bar{\phi}}\bar{p}_{\phi} - \bar{\mathcal{H}}\right] \tag{2.20}$$

where

$$\bar{\mathcal{H}} = -\frac{\bar{p}^2}{24\bar{a}} + \frac{\bar{p}_{\phi}^2}{2\bar{a}^3} + \bar{a}^3 V(\bar{\phi}). \tag{2.21}$$

The background spacetime metric with this parametrization, with $N^2 = 1$ in the dust-time gauge, is of the standard form

$$ds^2 = -dt^2 + \bar{a}^2(t) e_{ab} dx^a dx^b. \tag{2.22}$$

The background EOM are

$$\dot{\bar{a}} = -\frac{\bar{p}}{12\bar{a}} \tag{2.23a}$$

$$\dot{\bar{p}} = -\frac{\bar{p}^2}{24\bar{a}^2} + \frac{3\bar{p}_{\phi}^2}{2\bar{a}^4} - 3\bar{a}^2 V(\bar{\phi}) \tag{2.23b}$$

$$\dot{\bar{\phi}} = \frac{\bar{p}_{\phi}}{\bar{a}^3} \tag{2.23c}$$

$$\dot{\bar{p}}_{\phi} = -\bar{a}^3 V'(\bar{\phi}), \tag{2.23d}$$

where $V'(\bar{\phi}) = dV/d\phi|_{\bar{\phi}}$. The physical Hamiltonian is a constant of the motion in

the dust-time gauge, since it is not explicitly time dependent; this is unlike other time gauges, such as volume time $a^3 = t$. The background solution is of the type

$$\bar{\mathcal{H}} = \mu, \tag{2.24}$$

where μ is a constant, and therefore falls into one of the three classes: $\bar{\mathcal{H}} = 0$, $\bar{\mathcal{H}} > 0$, and $\bar{\mathcal{H}} < 0$. The first of these corresponds to the condition

$$\frac{\bar{p}^2}{24\bar{a}} = \frac{\bar{p}_\phi^2}{2\bar{a}^3} + \bar{a}^3 V(\bar{\phi}), \tag{2.25}$$

which by the equation of motion for $\bar{a}$ (and restoring the $8\pi G$ factor) is the Friedmann equation

$$\bar{H}^2 = \frac{8\pi G}{3}\left(\frac{\bar{p}_\phi^2}{2\bar{a}^6} + V(\bar{\phi})\right), \tag{2.26}$$

where $\bar{H} = \dot{\bar{a}}/\bar{a}$. For the cases $\bar{\mathcal{H}} = \mu \neq 0$, the conservation of the physical Hamiltonian may be written

$$\bar{H}^2 = \frac{8\pi G}{3}\left(\frac{\bar{p}_\phi^2}{2\bar{a}^6} + V(\bar{\phi}) - \frac{\mu}{\bar{a}^3}\right), \tag{2.27}$$

which shows that μ gives the dust energy density contribution to the Friedmann equation up to a minus sign. This completes our summary of the background solutions in the dust-time gauge.

2.3.1 Linearized theory

We define the following expansion of phase space variables and the shift vector:

$$q_{ab}(t,\vec{x}) = \bar{a}(t)^2 e_{ab} + h_{ab}(t,\vec{x}) \tag{2.28a}$$

$$\pi^{ab}(t,\vec{x}) = \frac{\bar{p}(t)}{6\bar{a}(t)} e^{ab} + p^{ab}(t,\vec{x}) \tag{2.28b}$$

$$N^a(t,\vec{x}) = 0 + \xi^a(t,\vec{x}) \tag{2.28c}$$

$$\Phi(t,\vec{x}) = \bar{\phi}(t) + \phi(t,\vec{x}) \tag{2.28d}$$

$$p_\Phi(t,\vec{x}) = \bar{p}_\phi(t) + p_\phi(t,\vec{x}). \tag{2.28e}$$

Here the fields $h_{ab}, p^{ab}, \phi, p_\phi$ are respectively the perturbations of the gravitational and scalar field phase space variables, and ξ^a is the perturbation of the shift vector.

These are substituted into the physical Hamiltonian and spatial diffeomorphism constraint, which are then expanded to second order in the perturbations. This leads to the second order action for the perturbations

$$S^{(2)} = \int dt d^3x \left[\dot{h}_{ab}p^{ab} + \dot{\phi}p_\phi - \mathcal{H}^{(2)} - \xi^a C_a^{(1)}\right], \tag{2.29}$$

where $\mathcal{H}^{(2)}$ is the second order perturbation of the Hamiltonian, and $C_a^{(1)}$ is first order perturbation of the spatial diffeomorphism constraint. The latter is all that is required since the shift is first order. We note also that terms linear in the perturbations vanish when the background solution is imposed; the first order symplectic term in the action combines with the first order term $\mathcal{H}^{(1)}|_{\bar{S}}$ to give zero, and the first order diffeomorphism term $\left(N^{a(0)}C_a^{(1)} + \xi^a C_a^{(0)}\right)|_{\bar{S}} = 0$. ($\bar{S}$ denotes evaluation on the background solution.) The expressions for

$$\mathcal{H}^{(2)} = \mathcal{H}^{G(2)} + \mathcal{H}^{\Phi(2)} \tag{2.30}$$

$$C_a^{(1)} = C_a^{G(1)} + C_a^{\Phi(1)} \tag{2.31}$$

are the following:

$$\begin{aligned}
\mathcal{H}^{G(2)} &= \bar{a}\left(p^{ab}p_{ab}-\frac{1}{2}p^2\right)+\frac{1}{\bar{a}}\left(\frac{\bar{p}}{6\bar{a}}\right)\left(p^{ab}h_{ab}-\frac{1}{2}hp\right) \\
&\quad +\frac{1}{8\bar{a}^3}\left(\frac{\bar{p}}{6\bar{a}}\right)^2\left(5h_{ab}h^{ab}-\frac{3}{2}h^2\right)-\frac{h}{2\bar{a}^3}\left(\partial_a\partial_b h^{ab}-\frac{1}{2}\partial^2 h\right) \\
&\quad +\frac{h^{ab}}{2\bar{a}^3}\left(\partial_b\partial^c h_{ca}-\frac{1}{2}\partial^2 h_{ab}\right) \qquad (2.32) \\
\mathcal{H}^{\phi(2)} &= \frac{p_\phi^2}{2\bar{a}^3}+\frac{\bar{a}}{2}e^{ab}\partial_a\phi\partial_b\phi+\frac{\bar{a}^3}{2}\,V''(\bar{\phi})\,\phi^2 \\
&\quad +\bar{a}\left(-\frac{\bar{p}_\phi}{2\bar{a}^6}\,p_\phi+\frac{1}{2}V'(\bar{\phi})\,\phi\right)h+\frac{\bar{p}_\phi^2}{8\bar{a}^7}\left(h_{ab}h^{ab}+\frac{1}{2}h^2\right) \\
&\quad -\frac{1}{4\bar{a}}V(\bar{\phi})\left(h_{ab}h^{ab}-\frac{1}{2}h^2\right) \qquad (2.33) \\
C_a^{(1)} &= -2\bar{a}^2\partial^b p_{ab}-\frac{\bar{p}}{3\bar{a}}\left(\partial^c h_{ac}-\frac{1}{2}\partial_a h\right)+\bar{p}_\phi\partial_a\phi. \qquad (2.34)
\end{aligned}$$

All indices in these equations are raised and lowered by the Euclidean metric e_{ab}; $\partial^2 = e^{ab}\partial_a\partial_b$, $h = h_{ab}e^{ab}$, and $p = p^{ab}e_{ab}$. The derivation of these expressions appears in Appendix A.1.

2.3.2 Linearized theory in momentum space

We next write the action for the perturbations and the shift in spatial Fourier modes, as this significantly simplifies the remaining analysis. We set

$$\begin{aligned}
h_{ab}(t,\vec{x}) &= \int d^3k\left[e^{i\vec{k}.\vec{x}}M^I_{ab}h_I(t,\vec{k})\right], \qquad (2.35) \\
p^{ab}(t,\vec{x}) &= \int d^3k\left[e^{i\vec{k}.\vec{x}}M^{ab}_I p^I(t,\vec{k})\right], \qquad (2.36) \\
\phi(t,\vec{x}) &= \int d^3k\left[e^{i\vec{k}.\vec{x}}\tilde{\phi}(t,\vec{k})\right], \qquad (2.37) \\
p_\phi(t,\vec{x}) &= \int d^3k\left[e^{i\vec{k}.\vec{x}}\tilde{p}_\phi(t,\vec{k})\right], \qquad (2.38) \\
\xi^a(t,\vec{x}) &= \int d^3k\left[e^{i\vec{k}.\vec{x}}\tilde{\xi}^a(t,\vec{k})\right]. \qquad (2.39)
\end{aligned}$$

Here the matrices $M^I_{ab},\ I = 1\cdots 6$ (to be defined below) form a time independent basis for 3×3 symmetric matrices that give a decomposition of the gravitational phase space variables into the canonical set (h^I, p_I), and the lowercase indices are lowered and raised using the flat Euclidean spatial metric and its inverse respectively. The matrices M^I must satisfy the orthogonality condition

$$\mathrm{Tr}(M^I M^J) = M^I_{ab} M^{Jab} = \delta^{IJ}, \tag{2.40}$$

to ensure that the symplectic structure is preserved when the canonical action for perturbations (2.29) is written in $k-$space, i.e.

$$\int d^3x dt\ p^{ab}\dot{h}_{ab} \longrightarrow \int d^3k dt\ p_I \dot{h}^I. \tag{2.41}$$

A suitable matrix basis that fulfills this requirement may be constructed using the unit mode vector and two unit orthogonal vectors in the plane transverse to k^a

$$\epsilon^a_3 \equiv k^a/|k|, \quad \epsilon^a_1, \quad \epsilon^a_2. \tag{2.42}$$

Since we would like to characterize the matrices M as having defined helicity with respect to rotations about the k^a axis, we replace $\epsilon^a_1, \epsilon^a_2$ with the eigenvectors of the rotation matrix J_θ about the k^a axis. These are $\epsilon^a_\pm = (\epsilon^a_1 \pm i\epsilon^a_2)/\sqrt{2}$, and satisfy $J_\theta \epsilon_\pm = e^{\pm i\theta}\epsilon_\pm$, $J_\theta \epsilon_3 = \epsilon_3$, and $e_{ab}\epsilon^a_- \epsilon^b_+ = 1$ and $e_{ab}\epsilon^a_\pm \epsilon^b_\pm = 0$. Using the set $(\epsilon_3, \epsilon_\pm)$, the Euclidean metric may be written as $e^{ab} = 2\epsilon^{(a}_+ \epsilon^{b)}_- + \epsilon^a_3 \epsilon^b_3$.

The six matrices M^I are constructed from the elements

$$\epsilon^a_3 \epsilon^b_3, \quad \epsilon^{(a}_- \epsilon^{b)}_+, \quad \epsilon^a_\pm \epsilon^b_\pm, \quad \epsilon^{(a}_3 \epsilon^{b)}_\pm. \tag{2.43}$$

Under J_θ, the first two transform as scalars, the second two as tensors, and the last two as vectors. However as they stand, these do not satisfy the desired orthogonality

conditions (2.40). This is achieved by the following linear combinations:

$$
\begin{aligned}
M_1^{ab} &= \frac{1}{\sqrt{3}}\, e^{ab}, && (2.44)\\
M_2^{ab} &= \sqrt{\frac{3}{2}}\left(\epsilon_3^a\epsilon_3^b - \frac{1}{3}e^{ab}\right), && (2.45)\\
M_3^{ab} &= \frac{i}{\sqrt{2}}\left(\epsilon_-^a\epsilon_-^b - \epsilon_+^a\epsilon_+^b\right), && (2.46)\\
M_4^{ab} &= \frac{1}{\sqrt{2}}\left(\epsilon_-^a\epsilon_-^b + \epsilon_+^a\epsilon_+^b\right), && (2.47)\\
M_5^{ab} &= i\left(\epsilon_-^{(a}\epsilon_3^{b)} - \epsilon_+^{(a}\epsilon_3^{b)}\right), && (2.48)\\
M_6^{ab} &= \epsilon_-^{(a}\epsilon_3^{b)} + \epsilon_+^{(a}\epsilon_3^{b)}, && (2.49)
\end{aligned}
$$

where again the first pair transform as scalars, the next pair as tensors, and the last pair as vectors. Let us also note a few other properties of these matrices:

$$
\begin{aligned}
e^{ab}M_{ab}^I &= 0, \quad I = 2\cdots 6;\\
k^a M_{ab}^I &= 0, \quad I = 3, 4;\\
k^a k^b M_{ab}^I &= 0, \quad I = 5, 6. && (2.50)
\end{aligned}
$$

Thus in the decomposition of the Fourier transform of the metric perturbation $\tilde{h}_{ab}(k,t) \equiv M_{ab}^I h_I(k,t)$, h_1, h_2 are the scalar modes, h_3, h_4 are the transverse traceless tensor modes, and h_5, h_6 are the transverse vector modes. The same properties hold for the momenta p_I conjugate to h^I. The shift perturbation may also be decomposed into longitudinal and transverse components:

$$
\tilde{\xi}^a(t,\vec{k}) = \xi_1(t,\vec{k})\epsilon_1^a + \xi_2(t,\vec{k})\epsilon_2^a + \xi_{||}(t,\vec{k})\epsilon_3^a. \qquad (2.51)
$$

In summary, so far we have decomposed the perturbations $h_{ab}(x,t), p^{ab}(x,t)$ into longitudinal and transverse Fourier modes $h^I(k,t), p_I(k,t),\ I = 1\cdots 6$, with well defined physical properties, and a related expansion for ξ^a. (The scalar field pertur-

bation of course does not require any decomposition.) We now write the canonical action in $k-$space using this decomposition.

2.3.3 Canonical action in momentum space

As is standard in field theory, writing an action in momentum space using (2.35) requires field redefinitions after implementing the reality conditions such as $\tilde{h}^*_{ab}(t,k) = \tilde{h}_{ab}(t,-k)$. One way to do this is to write $\tilde{h}_{ab}(k,t) = \tilde{h}^R_{ab}(k,t) + i\tilde{h}^I_{ab}(k,t)$, impose the reality condition, restrict the action to be over independent modes, and then redefine modes to give an action with integration over all k. Following these steps, and using the decompositions

$$\tilde{h}_{ab}(k,t) = M_{abI}h^I(k,t), \quad \tilde{p}^{ab}(k,t) = M^{abI}p_I(k,t), \quad I = 1\cdots 6, \tag{2.52}$$

gives the $k-$space action

$$S^{(2)} = \int dtd^3k \left[\dot{h}^I p_I + \dot{\tilde{\phi}}\tilde{p}_\phi - \tilde{H}^{(2)} - i\tilde{\xi}^a\tilde{C}^{(1)}_a\right], \tag{2.53}$$

where $\tilde{H}^{(2)} = \tilde{\mathcal{H}}^{G(2)} + \tilde{\mathcal{H}}^{\phi(2)}$, and

$$\begin{aligned}
\tilde{\mathcal{H}}^{G(2)} = {} & \bar{a}\left(p^I p_I - \frac{3}{2}p_1^2\right) + \frac{1}{\bar{a}}\left(\frac{\bar{p}}{6\bar{a}}\right)\left(p^I h_I - \frac{3}{2}h_1 p_1\right) \\
& + \frac{1}{8\bar{a}^3}\left(\frac{\bar{p}}{6\bar{a}}\right)^2\left(5h_I h^I - \frac{9}{2}h_1^2\right) \\
& - \frac{k^2}{6\bar{a}^3}\left[\left(h_1 - \frac{h_2}{\sqrt{2}}\right)^2 - \frac{3}{2}\left(h_3^2 + h_4^2\right)\right], \qquad (2.54a) \\
\tilde{\mathcal{H}}^{\phi(2)} = {} & \frac{\tilde{p}_\phi^2}{2\bar{a}^3} + \frac{\bar{a}}{2}k^2\tilde{\phi}^2 + \frac{\bar{a}^3}{2}V''(\bar{\phi})\tilde{\phi}^2 \\
& + \sqrt{3}\bar{a}\left(-\frac{\bar{p}_\phi}{2\bar{a}^6}\tilde{p}_\phi + \frac{1}{2}V'(\bar{\phi})\tilde{\phi}\right)h_1 \\
& + \frac{\bar{p}_\phi^2}{8\bar{a}^7}\left(h_I h^I + \frac{3}{2}h_1^2\right) - \frac{V(\bar{\phi})}{4\bar{a}}\left(h_I h^I - \frac{3}{2}h_1^2\right). \qquad (2.54b)
\end{aligned}$$

The linearized diffeomorphism constraint in momentum space $\tilde{C}_a^{(1)} = 0$ is

$$\begin{aligned}\tilde{C}_a^{(1)} &= \tilde{C}_a^G + \tilde{C}_a^\phi \\ &= -2\bar{a}^2 k^b M_{ab}^I p_I - \frac{\bar{p}}{3\bar{a}}\left(k^c M_{ac}^I h_I - \frac{\sqrt{3}k_a}{2}h_1\right) + \bar{p}_\phi k_a \tilde{\phi}. \end{aligned} \tag{2.55}$$

A further expansion of $\tilde{C}_a^{(1)}$ using the properties of the M^I basis reveals its longitudinal and transverse components:

$$\begin{aligned}\tilde{C}_a^{(1)} = k\left[-\frac{2\bar{a}^2}{\sqrt{3}}(p_1 + \sqrt{2}p_2) + \frac{\bar{p}}{6\sqrt{3}\bar{a}}(h_1 - 2\sqrt{2}h_2) + \bar{p}_\phi\tilde{\phi}\right]\epsilon_{3a} \\ - \sqrt{2}k\left[\bar{a}^2 p_6 + \left(\frac{\bar{p}}{6\bar{a}}\right)h_6\right]\epsilon_{1a} - \sqrt{2}k\left[\bar{a}^2 p_5 + \left(\frac{\bar{p}}{6\bar{a}}\right)h_5\right]\epsilon_{2a}. \end{aligned} \tag{2.56a}$$

Similarly, the gravitational Hamiltonian may be written as a sum of scalar (h_1, h_2), tensor (h_3, h_4), and vector (h_5, h_6) components, and their canonical momenta:

$$\tilde{H}^{G(2)} = H^S + H^V + H^T, \tag{2.57}$$

$$\begin{aligned} H^S &= \bar{a}\left(p_2^2 - \frac{1}{2}p_1^2\right) + \frac{1}{\bar{a}}\left(\frac{\bar{p}}{6\bar{a}}\right)\left(h_2 p_2 - \frac{1}{2}h_1 p_1\right) + \frac{1}{8\bar{a}^3}\left(\frac{\bar{p}}{6\bar{a}}\right)^2\left(\frac{1}{2}h_1^2 + 5h_2^2\right) \\ &\quad - \frac{1}{6\bar{a}}\left(\frac{k}{\bar{a}}\right)^2\left(h_1 - \frac{1}{\sqrt{2}}h_2\right)^2, \end{aligned} \tag{2.58a}$$

$$H^V = \bar{a}\left(p_5^2 + p_6^2\right) + \frac{1}{\bar{a}}\left(\frac{\bar{p}}{6\bar{a}}\right)(p_5 h_5 + p_6 h_6) + \frac{5}{8\bar{a}^3}\left(\frac{\bar{p}}{6\bar{a}}\right)^2\left(h_5^2 + h_6^2\right), \tag{2.58b}$$

$$\begin{aligned} H^T &= \bar{a}\left(p_3^2 + p_4^2\right) + \frac{1}{\bar{a}}\left(\frac{\bar{p}}{6\bar{a}}\right)(p_3 h_3 + p_4 h_4) \\ &\quad + \frac{1}{4\bar{a}}\left[\frac{5}{2\bar{a}^2}\left(\frac{\bar{p}}{6\bar{a}}\right)^2 + \left(\frac{k}{\bar{a}}\right)^2\right]\left(h_3^2 + h_4^2\right). \end{aligned} \tag{2.58c}$$

This shows that only the scalar canonical pairs (h_1, p_1) and (h_2, p_2) interact with each other, while all the other pairs are mutually decoupled. Denoting the longitudinal and transverse components of the diffeomorphism constraint by $C_\parallel$ and $C_\perp$, we note

also that

$$\{H^S, C_\perp\} = 0, \quad \{H^V, C_\parallel\} = 0, \quad \{H^T, C_a\} = 0. \tag{2.59}$$

Thus the graviton modes are diffeomorphism invariant (to this order in perturbation theory). All propagating modes appear with a factor k^2 so the vector modes are non-propagating; the last term in H^S is the curvature perturbation up to an overall factor.

2.3.4 Partial gauge fixing: removal of vector modes

At this stage it is useful to perform a gauge fixing to remove the vector modes. This involves imposing canonical gauge conditions on these modes and solving strongly the corresponding diffeomorphism constraint components. The above decomposition reveals the convenient choice

$$h_5 = h_6 = 0. \tag{2.60}$$

These are second class with the components $C_\perp$,

$$\{h_5, C_\perp\} = \{h_6, C_\perp\} = \sqrt{2}k\bar{a}^2, \tag{2.61}$$

unless $\bar{a} = 0$ or $k = 0$. Since we are interested in propagating modes (where the diffeomorphism constraint is not identically zero), and in regions far from a potential singularity, these gauge choices are sufficient. $C_\perp = 0$ is then solved by setting $p_5 = p_6 = 0$.

This result is different from the one obtained in the standard, covariant cosmological perturbation theory where the vector modes decay in an expanding universe due to which they are typically set to zero [6, 39]. In our framework one can use a

different gauge from (2.60) to arrive at decaying vector modes. However the current result is more useful since it shows that vector modes are gauge DOF.

The resulting $\tilde{H}^{G(2)}$ is now

$$\tilde{H}^{G(2)} = H^S + H^T, \tag{2.62}$$

and the second order scalar field Hamiltonian becomes

$$\begin{aligned}\tilde{\mathcal{H}}^{\phi(2)} &= \frac{\tilde{p}_\phi^2}{2\bar{a}^3} + \frac{\bar{a}}{2}k^2\tilde{\phi}^2 + \frac{\bar{a}^3}{2}V''(\bar{\phi})\tilde{\phi}^2 \\ &\quad +\sqrt{3}\bar{a}\left[-\left(\frac{\bar{p}_\phi}{2\bar{a}^6}\right)\tilde{p}_\phi + \frac{1}{2}V'(\bar{\phi})\tilde{\phi}\right]h_1 \\ &\quad +\frac{\bar{p}_\phi^2}{8\bar{a}^7}\left(h_I h^I + \frac{3}{2}h_1^2\right) - \frac{V(\bar{\phi})}{4\bar{a}}\left(h_I h^I - \frac{3}{2}h_1^2\right),\end{aligned} \tag{2.63}$$

where the sums $h_I h^I$ in the last line now exclude the vectors modes h_5, h_6. The first line is the standard Hamiltonian of the scalar field perturbation $(\tilde{\phi}, \tilde{p}_\phi)$ on the $(\bar{a}, \bar{\phi})$ homogeneous background; the second line contains the coupling of the scalar field perturbation to the metric scalar mode h_1; the last line is a potential for the graviton and metric-scalar modes.

The diffeomorphism constraint is reduced to only its longitudinal component

$$\tilde{C}_\parallel \equiv -2\bar{a}^2(p_1 + \sqrt{2}p_2) + \left(\frac{\bar{p}}{6\bar{a}}\right)(h_1 - 2\sqrt{2}h_2) + \sqrt{3}\bar{p}_\phi\tilde{\phi} = 0. \tag{2.64}$$

In summary, the gauge fixing (2.60) leaves a simpler system for the the remaining degrees of freedom: the metric scalar modes (h_1, h_2), graviton modes (h_3, h_4), and the scalar field mode $\tilde{\phi}$.

2.3.5 Graviton equation

The graviton part of the second order canonical action is

$$S^g \equiv \int dt d^3k \left[p^I \dot{h}_I - H^g \right], \quad I = 3, 4, \tag{2.65}$$

where H^g is the sum of H^T in (2.58c) and the graviton parts of $\mathcal{H}^{\phi(2)}$ in (2.54b). For comparison with covariant perturbation theory, where the expansion $q_{ab} = \bar{a}^2(t)\left(e_{ab} + h_{ab}\right)$ is used, let us make the transformation

$$h_I \longrightarrow \bar{a}^2 h_I, \quad p_I \longrightarrow \bar{a}^{-2} p_I. \tag{2.66}$$

With this, the symplectic term transforms to

$$\dot{h}_I p^I \longrightarrow \dot{h}_I p^I + 2\left(\frac{\dot{\bar{a}}}{\bar{a}}\right) h_I p^I = \dot{h}_I p^I - \frac{\bar{p}}{6\bar{a}^2} h^I p_I, \tag{2.67}$$

where the last step uses the EOM of the background. Therefore H^g transforms to

$$\begin{aligned} H^g \;=\; & \frac{1}{\bar{a}^3}\left(p_3^2 + p_4^2\right) + \left(\frac{\bar{p}}{3\bar{a}^2}\right)\left(p_3 h_3 + p_4 h_4\right) \\ & + \frac{\bar{a}^3}{4}\left[\frac{\bar{p}_\phi^2}{2\bar{a}^6} - V(\bar{\phi}) + \frac{5}{2}\left(\frac{\bar{p}}{6\bar{a}^2}\right)^2 + \left(\frac{k}{\bar{a}}\right)^2\right]\left(h_3^2 + h_4^2\right). \end{aligned} \tag{2.68}$$

Although this expression for H^g looks involved, it is readily verified that the canonical EOM

$$\dot{h}_I = \{h_I, H^g\}, \quad \dot{p}_I = \{p_I, H^g\}, \tag{2.69}$$

together with the equations (2.23) of the background $(\bar{a}, \bar{p})$, leads to the standard

wave equation

$$\ddot{h}_I + 3\left(\frac{\dot{\bar{a}}}{\bar{a}}\right)\dot{h}_I + \frac{k^2}{a^2}h_I = 0, \qquad I = 3, 4. \tag{2.70}$$

Thus the graviton mode equation is unchanged in the canonical dust-time gauge. The calculation leading to this has some non-trivial steps (see Appendix A.2).

2.4 Scalar modes

We have so far seen that the dust-time physical Hamiltonian in momentum space, in the time independent matrix basis M, provides a relatively simple way to analyze cosmological perturbations. Specifically we showed from a canonical perspective how the vector perturbations are removed, and the graviton equation remains unchanged.

We now turn to the remaining degrees of freedom $(h_1, h_2, \tilde{\phi})$, with dynamics described by H^S (2.58a) and $\tilde{\mathcal{H}}^{\phi(2)}$ (2.63),

$$\begin{aligned} H^{S\phi} \equiv\ & \bar{a}\left(p_2^2 - \frac{1}{2}p_1^2\right) + \frac{1}{\bar{a}}\left(\frac{\bar{p}}{6\bar{a}}\right)\left(h_2 p_2 - \frac{1}{2}h_1 p_1\right) + \frac{1}{8\bar{a}^3}\left(\frac{\bar{p}}{6\bar{a}}\right)^2\left(\frac{1}{2}h_1^2 + 5h_2^2\right) \\ & - \frac{1}{6\bar{a}}\left(\frac{k}{\bar{a}}\right)^2\left(h_1 - \frac{1}{\sqrt{2}}h_2\right)^2 + \frac{\bar{p}_\phi^2}{8\bar{a}^7}\left(\frac{5}{2}h_1^2 + h_2^2\right) + \frac{V(\bar{\phi})}{4\bar{a}}\left(\frac{1}{2}h_1^2 - h_2^2\right) \\ & + \frac{\tilde{p}_\phi^2}{2\bar{a}^3} + \frac{\bar{a}}{2}k^2\tilde{\phi}^2 + \frac{\bar{a}^3}{2}V''(\bar{\phi})\tilde{\phi}^2 + \sqrt{3}\bar{a}\left[-\left(\frac{\bar{p}_\phi}{2\bar{a}^6}\right)\tilde{p}_\phi + \frac{1}{2}V'(\bar{\phi})\tilde{\phi}\right]h_1, \end{aligned} \tag{2.71}$$

subject to the remaining diffeomorphism constraint $C_\parallel$ (2.64).

The Hamiltonian $H^{S\phi}$ is of the form of $h_S(h_i, p_i) + h_\phi(\tilde{\phi}, \tilde{p}_\phi) + h_{\rm Int}(\tilde{\phi}, \tilde{p}_\phi, h_1)$. It is notable that the scalar field perturbation $\tilde{\phi}$ interacts with only the metric-scalar mode h_1 in the last term. The constraint $C_\parallel$ depends on the remaining phase space variables, and is also explicitly time dependent through the background solution

$(\bar{a}, \bar{p}, \bar{p}_\phi)$; it is therefore useful to check that it is remains first class, i.e.

$$\dot{\tilde{C}}_\parallel = \left\{ \tilde{C}_\parallel, \int d^3k \; H^{S\phi} \right\} + \frac{\partial \tilde{C}_\parallel}{\partial t} = 0. \tag{2.72}$$

This is indeed the case (see Appendix A.3).

At this stage we have one first class constraint $C_\parallel$ and three configuration variables h_1, h_2, ϕ. Therefore there are two physical configuration degrees of freedom in the metric perturbation (in addition to the two graviton modes we have already discussed). We recall that this is unlike the standard cosmological perturbation theory where the starting point has only the metric and scalar field perturbations; in the model we are studying, there is also the dust field, which was fixed as the time coordinate, thereby leaving an additional physical configuration variable in the metric perturbation. We now turn to identifying two physical diffeomorphism invariant variables and their conjugate momenta. These satisfy

$$\{\mathcal{O}, \tilde{C}_\parallel\} = 0. \tag{2.73}$$

2.4.1 Diffeomorphism invariant observables

For linear perturbation we are interested in observables $\mathcal{O}$ defined by (2.73) that are linear in the phase space variables $(h_1, h_2, p_1, p_2, \tilde{\phi}, \tilde{p}_\phi)$. There are many choices. We are interested in diffeomorphism invariant canonical pairs and an expression for the physical Hamiltonian (2.71) in terms of such pairs. Let us note that $\tilde{\phi}$ is already

invariant since $\tilde{p}_\phi$ does not appear in $\tilde{C}_\parallel$. A few other elementary ones are

$$H \equiv h_1 - \frac{h_2}{\sqrt{2}}, \qquad P \equiv p_1 + \frac{p_2}{2\sqrt{2}}, \tag{2.74}$$

$$A_1 \equiv h_1 - \left(\frac{12\bar{a}^3}{\bar{p}}\right) p_1, \qquad A_2 \equiv h_2 + \left(\frac{6\bar{a}^3}{\bar{p}}\right) p_2, \tag{2.75}$$

$$B_1 = h_1 - \left(\frac{2\bar{a}^2}{\sqrt{3}\bar{p}_\phi}\right) \tilde{p}_\phi, \quad B_2 = h_2 - \left(\frac{2\sqrt{2}\bar{a}^2}{3\bar{p}_\phi}\right) \tilde{p}_\phi. \tag{2.76}$$

These may be used to construct invariant canonical pairs by taking linear combinations with coefficients that are functions of the background solution.

The first of these observables H is proportional to the Ricci curvature $R^{(3)}$ of the spatial slice. To see this we note that to linear order

$$R^{(3)} = \frac{1}{\bar{a}^4} \left(\partial_a \partial_b h^{ab} - \partial^2 h\right). \tag{2.77}$$

In the M basis in momentum space, this becomes

$$\tilde{R}^{(3)} = 4 \left(\frac{k}{\bar{a}}\right)^2 \left[\frac{1}{2\sqrt{3}\bar{a}^2} \left(h_1 - \frac{h_2}{\sqrt{2}}\right)\right] \equiv -4 \left(\frac{k}{\bar{a}}\right)^2 \psi; \tag{2.78}$$

the ψ in the last term defines the curvature perturbation used in the covariant theory. It is readily verified that a momentum conjugate to ψ is

$$P_\psi \equiv -\frac{8\bar{a}^2}{\sqrt{3}} \left(p_1 + \frac{p_2}{2\sqrt{2}}\right). \tag{2.79}$$

This satisfies

$$\{P_\psi, \tilde{C}_\parallel\} = 0, \quad \{\psi, P_\psi\} = 1. \tag{2.80}$$

A second canonical pair is found by noting that the scalar field perturbation ϕ is

diffeomorphism invariant,

$$\{\phi, \tilde{C}_{\|}\} = 0. \tag{2.81}$$

For notational convenience we define $\gamma \equiv \tilde{\phi}$. A diffeomorphism invariant variable canonically conjugate to γ is

$$P_\gamma = \tilde{p}_\phi + 2\sqrt{3}\ \frac{\bar{a}\bar{p}_\phi}{\bar{p}}\left(p_1 + \sqrt{2}p_2\right), \tag{2.82}$$

and this satisfies

$$\{P_\gamma, \tilde{C}_{\|}\} = \{P_\gamma, \psi\} = \{P_\gamma, P_\psi\} = 0, \quad \{\gamma, P_\gamma\} = 1. \tag{2.83}$$

(We note that $\tilde{p}_\phi$ is canonically conjugate to $\tilde{\phi}$, but it is not gauge invariant, hence the need to define an alternative conjugate momentum that is gauge invariant.) Although the Hamiltonian (2.71) may be written down in terms of these variables, it is more convenient to use a different set that is useful to make a comparison with the conventional perturbation theory without the dust field. For this reason we select the following diffeomorphism invariant canonical pairs. The first pair is

$$\mathcal{R} = \psi - \left(\frac{\bar{a}\bar{p}}{12\bar{p}_\phi}\right)\tilde{\phi} \tag{2.84}$$

$$P_{\mathcal{R}} = \left(\frac{48k^2\bar{a}^3}{\bar{p}}\right)\psi + \sqrt{\frac{2}{3}}\left(\frac{\bar{p}}{\bar{a}}\right)A_2, \tag{2.85}$$

and the second pair is

$$\chi = \left(\frac{\bar{a}^3}{\bar{p}_\phi}\right)\tilde{\phi}, \tag{2.86}$$

$$P_\chi = 4\bar{a}k^2\psi + \left(\frac{\sqrt{3}\bar{p}}{18\bar{a}}\right)\left(\frac{\dot{\bar{p}}_\phi}{\bar{p}_\phi} - 3\bar{H}\right)A_1 - \sqrt{\frac{2}{3}}\left(\frac{\bar{p}\dot{\bar{p}}_\phi}{3\bar{a}\bar{p}_\phi}\right)A_2 - \left(\frac{\sqrt{3}\bar{p}_\phi^2}{2\bar{a}^5}\right)B_1. \tag{2.87}$$

These satisfy

$$\{\mathcal{R}, P_\mathcal{R}\} = \{\chi, P_\chi\} = 1, \quad \{P_\mathcal{R}, P_\chi\} = \{P_\mathcal{R}, \chi\} = \{P_\chi, \mathcal{R}\} = \{\mathcal{R}, \chi\} = 0. \tag{2.88}$$

We can now write the Hamiltonian (2.71) in terms of these canonical variables. Before doing this it is convenient to fix a gauge and solve the diffeomorphism constraint $C_\parallel = 0$; since the variables are diffeomorphism invariant, their values would of course be unaffected. We choose the gauge

$$h_1 = 0. \tag{2.89}$$

This choice removes the interaction of h_1 and ϕ in the Hamiltonian (2.71), thereby simplifying it considerably. It is second class with $C_\parallel$:

$$\{h_1, C_\parallel\} = -2\bar{a}^2, \tag{2.90}$$

unless $\bar{a} = 0$. Setting $h_1 = 0$ and solving the diffeomorphism constraint for p_1,

$$p_1 = -\sqrt{2}\left(p_2 + \frac{\bar{p}}{6\bar{a}^3}h_2\right) + \frac{\sqrt{3}p_{\bar{\phi}}}{2\bar{a}^2}\tilde{\phi}, \tag{2.91}$$

gives the fully reduced theory for the gauge invariant pairs $(\mathcal{R}, P_\mathcal{R})$ and (χ, P_χ). The

final action is

$$S^{(2)}_{GF} \equiv \int dt d^3k \left[\dot{\mathcal{R}} P_{\mathcal{R}} + \dot{\chi} P_{\chi} - H^{(2)}\right], \tag{2.92}$$

where the $k-$space Hamiltonian density takes the remarkably simple form

$$H^{(2)} = \frac{1}{2\bar{a}}\left[\frac{1}{z^2}P^2_{\mathcal{R}} + k^2\left(z\mathcal{R}\right)^2\right] + \left(\frac{\bar{a}^3}{2\bar{p}^2_{\phi}}\right)P^2_{\chi} - \left(\frac{\bar{a}\bar{p}}{12\bar{p}^2_{\phi}}\right)P_{\mathcal{R}}P_{\chi}, \tag{2.93}$$

with

$$z = -\frac{12\bar{p}_{\phi}}{\bar{p}}. \tag{2.94}$$

The EOM following from this Hamiltonian are

$$\begin{aligned}
\dot{\mathcal{R}} &= \left(\frac{1}{\bar{a}z^2}\right)P_{\mathcal{R}} + \left(\frac{\bar{a}}{z\bar{p}_{\phi}}\right)P_{\chi}, && (2.95)\\
\dot{P}_{\mathcal{R}} &= -\left(\frac{k^2z^2}{\bar{a}}\right)\mathcal{R}, && (2.96)\\
\dot{\chi} &= \left(\frac{\bar{a}^3}{\bar{p}^2_{\phi}}\right)P_{\chi} + \left(\frac{\bar{a}}{z\bar{p}_{\phi}}\right)P_{\mathcal{R}} = \left(\frac{1}{\bar{H}}\right)\dot{\mathcal{R}} && (2.97)\\
\dot{P}_{\chi} &= 0 \implies P_{\chi} = C. && (2.98)
\end{aligned}$$

These lead to the second order equations

$$\begin{aligned}
\ddot{\mathcal{R}} + \left(\frac{\dot{\zeta}}{\zeta}\right)\dot{\mathcal{R}} + \left(\frac{k^2}{\bar{a}^2}\right)\mathcal{R} &= C\bar{f}(t), && (2.99)\\
\ddot{\chi} + \left(\frac{\dot{\alpha}}{\alpha}\right)\dot{\chi} &= \frac{1}{\bar{H}}\left(C\bar{f} - \frac{k^2}{\bar{a}^2}\mathcal{R}\right), && (2.100)
\end{aligned}$$

where $\zeta = \bar{a}z^2$, $\alpha = \bar{H}\zeta$ and $\bar{f}(t)$ is the following function of background solution

$$\bar{f} = \left(\frac{\bar{a}}{z\bar{p}_{\phi}}\right)^{\cdot} + \left(\frac{\dot{\zeta}}{\zeta}\right)\left(\frac{\bar{a}}{z\bar{p}_{\phi}}\right) = \frac{\dot{\bar{H}}}{\bar{a}^3\dot{\bar{\phi}}}. \tag{2.101}$$

Thus the equation for $\mathcal{R}$ resembles that obtained in the usual cosmological pertur-

bation theory, but now has a forcing term that is a function $\bar{f}$ of the background fields and $P_\chi = C$; for the choice $C = 0$ this equation is the same as that in usual cosmology. The equation for χ on the other hand is ultra-local because there is no term in it of the form $k^2\chi$, which would indicate the presence of spatial derivatives of χ; k dependence of χ therefore arises solely from the source term of (2.100). This is not surprising since we would not expect a second propagating degree of freedom starting with a theory containing pressureless dust. Indeed this is also what is obtained for perturbation theory on flat spacetime [40]. As a final comment in these equations we note that (2.100) may be rewritten using the variable

$$\tilde{\chi} \equiv \chi - \frac{\mathcal{R}}{\bar{H}}, \tag{2.102}$$

leading to

$$\ddot{\tilde{\chi}} + \left(\frac{\dot{\alpha}}{\alpha}\right)\dot{\tilde{\chi}} = \frac{1}{\alpha}\frac{d}{dt}\left[\left(\zeta\frac{\dot{\bar{H}}}{\bar{H}}\right)\mathcal{R}\right], \tag{2.103}$$

which removes the k^2 term on the r.h.s. of (2.100). This shows the ultralocality of $\tilde{\chi}$ due to the absence of the spatial derivative propagation term $k^2\tilde{\chi}$ – the same reasoning as for χ.

Let us summarize the results so far. We started with the theory of GR coupled to dust and a scalar field. This theory has four physical field degrees of freedom, of which 2 are gravitational. The Hamiltonian perturbation analysis we presented therefore must also have the same number. By fixing the dust-time gauge, one of the these four degrees of freedom manifests itself in the metric. Thus, after identifying the two graviton modes, we are left with an additional scalar mode, which as we have seen turns out to be ultralocal.

The general framework for the dust-time perturbation theory we develop has direct application to inflaton + matter cosmology. In particular, one of the perturbation

equations we derive is exactly the Mukhanov-Sasaki equation, with the difference that the time parameter in our framework refers to dust-time. This provides a direct connection with one of the standard results of covariant perturbation theory. Furthermore, the formalism we develop extends readily to matter fields in addition to dust and scalar field; the dust-time physical Hamiltonian and diffeomorphism constraints can be expanded to second order for any additional fields, and their corresponding perturbation equations derived in a manner similar to that which we display for the inflaton.

This work may also be viewed in a wider context of GR coupled to special types of matter. These include the Einstein-Aether models [53], where a dynamical vector field of timelike norm is added to the GR action. A linearized analysis of these models has been performed, with the result that the graviton modes decouple from the aether modes [54]. The other model is the so-called mimetic gravity [55, 56], where the conformal mode of the spacetime metric is encoded as a scalar field with an arbitrary potential. This extra mode in the gravitational field represents self-interacting matter with arbitrary potential [57, 58], and has been used to model inflationary and bouncing cosmologies [59]. Given these analogies, it is potentially useful to consider this work in the larger context of Einstein-Aether [60] and mimetic gravity theories. Indeed, the dust-time gauge we employ here may be considered a natural choice for all scalar-tensor theories of gravity, among which Einstein-Aether and mimetic gravity are but two examples.

2.5 Comparison with perturbation theory without dust

It is useful to compare the dust-time perturbation theory we have developed above with a similar Hamiltonian treatment of standard perturbation theory. Previously

this has been done and the salient results are the Mukhanov-Sasaki equation, the gravitational wave equation and the identification of vector modes as gauge DOF [14]. We will show that not only does our treatment reproduce these results, but it is also an improvement on [14].

Our treatment begins with the ADM Hamiltonian action of GR coupled to only a scalar field. This is eqn. (2.3) with $T = P_T = 0$. Expansion of this action about a homogeneous and isotropic background solution is of the form (2.28), with the additional expansion of the lapse function

$$N(x,t) = \bar{N}(t) + \delta N(x,t), \tag{2.104}$$

where we have taken $\bar{N}(t)$ as the lapse function of the background. The second order action changes from (2.29) to

$$\mathcal{S}^{(2)} \equiv \int d^3x dt \left[\dot{h}_{ab} p^{ab} + \dot{\phi} p_\phi - \delta N \mathcal{H}^{(1)} - \bar{N}(t) \mathcal{H}^{(2)} - \xi^a C_a^{(1)} \right], \tag{2.105}$$

where $\mathcal{H}^{(2)}$ and $C_a^{(1)}$ are exactly as given in (2.30), and

$$\begin{aligned} \mathcal{H}^{(1)} = & -\frac{1}{\bar{a}} \left\{ \left(\frac{\bar{p}}{6\bar{a}} \right) \left[\frac{1}{4} \left(\frac{\bar{p}}{6\bar{a}} \right) h + \bar{a}^2 p \right] + \partial_a \partial_b h^{ab} - \partial^2 h \right\} \\ & + \frac{\bar{p}_\phi}{\bar{a}^3} \left[p_\phi - \frac{\bar{p}_\phi}{4\bar{a}^2} h \right] + \bar{a} \left[\bar{a}^2 V'(\bar{\phi}) \phi + \frac{V(\bar{\phi})}{2} h \right]. \end{aligned} \tag{2.106}$$

We recall that $h = h_{ab} e^{ab}$ and $p = p^{ab} e_{ab}$. In the following we will take the background lapse $\bar{N}(t) = 1$. We see that this second order action has two constraints obtained by varying w.r.t. the lapse and shift perturbation $\delta N(x,t)$ and $\xi^a(x,t)$. It is worth noting that in [14] the lapse and the shift are not perturbed, and qualitative arguments are offered to explain the presence and justify the use of the first order Hamiltonian and diffeomorphism constraints. Our approach shows that these constraints appear in the second order action if the lapse and shift are perturbed. This

is an important way in which our treatment is an improvement on [14].

The second order action also displays a non-vanishing Hamiltonian $\bar{N}(t)\mathcal{H}^{(2)}$, where $\bar{N}(t)$ is a fixed background function that cannot be varied in the second order action; it is of course varied in the zeroth order action to give the background Hamiltonian constraint $\bar{\mathcal{H}} = 0$. Thus, in comparison to the dust-time gauge theory, we have the additional constraint $\mathcal{H}^{(1)} = 0$. In momentum space, in the basis (h_I, p^I) (2.41), this is expanded as

$$\begin{aligned}\tilde{\mathcal{H}}^{(1)} &= -\frac{1}{\bar{a}}\left\{\left(\frac{\bar{p}}{6\bar{a}}\right)\left[\frac{1}{4}\left(\frac{\bar{p}}{6\bar{a}}\right)\tilde{h} + \bar{a}^2\tilde{p}\right] - k_a k_b \tilde{h}^{ab} + k^2\tilde{h}\right\} \\ &\quad + \frac{\bar{p}_\phi}{\bar{a}^3}\left[\tilde{p}_\phi - \frac{\bar{p}_\phi}{4\bar{a}^2}\tilde{h}\right] + \bar{a}\left[\bar{a}^2 V'(\bar{\phi})\tilde{\phi} + \frac{V(\bar{\phi})}{2}\tilde{h}\right] \qquad (2.107a) \\ &= -\frac{\sqrt{3}}{\bar{a}}\left\{\left(\frac{\bar{p}}{6\bar{a}}\right)\left[\frac{1}{4}\left(\frac{\bar{p}}{6\bar{a}}\right)h_1 + \bar{a}^2 p_1\right] + \frac{\sqrt{2}k^2}{3}\left[\sqrt{2}h_1 - h_2\right]\right\} \\ &\quad + \frac{\bar{p}_\phi}{\bar{a}^3}\left[\tilde{p}_\phi - \frac{\sqrt{3}\bar{p}_\phi}{4\bar{a}^2}h_1\right] + \bar{a}\left[\bar{a}^2 V'(\bar{\phi})\tilde{\phi} + \frac{\sqrt{3}V(\bar{\phi})}{2}h_1\right]. \qquad (2.107b)\end{aligned}$$

It is important to note that $\tilde{\mathcal{H}}^{(1)}$ is a function of only the scalar metric modes h_1 and h_2 and their conjugate momenta p_1 and p_2, in addition to scalar field perturbations $(\tilde{\phi}, \tilde{p}_\phi)$ – the graviton modes appear only in $\tilde{\mathcal{H}}^{(2)}$. We will additionally point out that [14] uses a scale factor dependent basis to decompose the matrix perturbations and this results in a symplectic term that includes time derivatives of the basis elements. Thus, our choice to use a time-independent basis that leads to a preservation of the symplectic structure (2.41), is an improvement on [14].

After solving the transverse parts of the diffeomorphism constraints and removing the vector modes as before, only the parallel component of the constraint $C_\parallel = 0$ (2.64) remains. The momentum space action for the scalar perturbations (h_1, h_2, ϕ) becomes

$$S^{S\phi} \equiv \int dt d^3k \left[p_1\dot{h}_1 + p_2\dot{h}_2 + \tilde{p}_\phi\dot{\tilde{\phi}} - H^{S\phi} - \delta\tilde{N}\tilde{\mathcal{H}}^{(1)} - \tilde{\xi}_\parallel\tilde{C}^{(1)}_\parallel\right] \qquad (2.108)$$

where $H^{S\phi}$ is given in (2.71), and $\delta\tilde{N}(k,t)$ is the lapse perturbation in momentum space. We now note that the constraints obtained by varying this action w.r.t. $\tilde{\xi}_{\parallel}$ and $\delta\tilde{N}(k,t)$ are first class. We have already verified that $C_{\parallel}$ is first class (Appendix A.3). We also find that

$$\frac{d}{dt}\,\tilde{\mathcal{H}}^{(1)} = \{\tilde{\mathcal{H}}^{(1)}, H^{S\phi}\} + \frac{\partial}{\partial t}\tilde{\mathcal{H}}^{(1)} = \tilde{C}_{\parallel} = 0, \tag{2.109}$$

and

$$\{\tilde{\mathcal{H}}^{(1)}, \tilde{C}_{\parallel}\} = -\bar{\mathcal{H}} = 0, \tag{2.110}$$

where the last equality follows from the background Hamiltonian constraint $\bar{\mathcal{H}} = 0$; recall that this is the theory without dust. This is a satisfying structure demonstrating explicitly that the second order perturbed system is first class. It also shows that, of the three scalar perturbation modes $(h_1, h_2, \tilde{\phi})$, only one is a physical degree of freedom (due to the two constraints $\tilde{\mathcal{H}}^{(1)} = 0$ and $\tilde{C}_{\parallel} = 0$). We can now proceed to obtain gauge invariant observables, i.e. those that Poisson commute with $\tilde{C}_{\parallel}$ and $\tilde{\mathcal{H}}^{(1)}$. Unlike the case with dust, only one canonical pair of gauge invariant variables is required (due to the presence of two constraints instead of one). We note that our method of deriving gauge invariant variables is different from the one used in [14]; there the author uses Hamilton-Jacobi like equations to arrive at the gauge invariant variables.

2.5.1 Gauge invariant variables

Gauge invariant variables $\mathcal{O}$ must now satisfy

$$\{\mathcal{O}, \tilde{\mathcal{H}}^{(1)}\} = \{\mathcal{O}, \tilde{C}_{\parallel}\} = 0. \tag{2.111}$$

We have already noted that the curvature perturbation

$$\psi = -\frac{1}{2\sqrt{3}\bar{a}^2}\left(h_1 - \frac{h_2}{\sqrt{2}}\right) \tag{2.112}$$

defined in (2.78) satisfies $\left\{\psi, C_{\|}\right\} = 0$. However

$$\left\{\psi, \tilde{\mathcal{H}}^{(1)}\right\} = \frac{\bar{p}}{12\bar{a}^2} \neq 0, \tag{2.113}$$

therefore ψ is not invariant under the second constraint, and therefore not fully gauge invariant. By noting that

$$\left\{\tilde{\phi}, \tilde{\mathcal{H}}^{(1)}\right\} = \frac{\bar{p}_\phi}{\bar{a}^3}, \tag{2.114}$$

we observe that the linear combination

$$\mathcal{R} \equiv \psi - \left(\frac{\bar{a}\bar{p}}{12\bar{p}_\phi}\right)\ \tilde{\phi}, \tag{2.115}$$

satisfies

$$\left\{\mathcal{R}, \tilde{\mathcal{H}}^{(1)}\right\} = 0, \quad \left\{\mathcal{R}, \tilde{C}_{\|}\right\} = 0. \tag{2.116}$$

This $\mathcal{R}$ is exactly the same variable we used for the dust case. We have now learned that it is also invariant under the transformation generated by $\mathcal{H}^{(1)}$. Similarly we note that its conjugate momentum defined in (2.85) satisfies

$$\{\mathcal{R}, P_{\mathcal{R}}\} = 1, \quad \left\{P_{\mathcal{R}}, \tilde{\mathcal{H}}^{(1)}\right\} = 0, \quad \left\{P_{\mathcal{R}}, \tilde{C}_{\|}\right\} = 0. \tag{2.117}$$

Thus the canonically conjugate pair $(\mathcal{R}, P_{\mathcal{R}})$ are fully gauge invariant to this order.

We note also that any scaled variables of the type $(g\mathcal{R}, P_{\mathcal{R}}/g)$, where $g = g(\bar{a}, \bar{p}, \bar{\phi}, \bar{p}_\phi)$

is an arbitrary function of the background variables, are also gauge invariant (since the fixed background does not participate in the Poisson bracket for the perturbations). The choice

$$g = -\frac{12\bar{p}_\phi}{\bar{p}} \equiv z \tag{2.118}$$

gives the Mukhanov-Sasaki (MS) variable

$$\nu \equiv -\left(\frac{12\bar{p}_\phi}{\bar{p}}\right)\mathcal{R} = \left(\frac{\bar{a}\dot{\bar{\phi}}}{\bar{H}}\right)\mathcal{R} = \bar{a}\left(\tilde{\phi} + \frac{\dot{\bar{\phi}}}{\bar{H}}\,\psi\right), \tag{2.119}$$

where the second equality follows from the background equations (2.23).

2.5.2 Gauge fixed action

As the last step, we fix two gauges corresponding to the two first class constraints $\tilde{\mathcal{H}}^{(1)} = 0$ and $\tilde{C}_\parallel = 0$, and solve these constraints strongly to obtain the final canonical action from (2.108) for the remaining unconstrained gauge invariant physical degrees of freedom. The final action will be a functional of the canonical pair $\mathcal{R}, P_\mathcal{R}$. This may then be recast in terms of the MS variable ν and its conjugate momentum P_ν.

We set the gauge conditions

$$\tilde{\phi} = 0, \quad h_1 = 0. \tag{2.120}$$

These satisfy

$$\{\tilde{\phi}, \tilde{\mathcal{H}}^{(1)}\} = \frac{\bar{p}_\phi}{\bar{a}^3}; \quad \{h_1, \tilde{C}_\parallel\} = -2\bar{a}^2, \tag{2.121}$$

therefore the constraints and gauge conditions form second class pairs. Solving the

constraints for p_1 and $\tilde{p}_\phi$ gives

$$p_1 = -\frac{\sqrt{2}}{\bar{a}^2}\left[\left(\frac{\bar{p}}{6\bar{a}}\right)h_2 + \bar{a}^2 p_2\right] \tag{2.122}$$

$$\tilde{p}_\phi = -\frac{1}{\sqrt{6}\bar{p}_\phi}\left(\frac{\bar{p}^2}{6}h_2 + 2\bar{a}^2k^2h_2 + \bar{a}^3\bar{p}p_2\right). \tag{2.123}$$

In this gauge, the invariant variables $\mathcal{R}$ and $P_\mathcal{R}$ become

$$\mathcal{R} = \frac{1}{2\sqrt{6}\bar{a}^2}\ h_2, \quad P_\mathcal{R} = \sqrt{\frac{2}{3}}\left(\frac{\bar{p}}{\bar{a}} + \frac{12\bar{a}}{\bar{p}}k^2\right)\ h_2 + 2\sqrt{6}\bar{a}^2\ p_2. \tag{2.124}$$

Substituting the gauge conditions and solutions of the constraints into the action (2.108), and expressing variables in terms of $\mathcal{R}$ and $P_\mathcal{R}$, gives

$$S^S_{GF} \equiv \int dtd^3k\left[\dot{\mathcal{R}}P_\mathcal{R} - H^S_{GF}\right], \tag{2.125}$$

where

$$H^S_{GF} = \frac{1}{2\bar{a}}\left[\frac{1}{z^2}P^2_\mathcal{R} + k^2\left(z\mathcal{R}\right)^2\right]. \tag{2.126}$$

This is the same as the action for the dust-time case (2.93), but with $\chi = P_\chi = 0$.

As the last step in comparison with standard perturbation theory, we derive from this action the MS equation. We noted the definition of the MS variable ν in (2.119). The conjugate momentum is $P_\nu = P_\mathcal{R}/z$. The action (2.125) transforms to

$$S^S_{GF} = \int dtd^3k\left[P_\nu\dot{\nu} - H_\nu\right], \tag{2.127}$$

with

$$H_\nu = \frac{1}{2\bar{a}}\left(P^2_\nu + k^2\nu^2\right) + \frac{\dot{z}}{z}\nu P_\nu. \tag{2.128}$$

This gives the equation of motion

$$\ddot{\nu} + \bar{H}\dot{\nu} + \left(\frac{k^2}{\bar{a}^2} - \frac{\ddot{z}}{z} - \bar{H}\frac{\dot{z}}{z}\right)\nu = 0. \tag{2.129}$$

In conformal time $dt = \bar{a}d\tau$ this becomes the familiar MS equation

$$\nu'' + \left(k^2 - \frac{z''}{z}\right)\nu = 0. \tag{2.130}$$

Here a prime indicates a derivative with respect to conformal time.

To summarize this section, we have seen that the gauge invariant canonical variables $(\mathcal{R}, P_{\mathcal{R}})$ that we used in the dust-time setting are also invariant under the local time transformation generated by the additional constraint $\tilde{\mathcal{H}}^{(1)}$. This is in fact why we used these for the dust-time case, rather than variables that are only invariant under the diffeomorphism constraint $\tilde{C}_{\|}$. There are many other possibilities for canonical pairs invariant under only the latter, but these do not provide a direct connection with the standard perturbation theory.

2.6 Summary and discussion

We presented the Hamiltonian theory of cosmological perturbations for GR coupled to dust and a scalar field, in the dust-time gauge. The analysis demonstrates the following features: (i) the graviton modes decouple from other degrees of freedom and their EOM are unchanged, (ii) the vector modes are removed by gauge fixing in the same way as for flat space perturbation theory [40], (iii) there remain two coupled scalar modes, one of which $(\mathcal{R})$ satisfies a wave equation with a source, and the other (χ) satisfies an ultra-local equation with a source dependent on k; these two equations generalize the usual perturbation equations.

We also applied the same Hamiltonian decomposition, using the canonical vari-

ables (h_I, p^I) to the standard cosmological perturbation theory. This differs from the Hamiltonian formalism presented in [14] in several respects. These include our inclusion of the lapse and shift perturbations, use of a scale-factor-independent basis for decomposing metric perturbations, a demonstration that the perturbed constraints are first class, a calculation of the constraint algebra, and finally a step-by-step application of the reduction to physical degrees of freedom using the Dirac procedure. Thus our work provides a more detailed view of Hamiltonian perturbation theory for cosmology, in addition to its extension to the dust-time gauge.

Our final equations in the dust-time gauge (2.99) and (2.100) lead ultimately to the MS equation with an external forcing term dependent on the background solution, and an additional ultra-local equation for the field χ. These may have observational consequences which we intend to explore in future work. The special solution $P_\chi = 0$ removes the source term, and so leads to exactly the MS equations plus the equation for χ. However this case contributes no additional energy density since the terms proportional to P_χ in the Hamiltonian density (2.93) vanish for this case. Therefore the general case $P_\chi \neq 0$ is more interesting for exploring cosmological consequences.

Finally recall that in the dust-time gauge the metric acquires an additional DOF χ that represents dust. Therefore it may be possible to express χ as an entropy perturbation, which measures how misaligned the perturbations in the energy densities of the different fields are.

Chapter 3

Ising-like models on Euclidean black holes

3.1 Introduction

Spin models are useful tools in studying interacting degrees of freedom in thermal equilibrium. This is primarily due to two reasons. Firstly due to their simplicity spin models can be solved either exactly or approximately by analytical or numerical techniques. Secondly if the simple spin model shares some global features (such as symmetries of the Hamiltonian and the number of spatial dimensions) with a real system (such as a lattice of interacting atoms) then some results of the spin model match the behaviour of the real system [61]. Two well-studied spin systems are the Ising and Blume-Capel models [62, 63].

The Blume-Capel model is a spin-1 generalization of the Ising model with an additional self-interaction (or "mass" term) with Hamiltonian $H = -J \sum_{i,j;nn} s_i s_j + K \sum_i s_i^2$ where nn denotes that the sum is over nearest neighbors. It has richer physics than the Ising model; in two dimensions, if $K > 2J$ there is no phase

transition; if $K \leq 2J$ then the ratio $\frac{K}{2J}$ not only determines whether the phase transition is continuous (second order) or discontinuous (first order) but also fixes the critical temperature. The Blume-Capel model has been rigorously investigated using not only analytical techniques - such as the renormalization group (RG) [64] - but by numerical Monte-Carlo (MC) simulations also [65].

MC studies of the Ising and Blume-Capel models typically use periodic boundary conditions. Due to this choice the lattice has the topology of a 2 torus. There has been a growing interest in investigating the effects of using different topologies such as the 2 sphere [66] and a random topology [67]. This interest arises from multiple areas, including discrete models of quantum gravity, condensed matter physics and the statistical mechanics of complex networks such as the internet [68]. There is also a rich literature on investigating the effects of geometric curvature on the thermodynamic properties of spins. For example it is known that the Ising model on a 2d hyperbolic plane with free boundary conditions exhibits multiple phase transitions [69]. This model is expected to have applications to quantum information [70].

Our goal is to generalize the Ising and Blume-Capel models to Schwarzschild and AdS black hole backgrounds and study their physical content. This is of interest for several reasons: black hole backgrounds are inhomogeneous (i.e. have explicit dependence on radial location) and thus provide an interesting platform to generalize spin-models; Euclidean versions of black hole metrics are used in attempts to understand black hole thermodynamics [4, 35]; black holes metrics are considered as thermal backgrounds for quantum field theory where the radius of Wick-rotated time is proportional to black hole mass; the case with a cosmological constant provides a generalization of spin models where the connection between metric parameters and temperature is more involved [36]. We review these features before constructing the models.

Our approach is to start with a scalar field action on a general form of a Euclidean

black hole background, discretize the action on a suitably defined lattice, and then restrict the scalar field to take on spin values. This process naturally introduces a point interaction from the scalar field mass term, and nearest neighbour interactions from a finite difference of the kinetic term.

In Section 3.2 we review the MC scheme [71] and the correspondence between Euclidean time periodicity and inverse temperature [23, 24]; in Section 3.3 we review the construction of the Euclidean black holes [2, 35, 36]; in Section 3.4 we define the spin-models; in Section 3.5 we describe and present the MC calculations for the spin-1/2 and spin-1 models, followed by a summary of the work and possible extensions.

3.2 Background

3.2.1 Monte-Carlo scheme

In this section we briefly describe the Monte-Carlo scheme [71]; the reader can consult references [72, 73] for further details.

Consider the multidimensional integral

$$S = \int_{\mathcal{V}} dx_1 ... dx_d f(x_1, ...x_d), \tag{3.1}$$

where $\mathcal{V}$ is the region of the integration, the volume of which will be set to 1 for simplicity. Hereafter we will use $\mathbf{x}$ to denote a point in the integration region instead of $(x_1, ...x_d)$. The MC scheme

1. Randomly selects a point in $\mathcal{V}$,

2. Evaluates the function's value at that point,

3. Repeats the first two steps M times to estimate S as

$$S \sim \frac{1}{M} \sum_{i=1}^{M} f_i \tag{3.2}$$

$$=< f > . \tag{3.3}$$

The efficiency of this scheme is

$$\triangle S \sim \frac{1}{M^{\frac{1}{2}}}. \tag{3.4}$$

Given large M the estimated value of S converges to the actual value. This is called convergence. Also note that the efficiency is independent of dimension. This is unlike other integration schemes: for example the trapezoidal scheme has an efficiency

$$\triangle S \sim \frac{1}{M^{\frac{2}{d}}}. \tag{3.5}$$

In selecting points in $\mathcal{V}$ at which the function is evaluated one can choose a uniform or a non-uniform distribution. A way to do the latter was proposed by Metropolis and collaborators [74] and their method may be viewed as a Markov process. The Metropolis algorithm requires detailed balance, the basic idea of which is that in equilibrium the value of the non-uniform distribution function $p(\mathbf{x})$ at different points in $\mathcal{V}$ is related by

$$T(\mathbf{x} \rightarrow \mathbf{x}')p(\mathbf{x}) = T(\mathbf{x}' \rightarrow \mathbf{x})p(\mathbf{x}') \tag{3.6}$$

where $\mathbf{x}$ is the old point, $\mathbf{x}'$ is the new point, and T is the transition rate between the two. The transition $T(\mathbf{x} \rightarrow \mathbf{x}')$ is accepted if

$$\frac{T(\mathbf{x} \rightarrow \mathbf{x}')}{T(\mathbf{x}' \rightarrow \mathbf{x})} = \frac{p(\mathbf{x}')}{p(\mathbf{x})} \geq \text{rand}[0, 1]. \tag{3.7}$$

Therefore the new points in $\mathcal{V}$ are not selected randomly; rather they are selected following a Markov chain, a process that maximizes $p(\mathbf{x})$.

This discussion can be applied to multidimensional sums also, which (as will be shown later) are what we compute.

3.2.2 Euclidean time periodicity and temperature

In this section we investigate the relationship between Euclidean time periodicity and inverse temperature [23, 24]. Consider a particle that evolves from position q at time $t = 0$ to position q' at time $t = T$. The quantum transition amplitude is

$$\begin{aligned} F(q', T; q, 0) &= \langle q', T | q, 0 \rangle \\ &= \langle q' | \, e^{-iT\hat{H}} \, | q \rangle \, . \end{aligned} \tag{3.8}$$

Let's now impose Euclidean time compactification i.e the condition for the particle to return to its original position in Euclidean time β; hence β is Euclidean time periodicity. The resultant Euclidean transition amplitude is

$$F(q, -i\beta; q, 0) = \langle q | \, e^{-\beta\hat{H}} \, | q \rangle \, . \tag{3.9}$$

We will use this result shortly.

Consider now the quantum partition function of a system at temperature β^{-1}

$$Z(\beta) = \mathrm{Tr} \left(e^{-\beta\hat{H}} \right) . \tag{3.10}$$

One may evaluate the trace using the position basis

$$Z(\beta) = \sum_q \langle q | \, e^{-\beta\hat{H}} \, | q \rangle \, . \tag{3.11}$$

Note that the summand in the right hand side of the equation above is the transition

amplitude of a particle to return to its original position in Euclidean time β (3.9). Therefore (3.11) may be rewritten in the form

$$Z(\beta) = \sum_q F(q, -i\beta; q, 0) \tag{3.12}$$

which indicates a correspondence between Euclidean time periodicity and inverse temperature.

Let's express the right hand side of (3.12) as a path integral. We begin with the transition amplitude (3.8) expressed as a path integral:

$$F(q', T; q, 0) = \int D\bar{q}\ \exp(iI), \qquad I = \int_0^T dt L\left(\bar{q}, \frac{d\bar{q}}{dt}\right). \tag{3.13}$$

Here $\int D\bar{q}$ integrates over all paths the particle can take between the starting and finishing configurations, I is the Lorentzian action and L is the Lagrangian. Consequently the path integral of a particle to return to its original position in imaginary time β is

$$F(q, -i\beta; q, 0) = \int D\bar{q}\ \exp\left[i \int_0^{-i\beta} dt\, L\left(\bar{q}, \frac{d\bar{q}}{dt}\right)\right], \tag{3.14}$$

where $\int D\bar{q}$ is now over all paths that are periodic in imaginary time β. After a Wick rotation

$$t = -i\tau \tag{3.15}$$

the path integral is

$$F(q, -i\beta; q, 0) = \int D\bar{q}\ \exp\left[\int_0^\beta d\tau L\left(\bar{q}, \frac{d\bar{q}}{d\tau}\right)\right] \tag{3.16}$$

$$\equiv \int D\bar{q}\ \exp\left[-\int_0^\beta d\tau\, L_E\left(\bar{q}, \frac{d\bar{q}}{d\tau}\right)\right], \tag{3.17}$$

where L_E is the Euclidean Lagrangian. The equation above may be rewritten in terms of the Euclidean action I_E

$$F(q, -i\beta; q, 0) = \int D\bar{q} \, \exp\left(-I_E\right), \qquad I_E = \int_0^\beta d\tau \, L_E \left(\bar{q}, \frac{d\bar{q}}{d\tau}\right). \tag{3.18}$$

Now we will demonstrate the relationship between L and L_E through an example: we will consider a particle in an arbitrary potential, the Lagrangian for which is:

$$L = \left(\frac{dx}{dt}\right)^2 - V(x). \tag{3.19}$$

Wick rotation yields the Euclidean Lagrangian:

$$\begin{aligned} L &= -\left(\frac{dx}{d\tau}\right)^2 - V(x) \\ &= -\left[\left(\frac{dx}{d\tau}\right)^2 + V(x)\right] \\ &= -L_E. \end{aligned} \tag{3.20}$$

Since τ is like a space dimension, the Euclidean Lagrangian is like the Hamiltonian density of a field in one space dimension and the Euclidean action (3.18) is like a Hamiltonian. Therefore upon Wick rotation the action resembles a Hamiltonian for a system in one extra space dimension.

3.3 Euclidean black holes

As a prelude to defining spins models on Euclidean black hole backgrounds, in this section we summarize the main aspects of the metrics we will be using.

The Schwarzschild black hole metric in its original form is

$$ds^2 = -\left(1 - \frac{2M}{r}\right) dt^2 + \left(1 - \frac{2M}{r}\right)^{-1} dr^2 + r^2 d\Omega^2, \tag{3.21}$$

in the coordinates (t, r, θ, ϕ); it has a coordinate singularity at the horizon $r = 2M$ and a curvature singularity at $r = 0$. In the Kruskal-Szekeres (KS) coordinates (T, X, θ, ϕ) defined as

$$-T^2 + X^2 = \left(\frac{r}{2M} - 1\right) \exp\left(-\frac{r}{2M}\right) \tag{3.22}$$

$$\frac{T + X}{T - X} = \exp\left(\frac{t}{2M}\right) \tag{3.23}$$

the geometry is

$$ds^2 = \frac{32M^3}{r} \exp\left(-\frac{r}{2M}\right) \left(-dT^2 + dX^2\right) + r^2 d\Omega^2. \tag{3.24}$$

In these coordinates the event horizon $r = 2M$ is given by $T = \pm X$, and the singularity at $r = 0$ is $T^2 - X^2 = 1$. The KS coordinates provide a global extension of the original Schwarzschild metric, and are best suited to understanding its Euclidean version.

The Euclidean KS metric is defined by the Wick rotation $Y = iT$

$$ds^2 = \frac{32M^3}{r} \exp\left(-\frac{r}{2M}\right) \left(dY^2 + dX^2\right) + r^2 d\Omega^2, \tag{3.25}$$

where now

$$Y^2 + X^2 = \left(\frac{r}{2M} - 1\right) \exp\left(-\frac{r}{2M}\right) \tag{3.26}$$

$$\frac{-iY + X}{-iY - X} = \exp\left(\frac{t}{2M}\right). \tag{3.27}$$

This rotated metric is singularity free since $r = 0$ now corresponds to $Y^2 + X^2 = -1$ which has no solution; the horizon $r = 2M$ corresponds to $Y^2 + X^2 = 0$, which is the origin of (Y, X) plane. Thus, the Euclidean Schwarzschild geometry is singularity free and the interior of the Lorentzian Schwarzschild metric ($r < 2M$) is absent. The coordinates (Y, X) cover the entire manifold of a Euclidean Schwarzschild geometry. Finally to derive the temperature of Euclidean Schwarzschild we Wick-rotate the original time coordinate $\tau = it$ under which (3.27) becomes

$$\begin{aligned} \exp\left(\frac{-i\tau}{2M}\right) &= \frac{-iY + X}{-iY - X}, \quad \text{Use } z = X + iY, \\ &= \frac{z}{-z^*}, \quad \text{Substitute } z = re^{i\theta} \text{ where } \theta = [0, 2\pi), \\ &= \exp(-2i\theta) \implies \tau = 4M\theta. \end{aligned} \tag{3.28}$$

Therefore Euclidean time τ has periodicity $8\pi M$ and Euclidean Schwarzschild has a global temperature $(8\pi M)^{-1}$.

Before proceeding we will note that for Euclidean backgrounds, such as Euclidean Schwarzschild, there is an additional notion of local temperature. For this discussion consider a Euclidean background defined by the metric

$$ds^2 = u(r)^2 d\tau^2 + v(r)^2 dr^2 + w(r)^2 d\Omega^2 \tag{3.29}$$

and for this space to have a global temperature T. Local temperature is defined as

$$\begin{aligned} T_r &= \sqrt{\frac{1}{g_{00}}}\, T \\ &= \left(\frac{1}{u}\right) T. \end{aligned} \tag{3.30}$$

We do not consider local temperature in our work. This is because the standard Ising and Blume-Capel models are defined in terms of global temperatures and our goal is to generalize these models to Schwarzschild and AdS black hole backgrounds.

Hence using global temperature is a natural choice.

Having obtained the Euclidean Schwarzschild geometry in the KS coordinates, we now see that the same result is obtained in the original coordinates by simply restricting the radial coordinate to $r \in [2M, \infty)$, with $\tau = it$.

The near-horizon metric is obtained by setting $r = 2M + \nu$; then for $\nu \ll 1$ the $\tau - \nu$ part of the metric is

$$ds^2 = \frac{2M}{\nu} d\nu^2 + \frac{\nu}{2M} d\tau^2; \tag{3.31}$$

defining $d\rho^2 = (2M/\nu) d\nu^2$ gives

$$ds^2 = d\rho^2 + \left(\frac{\rho}{4M}\right)^2 d\tau^2. \tag{3.32}$$

The final observation is that absence of a conical singularity at $\rho = 0$ requires $\tau/4M \in [0, 2\pi)$.

This procedure is readily generalized [2] for obtaining a regular Euclidean black hole geometry starting from the $d-$dimensional metric

$$ds^2 = -F(r) dt^2 + F(r)^{-1} dr^2 + r^2 d\Omega_{d-2}{}^2, \tag{3.33}$$

where $F(r)$ is a one to one function such that there is an $r_0 \in [0, \infty)$ such that $F(r_0) = 0$ (the horizon), $F'(r_0) > 0$ and $\lim_{r \to 0} F(r) = \infty$ (the singularity). Then, the Wick rotation $\tau = it$, the restriction $r \in [r_0, \infty)$ and the coordinate transformation

$$\rho(r) = \beta_0 \sqrt{F(r)}, \qquad \beta_0 = \frac{2}{F'(r_0)} \tag{3.34}$$

gives the metric

$$ds^2 = \left(\frac{\rho}{\beta_0}\right)^2 d\tau^2 + \left(\frac{2}{\beta_0 F'(r)}\right)^2 d\rho^2 + \ r^2(\rho) \ d\Omega_{d-2}{}^2, \tag{3.35}$$

where $\tau \in (-\infty, \infty)$ and $\rho \in [0, \lim_{r\to\infty} \rho(r)]$. The near-horizon $r \approx r_0$ metric is

$$ds^2 = d\rho^2 + \left(\frac{\rho}{\beta_0}\right)^2 d\tau^2 + r^2(\rho) d\Omega_{d-2}{}^2. \tag{3.36}$$

Thus the $\tau - \rho$ part of the metric is flat space with no conical singularity provided $\tau\beta_0{}^{-1}$ is an angular coordinate with period 2π; this corresponds to τ having periodicity β

$$\tau \in [0, \beta), \quad \beta = 2\pi\beta_0. \tag{3.37}$$

The inverse of the Euclidean time periodicity is the natural temperature of the spacetime

$$T = (2\pi\beta_0)^{-1}. \tag{3.38}$$

In summary, we will use the metric (3.35) with the periodically identified τ as the background for defining spin models, with the function

$$F(r) = 1 - \frac{2M}{r^{d-3}} + \left(\frac{r}{L}\right)^2; \tag{3.39}$$

this is the AdS black hole in d spacetime dimensions where the scale L is related to d and the cosmological constant by $\Lambda = -(d-1)(d-2)/(2L^2)$. The cases we consider are 4d Schwarzschild ($L \to \infty$) and Schwarzschild AdS in 4d and 5d.

The temperature-mass relation for the 4d Schwarzschild case is $T = (4\pi r_0)^{-1} = (8\pi M)^{-1}$. However for the 4d AdS case it is

$$T = \frac{3r_0{}^2 + L^2}{4\pi r_0 L^2}; \quad M = \frac{r_0}{2}\left[1 + \left(\frac{r_0}{L}\right)^2\right]. \tag{3.40}$$

$T(M)$ has a minimum at $T_{min} = \sqrt{3}/(2\pi L)$ at mass $M_* = 2L/(3\sqrt{3})$ (Figure 3.1)

and horizon radius $r_{0*} = L/\sqrt{3}$; $T > T_{\rm min}$ corresponds to either a small or a large mass black hole. A similar treatment applies to 5d Schwarzschild AdS also: here

$$T = \frac{2{r_0}^2 + L^2}{2\pi r_0 L^2}; \quad M = \frac{{r_0}^2}{2}\left[1 + \left(\frac{r_0}{L}\right)^2\right], \tag{3.41}$$

$T(M)$ has a minimum at $T_{min} = \sqrt{2}/(\pi L)$ at mass $M_* = 3L^2/8$. This discussion will be relevant below where we discuss phase transitions in spin models as functions of T and M.

3.4 Spin models on black holes

Spin models on Euclidean black hole backgrounds may be defined by starting with the Euclidean action of a scalar field on the metrics reviewed in the last section, discretizing the action, and then restricting the scalar field variable to take discrete values, ± 1 for Ising, and $0, \pm 1$ for Blume-Capel models. The d-dimensional Euclidean action for a massive scalar field on a background metric g_{ab} is

$$I_E[\Phi] = \frac{1}{2}\int d^d x\, \sqrt{g}\left(g^{ab}\partial_a\Phi\partial_b\Phi + \mu^2\Phi^2\right). \tag{3.42}$$

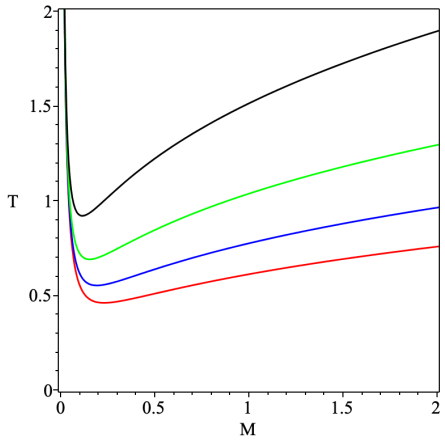

Figure 3.1: Temperature-Mass relation for 4d Euclidean AdS-Schwarzschild for $L = 0.3, 0.4, 0.5, 0.6$ (top to bottom).

The Euclidean black hole metrics (3.35) have the form

$$ds^2 = u(\rho)d\tau^2 + v(\rho)d\rho^2 + w(\rho)d\Omega_{d-2}{}^2. \tag{3.43}$$

We consider only the $\tau - \rho$ plane since the sphere is not relevant for the black hole properties of interest. Therefore the scalar field we consider is $\Phi \equiv \Phi(\tau, \rho)$ with the Euclidean time periodicity $\Phi(0, \rho) = \Phi(\beta, \rho)$. With these assumptions the Euclidean action reduces to

$$\begin{aligned} I_E[\Phi] &= \frac{A_{d-2}}{2}\int_0^\beta \int_0^{\rho_0} d\tau d\rho \sqrt{w^{d-2}} \\ &\quad \cdot \left(\sqrt{\frac{v}{u}}\dot{\Phi}^2 + \sqrt{\frac{u}{v}}\Phi'^2 + \mu^2\sqrt{uv}\Phi^2\right) \end{aligned} \tag{3.44}$$

where A_{d-2} is the area of S^{d-2} and dots and primes denote partial derivatives with respect to τ and ρ; the ρ integration is restricted to a finite value ρ_0 to define a discrete model on a finite lattice. The object of interest is the partition function

$$Z = \int D\Phi \exp\left(-I_E[\Phi]\right) \tag{3.45}$$

where $D\Phi$ integrates over all possible field configurations that have periodicity β in imaginary time.

3.4.1 Discretization

Consider the $\tau - \rho$ plane as an $N_\beta \times N_\rho$ lattice with spacing

$$\epsilon = \frac{\beta}{N_\beta} = \frac{\rho_0}{N_\rho}. \tag{3.46}$$

Through β the lattice spacing depends on the metric parameters M and Λ, and a

simple discretization is given by

$$\begin{aligned}
&\tau \to \tau_m = m\epsilon, \qquad \rho \to \rho_n = n\epsilon; \\
&f(\tau,\rho) \to f_{m,n}, \\
&\dot{f} \to \frac{f_{m+1,n} - f_{m,n}}{\epsilon}, \\
&f' \to \frac{f_{m,n+1} - f_{m,n}}{\epsilon}.
\end{aligned} \tag{3.47}$$

Lastly, the scalar field values are restricted to the set

$$\Phi = \{-s,\, -s+1,\, ...\, s-1,\, s\} \times s^{-1}, \tag{3.48}$$

where s is a half integer, so that the values of Φ are rational numbers in the interval $[-1, 1]$. With this discretization the Euclidean action becomes the sum

$$\begin{aligned}
I_E\left[\Phi\right] =& A_{d-2} \sum_{m,n=1}^{N_\beta, N_\rho} \Bigg\{ - \Phi_{m,n} \left[\sqrt{\frac{v_n {w_n}^{d-2}}{u_n}}\, \Phi_{m+1,n} + \sqrt{\frac{u_n {w_n}^{d-2}}{v_n}}\, \Phi_{m,n+1} \right] \\
&+ {\Phi_{m,n}}^2 \Bigg[\sqrt{\frac{v_n {w_n}^{d-2}}{u_n}} + \frac{1}{2} \left(\sqrt{\frac{u_n {w_n}^{d-2}}{v_n}} + \sqrt{\frac{u_{n-1} {w_{n-1}}^{d-2}}{v_{n-1}}} \right) \\
&+ \frac{\mu^2 \epsilon^2}{2} \sqrt{u_n v_n {w_n}^{d-2}} \Bigg] \Bigg\}.
\end{aligned} \tag{3.49}$$

This is the desired "spin" model. It is apparent that the coupling "constants" vary across the lattice and depend on the metric functions from point to point; the first line contains metric function-weighted nearest neighbour interactions in the τ and ρ directions, the second line represents spin self-interactions which are weighted by the metric functions, and the third line contains self-interactions that are weighted by the determinant of the metric, scalar field mass and ϵ^2 (this factor cancels out for the remaining terms); the choice $s = 1/2$ or $s = 1$ gives an Ising or Blume Capel like

model on a Euclidean black hole background respectively; the self interaction terms only affect statistical averages in the latter case.

For the 4d Euclidean AdS-Schwarzschild geometry the metric functions are

$$u(\rho) = \left[\left(\frac{3{r_0}^2 + L^2}{2r_0L^2}\right)\rho\right]^2 \tag{3.50}$$

$$v(\rho) = \left[\left(\frac{3{r_0}^2 + L^2}{2r_0L^2}\right)\left(\frac{L^2\, r^2(\rho)}{r^3(\rho) + ML^2}\right)\right]^2 \tag{3.51}$$

$$w(\rho) = r^2(\rho), \tag{3.52}$$

where $r(\rho)$ is given by (3.34) with $F(r) = (1 - 2M/r + r^2/L^2)$. It is readily verified that for this F there is a single real root for $r(\rho)$, a fact that leads to unambiguous values of $w(\rho)$. The details of this verification are presented in Appendix B.1. On the lattice these functions are discretized with the replacements $\rho \to \rho_n = n\epsilon$ and $r_n(\rho_n)$. This results in the specific spin model

$$\begin{aligned} I_E\left[\Phi\right] = 4\pi \sum_{m,n=1}^{N_\beta, N_\rho} \Bigg\{ & -\Phi_{m,n}\left[\left(\frac{{r_n}^4}{\rho_n}\right)\left(\frac{L^2}{ML^2 + {r_n}^3}\right)\Phi_{m+1,n}\right. \\ & \left. + (\rho_n)\left(\frac{ML^2 + {r_n}^3}{L^2}\right)\Phi_{m,n+1}\right] \\ & + \left[\left(\frac{{r_n}^4}{\rho_n}\right)\left(\frac{L^2}{ML^2 + {r_n}^3}\right) + \left(\frac{ML^2 + {r_n}^3}{2L^2}\right)(\rho_n + \rho_{n-1})\right]{\Phi_{m,n}}^2 \\ & + \left(\frac{\rho_n {r_n}^4 L^2}{ML^2 + {r_n}^3}\right)\left(\frac{3{r_0}^2 + L^2}{2r_0L^2}\right)^2 \epsilon^2 \left(\frac{\mu^2}{2}\right){\Phi_{m,n}}^2 \Bigg\}. \end{aligned} \tag{3.53}$$

The limit $L \to \infty$ gives the model on 4d Euclidean Schwarzschild background:

$$
\begin{aligned}
I_E\left[\Phi\right] =& 4\pi \sum_{m,n=1}^{N_\beta, N_\rho} \Bigg\{ - \Phi_{m,n} \left[\frac{16M^3}{\rho_n \left(1 - \left(\frac{\rho_n}{4M}\right)^2\right)^4} \, \Phi_{m+1,n} + \left(\rho_n M\right) \Phi_{m,n+1} \right] \\
&+ \left[\frac{16M^3}{\rho_n \left(1 - \left(\frac{\rho_n}{4M}\right)^2\right)^4} + \frac{M}{2} \left(\rho_n + \rho_{n-1}\right) \right] {\Phi_{m,n}}^2 \\
&+ \left[\frac{M\rho_n}{\left(1 - \left(\frac{\rho_n}{4M}\right)^2\right)^4} \right] \epsilon^2 \left(\frac{\mu^2}{2}\right) {\Phi_{m,n}}^2 \Bigg\}.
\end{aligned}
\tag{3.54}
$$

A similar procedure gives the model on the 5d AdS-Schwarzschild metric, and indeed any metric of the form (3.43).

This completes the prescription for defining spin models on Euclidean black holes. The process we have followed is similar to discretizing any continuum theory on a lattice where certain discretization choices are made; in our case this is the representation for time and space derivatives. The procedure we have followed is analagous to discretized thermal quantum field theory (TQFT) on Euclideanized Minkowski spacetime with periodic identification of Wick rotated time. But there are important differences: in the black hole case the metric comes with the mass and cosmological constant parameters, and the periodicity of Euclidean time (which is guided by the requirement to remove the conical singularity) depends on these parameters.

3.5 Simulation details and results

As we have noted, in accordance with the relation (3.37) between the τ dimension size and black hole mass, the lattice size in the τ direction varies with M. Thus the thermodynamics properties of spins are best studied as a function of M with fixed lattice spacing ϵ but varying τ-dimension lattice size. We perform MC simulations

with $\epsilon = 0.01$, take

$$N_\beta = \left\lfloor \frac{\beta}{\epsilon} \right\rfloor, \quad N_\rho = \left\lfloor \frac{\rho_0}{\epsilon} \right\rfloor \tag{3.55}$$

where β is given by (3.37) and we choose $\rho_0 = \rho(5r_0)$ as the radial extent of the lattice. For convenience we use periodic boundary conditions in the ρ direction. This choice does identify radial infinity with the horizon. However the effect of this on the global thermodynamic properties of interest is negligible if the lattices are large, which is what we ensure. Additionally we consider $\mu = 0$ for all simulations and choose $\Lambda = -4$ for the AdS simulations. Note that this choice corresponds to an AdS scale of

$$L \approx 0.9 \tag{3.56}$$

in 4d and

$$L \approx 1.2 \tag{3.57}$$

in 5d. Since this work uses natural units, the AdS scales are close to the Planck length. It is also worth noting that the amplitude for Λ we choose is much larger than that of the observed cosmological constant $\sim 10^{-120}$.

After choosing a Euclidean black hole metric (Schwarzschild, 4d Schwarzschild-AdS or 5d Schwarzschild-AdS), we select a set of M values; each value of M fixes the lattice size. We use an aligned lattice (a cold start) once an M value is selected. Subsequent configurations are generated according to the probability distribution $P(x) = \exp[-I_E(x)]$ using a MC Markov Chain. We use the standard procedure where a single MC step entails flipping a randomly selected spin, computing the resulting change in the action ΔI_E, and keeping the new configuration provided

$\exp(-\Delta I_E) \geq \text{rand}[0,1]$; a sweep is defined as $N_\beta \times N_\rho$ MC steps.

Thermalization requires a number of sweeps from the starting cold configurations. This is determined by computing I_E as a function of the number of sweeps until a steady state is reached. Figure 3.2 shows that the required number of sweeps to thermalization is about 50 for the Euclidean Schwarzschild case with $M = 0.025$.

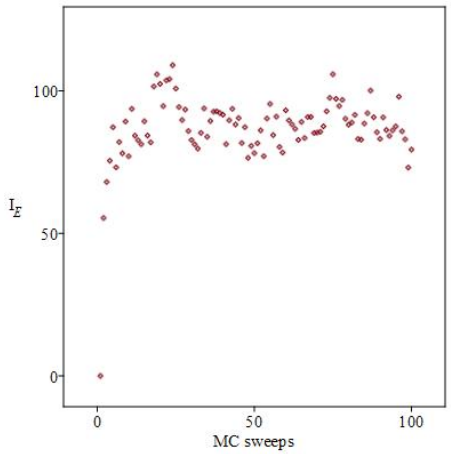

Figure 3.2: Spins on Euclidean Schwarzschild background with $M = 0.025$ are thermalized at around the 50^{th} MC sweep.

After thermalization we compute the average values of several thermodynamic quantities $\mathcal{O}$ with an additional $N_M = 2000$ sweeps for each value of mass M on its corresponding lattice using the formula

$$\langle \mathcal{O} \rangle = \frac{1}{N_M} \sum_{k=1}^{N_M} \mathcal{O}_i. \tag{3.58}$$

Here i is the number of the sweep and $\mathcal{O}_i$ is the corresponding measurement of the thermodynamic quantity. The specific quantities $\mathcal{O}$ we calculate include the

alignment A, energy E, susceptibility χ and specific heat C:

$$A = \left(\frac{1}{N_\beta N_\rho}\right) \left| \sum_{m,n=1}^{N_\beta,N_\rho} \Phi_{m,n} \right|, \tag{3.59}$$

$$E = \left(\frac{1}{N_\beta N_\rho}\right) I_E, \tag{3.60}$$

$$\chi = \frac{1}{T} \left(\langle A^2\rangle - \langle A\rangle^2\right), \tag{3.61}$$

$$C = \frac{1}{T^2} \left(\langle E^2\rangle - \langle E\rangle^2\right). \tag{3.62}$$

Another observable we calculate is entropy $S(T)$. A computation of $S(T)$ without using the partition function Z (which is not available) is to utilize a discrete version of the formula

$$S(T) = \int_0^T \frac{C(T')}{T'} dT'. \tag{3.63}$$

A discrete estimate is

$$S(T) \approx \sum_{i=1}^{N_T} \left[\frac{C(T_i)}{T_i}\right] (T_i - T_{i-1}), \tag{3.64}$$

where N_T is the total number of temperatures simulated till T in MC runs, T_i represents the i^{th} temperature in that list (where T_0 is the minimum temperature possible due to computational or theoretical constraints) and $C(T_i)$ is the heat capacity numerically evaluated at T_i.

We will now illustrate how this formula is used. Consider a spin model on a Euclidean Schwarzschild background where T_0 is the minimum temperature used due to computational constraints. To calculate $S(T_1)$ where T_1 is the next largest temperature to T_0 the formula (3.63) is used; in this case there is only one relevant term: $\left[\frac{C(T_1)}{T_1}\right](T_1 - T_0)$. The entropy at all other temperatures is calculated similarly. For the AdS black hole background T_0 is the minimum temperature theoretically

possible and a $T > T_0$ corresponds to a small and a large black hole. In this case $S(T_1)$ for a spin model on a small/large AdS black hole background is $\left[\frac{C^{S/L}(T_1)}{T_1}\right](T_1 - T_0)$ where $C^{S/L}(T_1)$ is the heat capacity for the spin model on the small/large AdS black hole background.

Since for the AdS cases a value of M uniquely determines T, but not vice versa (Figure 3.1), the thermodynamic observables are best visualized as functions of M. However it is also useful to see these quantities as functions of T; for a given T there are two values of M, the small and large black holes; these correspond to two different lattices, one for each mass. Therefore we expect two sets of results for each thermodynamic observable as functions of T, one for the small black hole and the other for the large black hole.

3.5.1 Numerical results

We computed the alignment, susceptibility, specific heat, and entropy for spin-1/2 and spin-1 models for Schwarzschild, and 4d and 5d Schwarzschild AdS. In each case we find evidence of a phase transition at a critical value of mass M_c; in each case it turns out that M_c is sub-Planckian with value indicated in the figures. We first plot these quantities as functions of M/M_c, and again as functions of T/T_c, where T_c for the AdS cases is uniquely determined (as for $\Lambda = 0$) by M_c.

Figures 3.3 and 3.4 exhibit thermodynamic quantities for the spin-1/2 case for the three Euclidean black hole backgrounds, as functions of M/M_c and T/T_c respectively; Figures 3.5 and 3.6 show the same for spin-1.

Evidence of a second order phase transition is apparent in the figures; specifically the specific heat and susceptibility exhibit an approximate divergence at the respective critical values of the masses, whereas the alignment indicates a transition from disorder to order as the mass increases. A curious feature is that the value of the critical masses is sub-Planckian (in the geometrized units $\hbar = c = G = 1$).

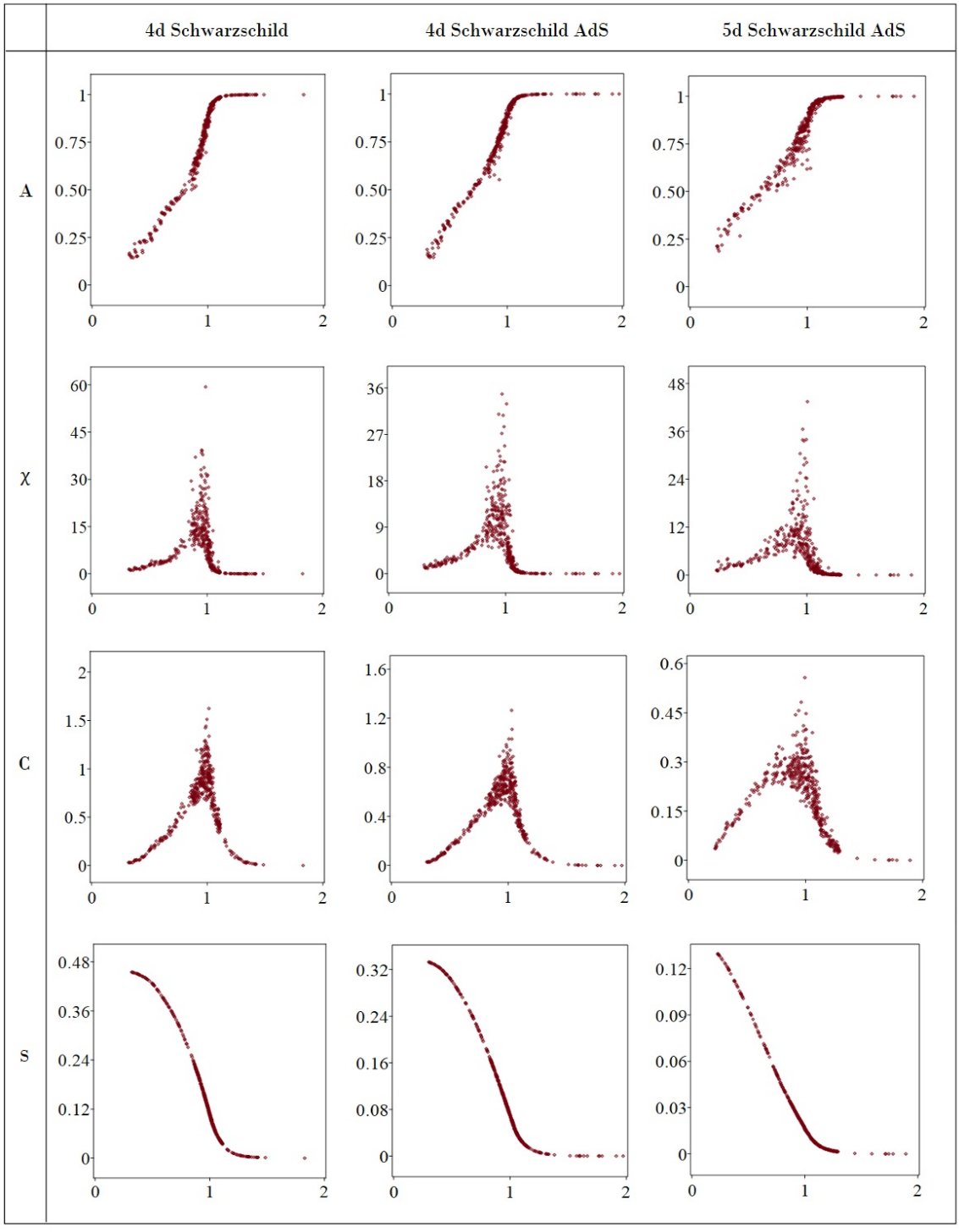

Figure 3.3: Plots of thermodynamic quantities for spin 1/2 models on Euclidean black holes with respect to $\frac{M}{M_c}$. The critical masses for Schwarzschild, and 4d and 5d Schwarzschild AdS ($\Lambda = -4$) are 0.070, 0.072 and 0.023 respectively in Planck units.

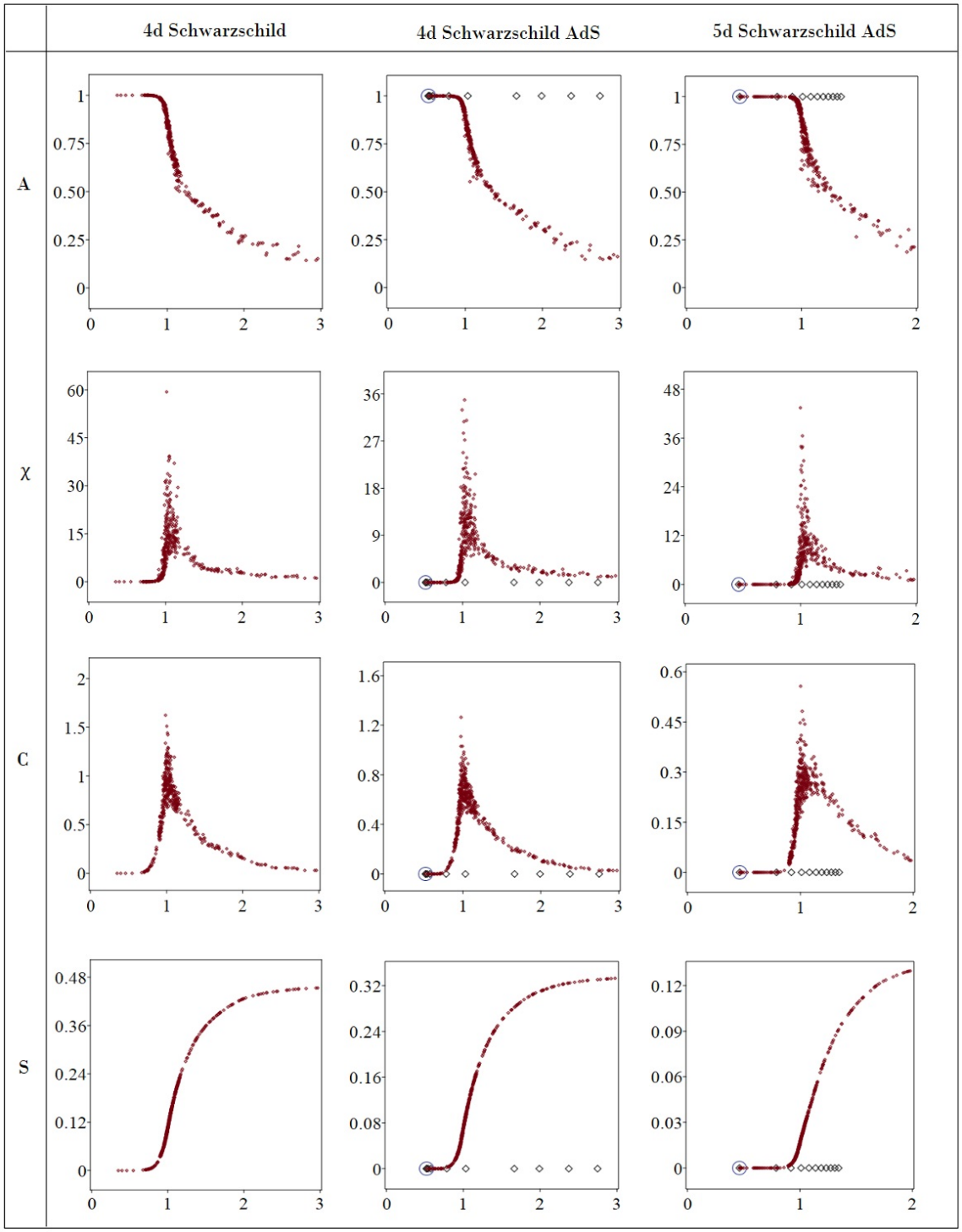

Figure 3.4: Plots of thermodynamic quantities for spin 1/2 models on Euclidean black holes with respect to $\frac{T}{T_c}$. The critical temperatures for Schwarzschild, 4d Schwarzschild AdS and 5d Schwarzschild AdS are 0.57, 0.61 and 0.80 respectively. For the AdS cases the point circled blue represents the black hole that corresponds to T_{min}, the black diamonds correspond to the large black holes, and the red dots correspond to the small black holes.

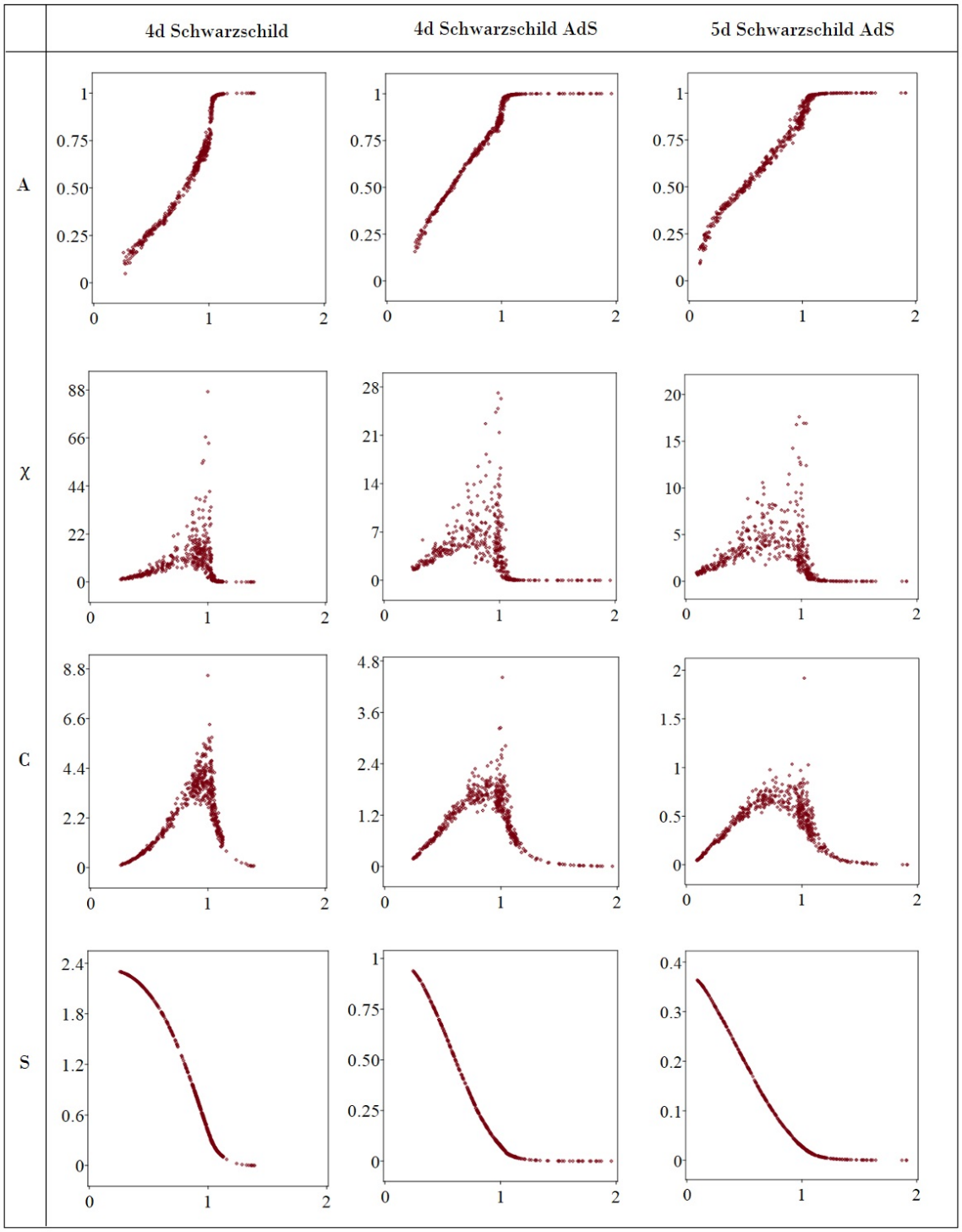

Figure 3.5: Plots of thermodynamic quantities for spin 1 models on Euclidean black holes with respect to $\frac{M}{M_c}$. The critical masses for Schwarzschild, 4d Schwarzschild AdS and 5d Schwarzschild AdS are 0.14, 0.17 and 0.065 respectively.

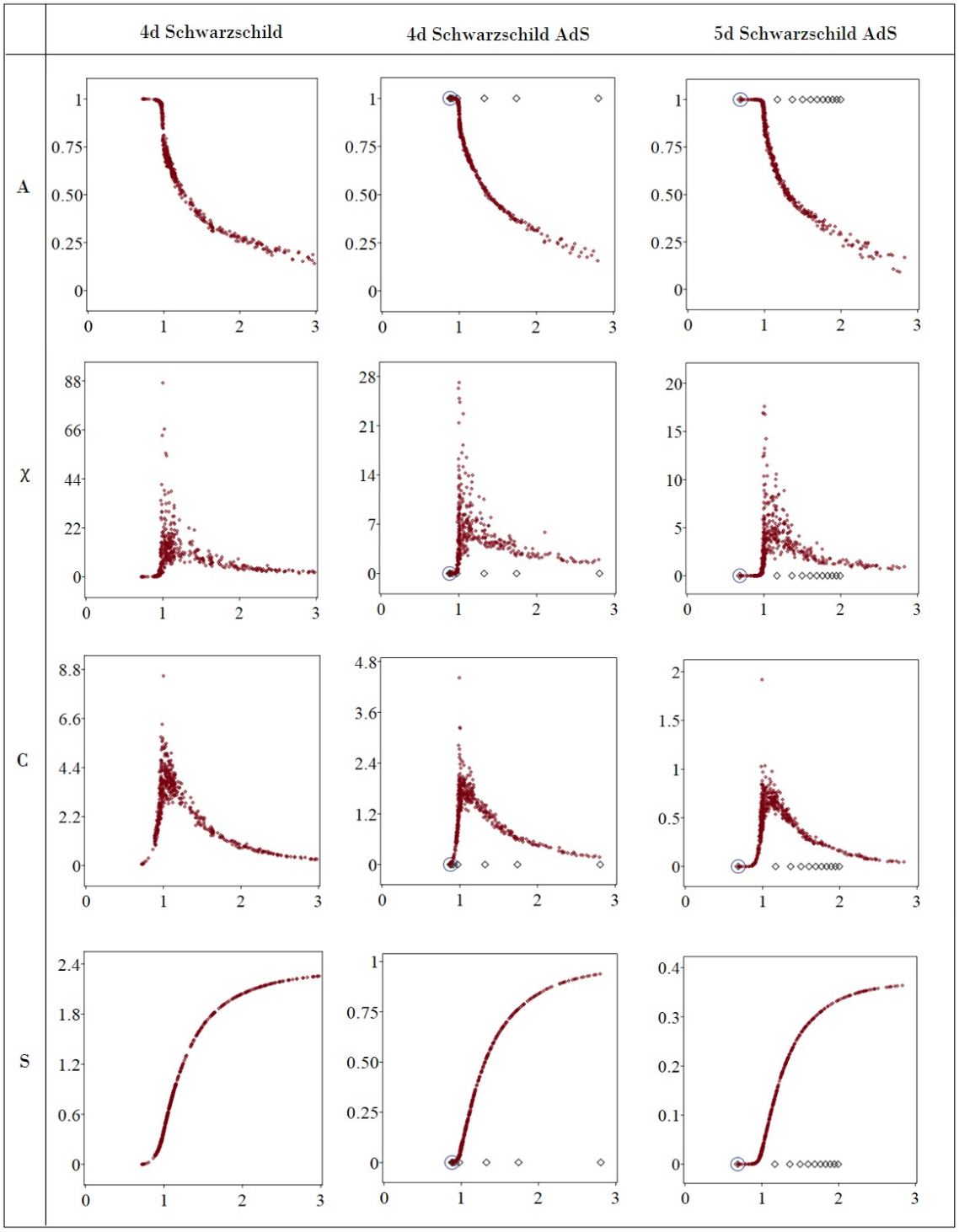

Figure 3.6: Plots of thermodynamic quantities for spin 1 models on Euclidean black holes with respect to $\frac{T}{T_c}$. The critical temperatures for Schwarzschild, 4d Schwarzschild AdS and 5d Schwarzschild AdS are 0.28, 0.36 and 0.53 respectively. For the AdS cases the point circled blue represents the black hole that corresponds to T_{min}, the black diamonds correspond to the large black holes, and the red dots correspond to the small black holes.

Euclidean background	Spin 1/2		Spin 1	
	M_c	T_c	M_c	T_c
4d Schwarzschild	0.070	0.57	0.14	0.28
4d Schwarzschild AdS	0.072	0.61	0.17	0.36
5d Schwarzschild AdS	0.023	0.80	0.065	0.53

Table 3.1: Table of critical masses and critical temperatures for spin 1/2 and spin 1 models on the Euclidean black hole backgrounds considered.

The graphs of the thermodynamic variables as a function of T/T_c contain two curves for the AdS cases; these are constructed by identifying the two possible black hole masses corresponding to a fixed T value as in Figure 3.1. To illustrate the procedure, consider for example the alignment graph as a function of T/T_c for 4d Schwarzschild-AdS: a fixed T identifies a large and a small black hole mass above the minimum value T_{min}; we take the two alignment values for these two masses from the alignment vs. mass graph and plot these values at the fixed T; this process is repeated for all data. The critical temperature is obtained uniquely from the critical mass value. Thus for example, in the alignment vs. T/T_c graphs in Figure 3.4, the circled point corresponds to the minimum (T_{min}) of the T vs. M curve in Figure 3.1; the black diamonds correspond to the large black holes, and the red dots correspond to the small black holes; in the range of T shown, the spins are ordered (as functions of T) for the large black hole, but exhibit a transition to disorder for the small black hole. Similar results hold for all the other thermodynamic quantities: spins on the background of the small black hole exhibit a phase transition as functions of T, but spins on the background of the large black hole do not, at least for the range of T values we were able to efficiently compute. Table 3.1 lists the critical masses and corresponding temperatures for all the cases studied.

Lastly Figures 3.7 and 3.8 are log-log graphs of the thermodynamics quantities for the spin-half and spin-one models as functions of the reduced temperature t, where $t = 1 - \frac{T}{T_c}$; these figures exhibit linear behaviour and therefore power laws of the

form

$$\begin{aligned} A &\approx t^b, \\ \chi &\approx t^{-g}, \\ C &\approx t^{-a}, \end{aligned} \tag{3.65}$$

together with least square fit estimates for the critical exponents b, g and a. It is worth mentioning that for the Ising or Blume-Capel models, χ and C from equation (3.65) depend on $|t|$ and conventionally the critical exponents are calculated separately for $t > 0$ and $t < 0$ following which they are averaged; we use $t > 0$ only since it corresponds to larger lattices and therefore more accurate results.

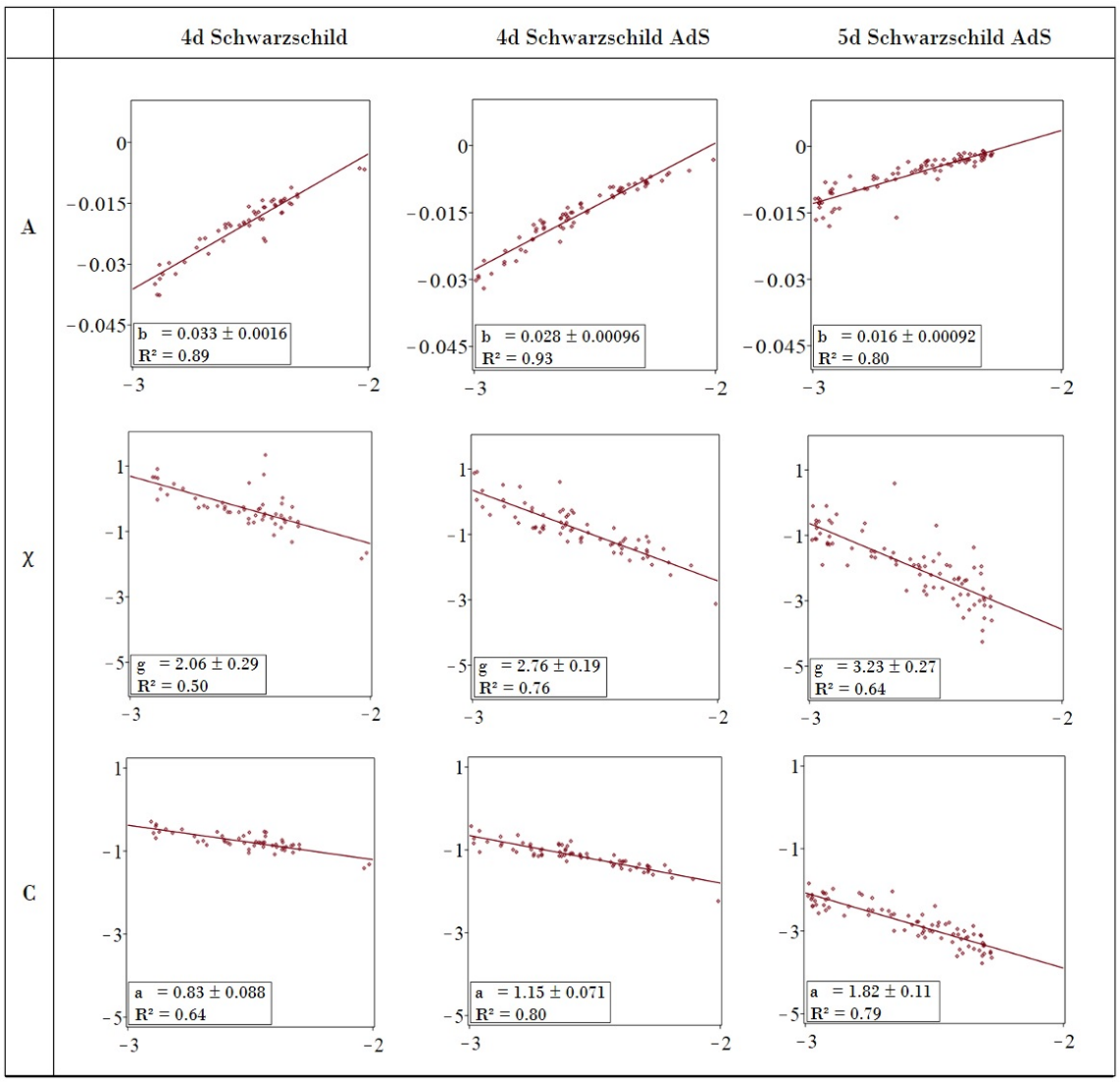

Figure 3.7: Estimating critical exponents of thermodynamic quantities for spin 1/2 models on Euclidean black holes. The horizontal axis is $\ln(t)$ and the vertical axis is the ln of the thermodynamic variable in the corresponding row.

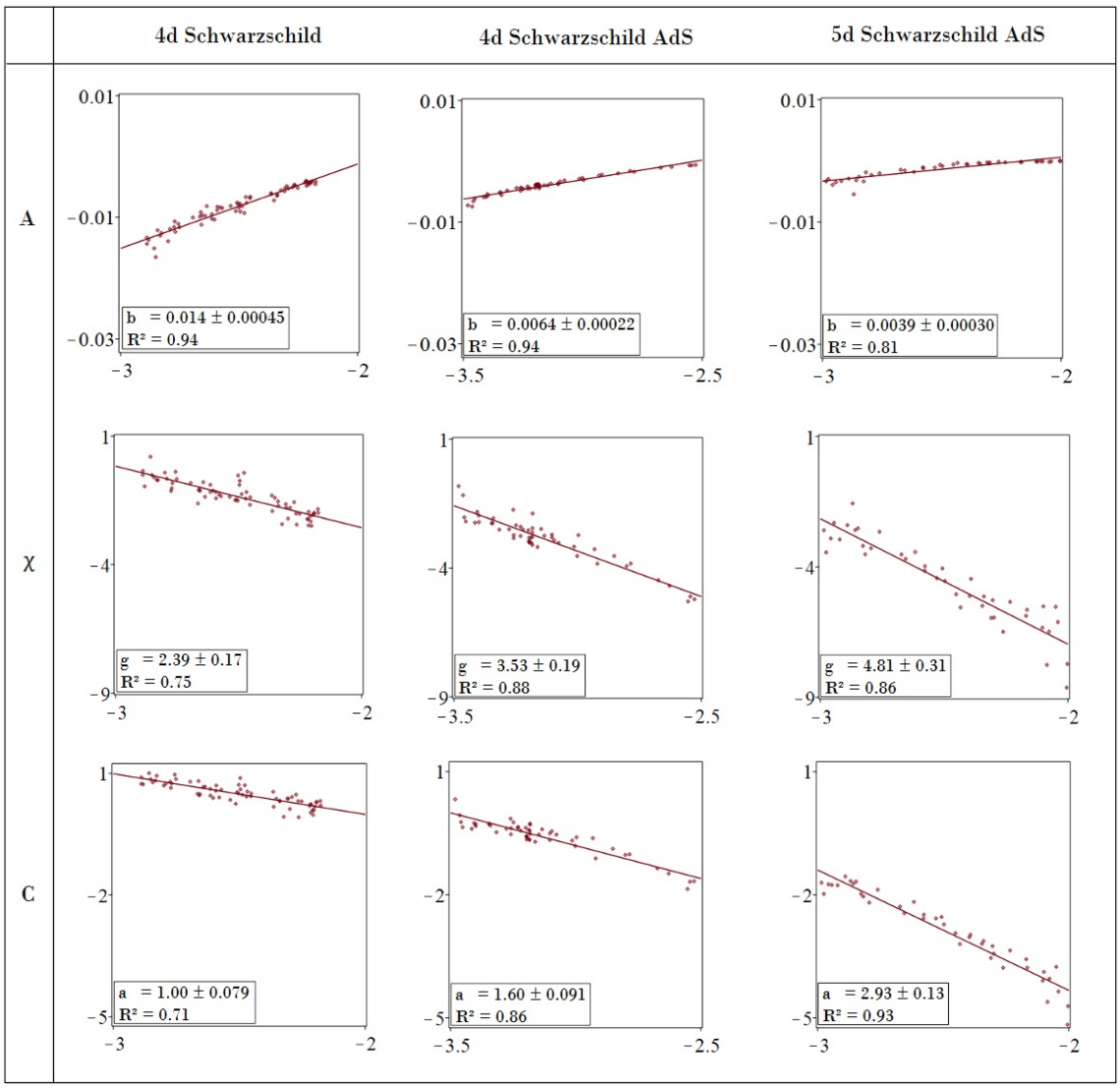

Figure 3.8: Estimating critical exponents of thermodynamic quantities for spin 1 models on Euclidean black holes. The horizontal axis is $\ln(t)$ and the vertical axis is the ln of the thermodynamic variable in the corresponding row.

This completes the description of the results: our main observation is that spins on Euclidean black hole geometries in four and five dimensions undergo phase transitions as a function of the mass parameter associated to the geometries. Perhaps surprisingly, the phase transitions to order occur at approximately a tenth of Planck mass in 4d (Table 3.1), whereas an intuitive expectation might be a few Planck masses. Nevertheless a transition in this range is not surprising considering the

Planck mass is the only natural scale in the spin model.

3.5.2 Correlation lengths at criticality

For the Ising model the interaction strength is homogeneous; there is a second order phase transition at the critical temperature T_c and the phase transition is indicative of diverging correlation length if the lattice is infinite (for a finite NxN lattice at T_c the correlation length equals N). Let's ascertain if this relationship holds when the spin model is inhomogeneous as is the case with the Ising-like models on Euclidean black holes.

Figure 3.9 presents thermalized Ising-like models on Euclidean Schwarzschild background for black hole masses at and close to the critical mass $M_c = 0.07$.

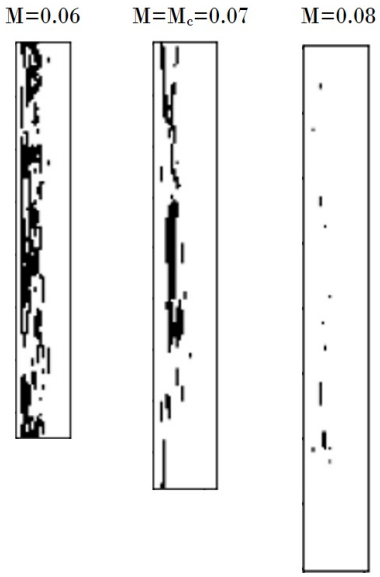

Figure 3.9: Thermalized Ising-like models on Euclidean Schwarzschild background at and close to criticality.

Note that the lattice corresponding to M_c is disordered on its left side and ordered on the right side. This is indicative of small correlation length. Therefore for the inhomogeneous Ising-like model on Euclidean Schwarzschild background a phase transition does not correspond to maximal correlations.

This indicates that the relationship between second order phase transition and maximal correlations holds if the couplings are homogeneous.

3.6 Discussion

The model and results we have described may be viewed as falling in the broad area of quantum fields on curved spacetime [33, 34]. Most work in this area is concerned mainly with quantum fields on Lorentzian rather than Euclidean curved geometries; the exception is thermal QFT which is quantum fields on Wick rotated Minkowski space [25, 26, 27, 28]. The model and the calculations we have performed are new in that (to our knowledge) there are no prior studies of inhomogeneous spin models on Euclidean black holes. Our work may be viewed as exploring the extent to which a Euclidean black hole is equivalent to a thermal heat bath for matter degrees of freedom propagating on such a geometry; our work does not concern or provide comment on the use of such solutions as contributions to the path integral of Euclidean quantum gravity without matter, which is the arena for the Hawking-Page transition [36].

The inhomogeneity of the spin models comes from the radial dependence of the coupling strength evident in the actions (3.53) and (3.54). This variation of coupling strength across the lattice means that the probability of a spin flip is dependent on radial position in the lattice; e.g. for Euclidean Schwarzschild the nearest-neighbour coupling in the τ-direction varies as $M^3/[\rho_n(1-(\rho_n/4M)^2)]^4$, whereas the coupling in the ρ-direction varies as $\rho_n M$. This not only makes apparent the inhomogeneous nature of the model but it also confirms that for small/large M the couplings are weak/strong which accounts for the observed disorder/order. The radial dependence of couplings also means that the transition point from order to disorder does not correspond to diverging correlations as is the case for homogeneous models. This in

turn indicates that the assignment of the term "second-order transition" comes with qualifications despite the linearity observed in the log-log graphs in Figures 3.7 and 3.8.

Due to the inhomogeneity it is also appropriate to study the spin behaviour as a function of column number n. Consider Figure 3.9; here for a fixed M it is possible to plot average alignment of each column vs. the column number. Physically this would amount to exploring the average spin behaviour for all allowed values of Euclidean time as a function of distance from the horizon. The horizontal axis of the resultant graph can be recast in terms of local temperature (3.30). Consider Euclidean Schwarzschild in $\tau - \rho$ coordinates (3.32); the local temperature for the discretized background is

$$T_n = \frac{1}{2\pi\rho_n}, \quad \rho_n = n\epsilon. \tag{3.66}$$

We can use Figure 3.9 to speculate that for some fixed masses (such as $M = 0.06$) we can expect a phase transition from order to disorder as the local temperature is increased.

The numerical accuracy of our results can be improved. This may be accomplished by an MC algorithm that is more efficient than the single spin flip one used in this work. However it is worth noting that most MC algorithms - such as Wolff's algorithm [75, 76] and that proposed in [77] - are designed to study spins on a flat Euclidean background for which temperature is an external parameter and is not related to lattice size. Therefore the MC algorithm being used must first be redesigned to apply to the type of inhomogeneous models that arise on black hole backgrounds. Another way to improve accuracy is via the finite size scaling technique [75, 78, 72], where successively finer lattices are used to approach the continuum limit.

Beyond improving MC methods, there are several directions for extending this work on spin models on Euclidean black hole backgrounds: exploring thermodynamic

properties while varying both mass and cosmological constant; Reissner-Nördstrom black holes and other black holes, including extremal cases; higher spin; a continuum of scalar field values within a given range rather than discrete values; and adding mass and other self-interaction terms.

Chapter 4

Reflections

This thesis investigated gravity-matter systems within the context of cosmology and black holes. In this chapter the important results are summarized and possible extensions are discussed.

Chapter 2 is a study of perturbations in cosmology with a dust clock [79]. The physical system used includes gravity, a scalar field and pressureless dust [13]. After expressing the system in the canonical framework, the Dirac procedure [9] is used to fix the dust-time gauge [13]. This yields a physical Hamiltonian and leaves untouched the diffeomorphism constraint. The perturbed phase space variables for cosmology are substituted in the canonical action, following which it is expanded to second order in the perturbations. Next the perturbations are expressed in terms of spatial Fourier modes and decomposed in scalar, vector and tensor modes. The tensor modes lead to the graviton equation, the vector modes are gauge-fixed away and the scalar modes lead to the equation of motion for an ultralocal degree of freedom and the Mukhanov-Sasaki equation with a source term. Following this a system of gravity and scalar field is considered and the same steps are used to derive the standard results for this model in a detailed and transparent fashion.

Since the method presented here is different in several respects to other methods, let's reflect on the differences.

Firstly the physical system used in this work involves gravity and two matter fields. In general CPT can contain any number of matter fields [80, 81, 82, 83]. Secondly the dust is fixed as a clock at the outset by fixing a gauge and solving the Hamiltonian constraint strongly. This is unlike the relational approach to CPT where the evolution of one variable is analyzed relative to the chosen clock variable [20, 84]. Thirdly the algebraic form of the physical Hamiltonian in the dust-time gauge is identical to that of the Hamiltonian constraint. It is worth reiterating that this desirable feature is unique to the model considered and is absent from other models that use geometric variables (such as volume or extrinsic curvature) [46] or other matter fields (such as a scalar field and Brown-Kuchař dust) [12, 47, 20] as clocks. Fourthly the spatial Fourier transforms of the perturbations are decomposed into scalar, vector and tensor modes using a time-independent basis unlike [14] which uses a time-dependent basis. Lastly gauge invariant scalar modes are constructed and the physical phase space is arrived at using a transparent and detailed application of the Dirac procedure. This is different from [14] which uses Hamilton-Jacobi like equations instead.

There are several applications and extensions of this work. Recall that in the dust-time gauge the physical background Hamiltonian is a constant of motion due to which its solutions are of the type $\bar{\mathcal{H}} = \mu$ where μ is a constant (refer to (2.24) for details). While this work considers $\mu = 0$, whereby one has the standard Friedmann equation (2.26), one can choose $\mu \neq 0$ and work with (2.27) instead. This will generalize the equations of motion of the background and the linear perturbations to include the background energy density μ and it will be enlightening to check how this changes the current results. One can also generalize the current work by considering a system of gravity, dust and two matter fields, fixing the dust-time gauge and using

the partially gauge-fixed system to study CPT. Here one can compare the results with CPT which uses and perturbs two matter fields and check how the standard result regarding entropy perturbation is modified [81, 82, 83]. It is unreasonable to expect no modification since the dust field is time and will contribute an energy density. Of particular interest to the author is the quantization of the system arrived at in this research and the calculation of the power spectra for the gauge invariant degrees of freedom. It will be interesting to explore how the contributions due to dust relate to the observed CMB data. Lastly the method presented here and in the earlier paper [40] can be used to study perturbation theory on different solutions of Einstein's equations such as AdS spacetime.

In chapter 3 spin models are constructed on Euclidean black holes after which the thermodynamic properties of the spins are studied as a function of black hole mass M using Monte-Carlo simulations. The starting point is the Euclidean action of a scalar field on a black hole space; Euclidean Schwarzschild in four dimensions and Euclidean Schwarzschild AdS in four and five dimensions are the backgrounds used [1]. The selected background is discretized and the scalar field values are restricted to ± 1 or to 0 and ± 1 to yield an Ising-like or Blume-Capel-like model respectively on the chosen Euclidean black hole background. Thermodynamic properties of spins (namely alignment, alignment susceptibility, heat capacity and entropy) are numerically investigated for different M using Monte-Carlo simulations and the resultant plots indicate a second order phase transition at sub-Planckian M. This result enriches the pre-existing knowledge regarding the thermal properties of black holes (that black holes have characteristic temperatures, entropies, etc. [4] and these have a statistical mechanics explanation [35]).

One may also view temperature T as the fundamental parameter that needs to be varied as opposed to M. The author believes that this view has two drawbacks.

[1] Where applicable the cosmological constant Λ is held fixed.

Firstly, while T is indeed an attractive choice for a Euclidean Schwarzschild background where the relationship between T and M is one to one, this is not the case for backgrounds that are asymptotically AdS where a $T > T_{min}$ corresponds to two data points. Due to this one has to revert back to M which is a metric parameter. Secondly, recall that the T associated with a Euclidean background is the result of three steps: Euclideanization of time; compactification; ensuring that the compactification circumference removes the conical singularity. The third step depends on M and therefore M is more fundamental.

Despite being a study of spins on Euclidean black holes, this work offers a comprehensive proof of concept for studying more general matter on these Euclidean geometries using Monte-Carlo simulations. Therefore the framework developed here can be extended to study not only higher spin models ($3/2, 2, 5/2$, etc.) but also a scalar field that can take any value in a specified interval. The latter - which is an example of lattice field theory - describes the behaviour of matter on a background of interest. The existence of phase transitions for the spin $1/2$ and the more general spin 1 model can be used to infer the existence of phase transitions for not only a higher spin model but also a scalar field on Euclidean black hole geometry.

The aforementioned study - and even the spirit of the current one - is different from thermal field theory (TFT) in three ways. Firstly, in TFT the background chosen is flat Euclidean space which has no metric parameters. Here one has Euclidean black hole backgrounds, the metrics for which have M [2]. Secondly, in TFT the compactification of Euclidean time stems from a choice to establish a correspondence with statistical mechanics. In this work the compactification of Euclidean time is additionally guided by the requirement to remove the conical singularity. Thirdly, here the compactification circumference depends on M. Hence the parameter in the metric is related to the compactification circumference and therefore to the tem-

[2]Since Λ is held fixed one need only consider M for this discussion.

perature of the background. This is not the case in TFT since the metric has no parameters and there exists no conical singularity, due to which one can choose the compactification circumference arbitrarily.

Lastly, one may view this work as a generalization of spin models on Euclidean background. This is because here the coupling between spins is position dependent and the black hole mass M affects vertical interactions differently from the horizontal ones. Already the results of this work provide commentary on the known relationship between second order phase transitions and diverging correlation lengths. Consider the homogeneous Ising model for which it is known that these occur at the critical temperature. This work demonstrates that criticality does not coincide with diverging correlations for the Ising-like model on a Euclidean Schwarzschild background.

Bibliography

[1] Albert Einstein. The Field Equations of Gravitation. *Sitzungsber. Preuss. Akad. Wiss. Berlin (Math. Phys.)*, 1915:844–847, 1915.

[2] Robert M. Wald. *General Relativity*. Chicago University Pr., Chicago, USA, 1984.

[3] Karl Schwarzschild. On the gravitational field of a mass point according to Einstein's theory. *Sitzungsber. Preuss. Akad. Wiss. Berlin (Math. Phys.)*, 1916:189–196, 1916.

[4] James M. Bardeen, B. Carter, and S. W. Hawking. The four laws of black hole mechanics. *Commun. Math. Phys.*, 31:161–170, 1973.

[5] S. W. Hawking. Particle creation by black holes. *Commun. Math. Phys.*, 43:199–220, 1975.

[6] Daniel Baumann. TASI Lectures on Inflation. *ArXiv:0907.5424v2*, 2012.

[7] Viatcheslav F. Mukhanov. Quantum Theory of Gauge Invariant Cosmological Perturbations. *Sov. Phys. JETP*, 67:1297–1302, 1988.

[8] R. Arnowitt, S. Deser, and C. W. Misner. Dynamical Structure and Definition of Energy in General Relativity. *Phys. Rev.*, 116:1322–1330, Dec 1959.

[9] P.A.M. Dirac. *Lectures on Quantum Mechanics*. Belfer Graduate School of Science, monograph series. Dover Publications, 2001.

[10] Karel V. Kuchař. Time and Interpretations of Quantum Gravity. *Inter. J. of Mod. Phys. D*, 20(supp01):3–86, Jul 2011.

[11] W. F. Blyth and C. J. Isham. Quantization of a Friedmann universe filled with a scalar field. *Phys. Rev. D*, 11:768–778, Feb 1975.

[12] J. David Brown and Karel V. Kuchař. Dust as a standard of space and time in canonical quantum gravity. *Phys.Rev.*, D51:5600–5629, 1995.

[13] Viqar Husain and Tomasz Pawlowski. Time and a Physical Hamiltonian for Quantum Gravity. *Phys. Rev. Lett.*, 108:141301, Apr 2012.

[14] David Langlois. Hamiltonian formalism and gauge invariance for linear perturbations in inflation. *Class.Quant.Grav.*, 11:389–407, 1993.

[15] Bianca Dittrich and Johannes Tambornino. A perturbative approach to Dirac observables and their spacetime algebra. *Class. Quant. Grav.*, 24(4):757, Jan 2007.

[16] Bianca Dittrich and Johannes Tambornino. Gauge-invariant perturbations around symmetry-reduced sectors of general relativity: applications to cosmology. *Class. Quant. Grav.*, 24(18):4543, Aug 2007.

[17] K Giesel, S Hofmann, T Thiemann, and O Winkler. Manifestly gauge-invariant general relativistic perturbation theory: I. Foundations. *Class. Quant. Grav.*, 27(5):055005, Feb 2010.

[18] K Giesel, S Hofmann, T Thiemann, and O Winkler. Manifestly gauge-invariant general relativistic perturbation theory: II. FRW background and first order. *Class. Quant. Grav.*, 27(5):055006, Feb 2010.

[19] Kristina Giesel, Parampreet Singh, and David Winnekens. Dynamics of Dirac observables in canonical cosmological perturbation theory. *Class. Quant. Grav.*, 36(8):085009, Apr 2019.

[20] Kristina Giesel, Laura Herold, Bao-Fei Li, and Parampreet Singh. Mukhanov-Sasaki equation in a manifestly gauge-invariant linearized cosmological perturbation theory with dust reference fields. *Phys. Rev. D*, 102:023524, Jul 2020.

[21] Tom Lancaster and Stephen Blundell. *Quantum Field Theory for the Gifted Amateur*. Oxford University Press, 2014.

[22] M. Srednicki. *Quantum Field Theory*. Cambridge University Press, 2007.

[23] A.M Polyakov. *Gauge Fields and Strings*. Harwood Academic Publishers, 1987.

[24] Michel Le Bellac. *Thermal field theory*. Cambridge University Press, Cambridge, UK, 1996.

[25] J. Schwinger. On the Euclidean structure of relativistic field theory. *Proc. Nat. Acad. Sc.*, 44:956–965, 1958.

[26] Tadao Nakano. Quantum Field Theory in Terms of Euclidean Parameters. *Progress of Theoretical Physics*, 21(2):241–259, 02 1959.

[27] K. Symanzik. Euclidean Quantum Field Theory. I. Equations for a Scalar Model. *Journal of Mathematical Physics*, 7(3):510–525, 12 2004.

[28] K. Symanzik. *Euclidean Quantum Field Theory*. Academic Press, Chicago, USA, 1969.

[29] Konrad Osterwalder and Robert Schrader. Axioms for Euclidean Green's functions. *Commun. Math. Phys.*, 31:83–112, 1972.

[30] Roy P. Kerr. Gravitational Field of a Spinning Mass as an Example of Algebraically Special Metrics. *Phys. Rev. Lett.*, 11, 1963.

[31] M. Visser. How to Wick rotate generic curved spacetime. *ArXiv:1702.05572*, 2017.

[32] F. Gray. Black Hole Radiation, Greybody Factor, and Generalised Wick Rotation. *Victoria University of Wellington MSc. Thesis*, 2016.

[33] N. D. Birrell and P. C. W. Davies. *Quantum Fields in Curved Space*. Cambridge Monographs on Mathematical Physics. Cambridge University Press, 1982.

[34] Leonard Parker and David Toms. *Quantum Field Theory in Curved Spacetime*. Cambridge University Press, Cambridge, UK, 2009.

[35] G. W. Gibbons and S. W. Hawking. Action Integrals and Partition Functions in Quantum Gravity. *Phys. Rev. D*, 15:2752–2756, 1977.

[36] S. W. Hawking and Don N. Page. Thermodynamics of Black Holes in anti-De Sitter Space. *Commun. Math. Phys.*, 87:577, 1983.

[37] Juan Maldacena. The large-N limit of superconformal field theories and supergravity. *International journal of theoretical physics*, 38(4):1113–1133, 1999.

[38] Makoto Natsuume. AdS/CFT duality user guide. *ArXiv:1409.3575*, 8(9):20, 2014.

[39] M. Saeed. Cosmological Perturbation Theory in a Matter-Time Gauge. *UNB MSc. Thesis*, 2019.

[40] Masooma Ali, Viqar Husain, Shohreh Rahmati, and Jonathan Ziprick. Linearized gravity with matter time. *Class. Quant. Grav.*, 33(10):105012, Apr 2016.

[41] Ernst Ising. Beitrag zur Theorie des Ferromagnetismus. *Zeitschrift für Physik*, 31:253 – 258, 1925.

[42] M. Blume. Theory of the First-Order Magnetic Phase Change in UO_2. *Phys. Rev.*, 141:517–524, Jan 1966.

[43] H. Capel. On the possibility of first-order phase transitions in Ising systems of triplet ions with zero-field splitting. *Physica*, 32(5):966–988, 1966.

[44] Richard L. Arnowitt, Stanley Deser, and Charles W. Misner. The Dynamics of General Relativity. *Gen. Rel. Grav.*, 40:1997–2027, 2008.

[45] Andrew J. Hanson, Tullio Regge, and Claudio Teitelboim. *Constrained Hamiltonian Systems*. Accademia Nazionale dei Lincei, 1976.

[46] James W. York Jr. Role of conformal three geometry in the dynamics of gravitation. *Phys. Rev. Lett.*, 28:1082–1085, 1972.

[47] W.F. Blyth and C.J. Isham. Quantization of a Friedmann Universe Filled with a Scalar Field. *Phys. Rev. D*, 11:768–778, 1975.

[48] Viqar Husain and Tomasz Pawlowski. Dust reference frame in quantum cosmology. *Class. Quant. Grav.*, 28(22):225014, Oct 2011.

[49] K Giesel and T Thiemann. Scalar material reference systems and loop quantum gravity. *Class. Quant. Grav.*, 32(13):135015, Jun 2015.

[50] Mehdi Assanioussi, Jerzy Lewandowski, and Ilkka Mäkinen. Time evolution in deparametrized models of loop quantum gravity. *Physical Review D*, 96(2), Jul 2017.

[51] Johannes Tambornino. Relational Observables in Gravity: a Review. *SIGMA*, 8:017, 2012.

[52] Jcedrzej Swiezewski. On the properties of the irrotational dust model. *Class.Quant.Grav.*, 30:237001, 2013.

[53] Christopher Eling, Ted Jacobson, and David Mattingly. Einstein-Aether theory. In *Deserfest: A celebration of the life and works of Stanley Deser. Proceedings, Meeting, Ann Arbor, USA, April 3-5, 2004*, pages 163–179, 2004.

[54] T. Jacobson and D. Mattingly. Einstein-Aether waves. *Phys. Rev.*, D70:024003, 2004.

[55] Ali H. Chamseddine and Viatcheslav Mukhanov. Mimetic Dark Matter. *JHEP*, 11:135, 2013.

[56] Alexey Golovnev. On the recently proposed mimetic Dark Matter. *Physics Letters B*, 728:39–40, Jan 2014.

[57] Eugene A. Lim, Ignacy Sawicki, and Alexander Vikman. Dust of Dark Energy. *JCAP*, 1005:012, 2010.

[58] Ali H. Chamseddine, Viatcheslav Mukhanov, and Alexander Vikman. Cosmology with Mimetic Matter. *JCAP*, 2014(06):017, 2014.

[59] Ali H. Chamseddine and Viatcheslav Mukhanov. Resolving cosmological singularities. *Journal of Cosmology and Astroparticle Physics*, 2017(03):009–009, Mar 2017.

[60] Ted Jacobson and Antony J. Speranza. Variations on an aethereal theme. *Phys. Rev.*, D92:044030, 2015.

[61] John Cardy. *Scaling and Renormalization in Statistical Physics*. Cambridge Lecture Notes in Physics. Cambridge University Press, 1996.

[62] M. Blume. *Phys. Rev.*, 141:517, 1966.

[63] H. W. Capel. *Physica*, 32:966, 1966.

[64] Theodore W. Burkhardt. Application of Kadanoff's lower-bound renormalization transformation to the Blume-Capel model. *Phys. Rev. B*, 14:1196–1201, Aug 1976.

[65] C. J. Silva, A. A. Caparica, and J. A. Plascak. Wang-Landau Monte Carlo simulation of the Blume-Capel model. *Phys. Rev. E*, 73:036702, Mar 2006.

[66] Ch. Hoelbling and C. B. Lang. Universality of the Ising model on spherelike lattices. *Phys. Rev. B*, 54:3434–3441, Aug 1996.

[67] F.P. Fernandes, F.W.S. Lima, and J.A. Plascak. Blume–Capel model on directed and undirected small-world Voronoi–Delaunay random lattices. *Computer Physics Communications*, 181(7):1218–1223, 2010.

[68] Réka Albert and Albert-László Barabási. Statistical mechanics of complex networks. *Rev. Mod. Phys.*, 74:47–97, Jan 2002.

[69] C. Chris Wu. Ising models on hyperbolic graphs. *Journal of Statistical Physics*, 85, 1996.

[70] Nikolas P. Breuckmann, Benedikt Placke, and Ananda Roy. Critical properties of the Ising model in hyperbolic space. *Phys. Rev. E*, 101:022124, Feb 2020.

[71] Tao Pang. *An Introduction to Computational Physics*. Cambridge University Press, 2006.

[72] Jos Thijssen. *Computational Physics*. Cambridge University Press, 2 edition, 2007.

[73] Colin Morningstar. The Monte Carlo method in quantum field theory. *Arxiv: 0702020*, 2007.

[74] Nicholas C. Metropolis, Arianna W. Rosenbluth, Marshall N. Rosenbluth, and A. H. Teller. Equation of state calculations by fast computing machines. *Journal of Chemical Physics*, 21:1087–1092, 1953.

[75] D. P. Landau and K Binder. *A Guide to Monte Carlo Simulations in Statistical Physics*. Cambridge University Press, Cambridge, UK, 2015.

[76] Tao Pang. *An Introduction to Computational Physics*. Cambridge University Press, Cambridge, UK, 2006.

[77] Fugao Wang and D. P. Landau. Efficient, Multiple-Range Random Walk Algorithm to Calculate the Density of States. *Phys. Rev. Lett.*, 86:2050–2053, Mar 2001.

[78] D. P. Landau. Finite-size behavior of the Ising square lattice. *Phys. Rev. B*, 13:2997–3011, Apr 1976.

[79] Viqar Husain and Mustafa Saeed. Cosmological perturbation theory with matter time. *Phys. Rev. D*, 102:124062, Dec 2020.

[80] Jai chan Hwang and Hyerim Noh. Cosmological perturbations with multiple scalar fields. *Physics Letters B*, 495:277–283, 1996.

[81] Christopher Gordon, David Wands, Bruce A. Bassett, and Roy Maartens. Adiabatic and entropy perturbations from inflation. *Phys. Rev. D*, 63:023506, Dec 2000.

[82] David Langlois. Correlated adiabatic and isocurvature perturbations from double inflation. *Phys. Rev. D*, 59:123512, May 1999.

[83] David Polarski and A. A. Starobinsky. Isocurvature perturbations in multiple inflationary models. *Phys. Rev. D*, 50:6123–6129, Nov 1994.

[84] Kristina Giesel and Adrian Herzog. Gauge invariant canonical cosmological perturbation theory with geometrical clocks in extended phase-space — a review and applications. *International Journal of Modern Physics D*, 27(08):1830005, May 2018.

Appendix A

Cosmological perturbation theory with matter-time

A.1 Derivation of second order Hamiltonian

Recall that the physical Hamiltonian density for general relativity consists of a curvature and kinetic part:

$$\mathcal{H}^{GR} = -\sqrt{q}R^{(3)} + \frac{\pi_{ab}\pi^{ab}}{\sqrt{q}} - \frac{\pi^2}{2\sqrt{q}}. \tag{A.1}$$

We list the expansions of the different pieces. The metric and its inverse are:

$$q_{ab} = \bar{a}^2 e_{ab} + \epsilon h_{ab} \tag{A.2a}$$

$$q^{ab} = \frac{e^{ab}}{\bar{a}^2} - \epsilon\frac{h^{ab}}{\bar{a}^4} \tag{A.2b}$$

where ϵ tracks the order in perturbation. We will first compute the determinant using the usual definition:

$$q = \frac{\varepsilon^{abc}\varepsilon^{def}}{3!} q_{ad}q_{be}q_{cf} \tag{A.3}$$

where ε^{abc} is the Levi-Civita symbol. We expand the metric as defined in equation (A.2a) and follow the steps detailed below to obtain the metric determinant.

$$\begin{aligned} q &= \frac{\varepsilon^{abc}\varepsilon^{def}}{3!}\left(\bar{a}^2 e_{ad} + \epsilon h_{ad}\right)\left(\bar{a}^2 e_{be} + \epsilon h_{be}\right)\left(\bar{a}^2 e_{cf} + \epsilon h_{cf}\right) \\ &= \frac{\bar{a}^6}{3!}\varepsilon^{abc}\varepsilon^{def}e_{ad}e_{be}e_{cf} + \frac{\epsilon\bar{a}^4}{2}\varepsilon^{abc}\varepsilon^{def}e_{ad}e_{be}h_{cf} + \frac{\epsilon^2\bar{a}^2}{2}\varepsilon^{abc}\varepsilon^{def}e_{ad}h_{be}h_{cf} \\ &= \frac{\bar{a}^6}{3!}\varepsilon_{def}\varepsilon^{def} + \frac{\epsilon\bar{a}^4}{2}\varepsilon_{de}{}^{c}\varepsilon^{def}h_{cf} + \frac{\epsilon\bar{a}^2}{2}\varepsilon_{d}{}^{bc}\varepsilon^{def}h_{be}h_{cf} \\ &= \bar{a}^6 + \epsilon\bar{a}^4 e^{cf}h_{cf} + \frac{\epsilon^2\bar{a}^2}{2}\left(e^{be}e^{cf} - e^{bc}e^{ef}\right)h_{be}h_{cf} \\ &= \bar{a}^6 + \epsilon\bar{a}^4 h + \frac{\epsilon^2\bar{a}^2}{2}\left(h^2 - h^{ab}h_{ab}\right). \end{aligned} \tag{A.4}$$

We can calculate $q^{\pm\frac{1}{2}}$ using a Taylor expansion to second order in perturbations. We list the results below:

$$\sqrt{q} = \bar{a}^3 + \frac{\epsilon\bar{a}h}{2} + \frac{\epsilon^2}{8\bar{a}}\left(h^2 - 2h^{ab}h_{ab}\right) \tag{A.5a}$$

$$\frac{1}{\sqrt{q}} = \frac{1}{\bar{a}^3} - \frac{\epsilon h}{2\bar{a}^5} + \frac{\epsilon^2}{8\bar{a}^7}\left(h^2 + 2h^{ab}h_{ab}\right). \tag{A.5b}$$

We will now calculate the curvature terms. It is natural to start with the Christoffel symbols

$$\begin{aligned} \Gamma^a_{bc} &= \epsilon\frac{q^{ad}}{2}\left(h_{bd,c} + h_{cd,b} - h_{bc,d}\right) \\ &= \epsilon\left[\frac{e^{ad}}{2\bar{a}^2}\left(h_{bd,c} + h_{cd,b} - h_{bc,d}\right)\right] - \epsilon^2\left[\frac{h^{ad}}{2\bar{a}^4}\left(h_{bd,c} + h_{cd,b} - h_{bc,d}\right)\right] \end{aligned} \tag{A.6}$$

where every partial derivative is spatial. The three Ricci scalar is:

$$\begin{aligned} R^{(3)} =& \frac{\epsilon}{\bar{a}^4}\left(\partial_a\partial_b h^{ab} - \partial^2 h\right) + \frac{\epsilon^2}{\bar{a}^6}\left[h^{ab}\partial_a\partial_b h + h^{ab}\partial^2 h_{ab} - 2h^{ai}\partial_b\partial_i h_a{}^b - \left(\partial_a h^{ab}\right)\left(\partial_c h_b{}^c\right)\right] \\ &+ \frac{\epsilon^2}{\bar{a}^6}\left[\left(\partial_a h^{ab}\right)\left(\partial_b h\right) - \frac{1}{4}\left(\partial_a h\right)\left(\partial^a h\right) + \frac{3}{4}\left(\partial_c h^{ab}\right)\left(\partial^c h_{ab}\right) - \frac{1}{2}\left(\partial_c h^{ab}\partial_a h_b{}^c\right)\right]. \end{aligned} \tag{A.7}$$

Now we will calculate the momentum terms. We start with the specification for π^{ab}:

$$\pi^{ab} = \frac{\bar{p}}{6\bar{a}} e^{ab} + \epsilon p^{ab}. \tag{A.8}$$

We will calculate π in detail; we start with the definition:

$$\begin{aligned} \pi &= q_{ab}\pi^{ab} \\ &= \left(\bar{a}^2 e_{ab} + \epsilon h_{ab}\right)\left(\frac{\bar{p}}{6\bar{a}} e^{ab} + \epsilon p^{ab}\right) \\ &= 3\bar{a}^2\left(\frac{\bar{p}}{6\bar{a}}\right) + \epsilon\left[\bar{a}^2 p + \left(\frac{\bar{p}}{6\bar{a}}\right) h\right] + \epsilon^2 h_{ab} p^{ab}. \end{aligned} \tag{A.9}$$

A similar calculation for π_{ab} reveals:

$$\pi_{ab} = \left(\bar{a}^2\right)^2\left(\frac{\bar{p}}{6\bar{a}}\right) e_{ab} + \epsilon\left[2\bar{a}^2\left(\frac{\bar{p}}{6\bar{a}}\right) h_{ab} + \left(\bar{a}^2\right)^2 p_{ab}\right] + \epsilon^2\left[2\bar{a}^2 p^d{}_{(a} h_{b)d} + \left(\frac{\bar{p}}{6\bar{a}}\right) h_a{}^d h_{bd}\right]. \tag{A.10}$$

We substitute these results in the expression for the Hamiltonian density, expand to second order in perturbations and simplify where possible using integration by parts. The curvature and kinetic terms from (A.1) are respectively:

$$-\sqrt{q}R^{(3)} = \frac{h^{ab}}{2\bar{a}^3}\left(\partial_b\partial^c h_{ac} - \frac{\partial^2 h_{ab}}{2}\right) - \frac{h}{2\bar{a}^3}\left(\partial_a\partial_b h^{ab} - \frac{\partial^2 h}{2}\right) \tag{A.11a}$$

$$\begin{aligned} \frac{\pi_{ab}\pi^{ab}}{\sqrt{q}} - \frac{\pi^2}{2\sqrt{q}} =& \frac{1}{\bar{a}}\left(\frac{\bar{p}}{6\bar{a}}\right)\left(p^{ab} h_{ab} - \frac{hp}{2}\right) + \bar{a}\left(p^{ab} p_{ab} - \frac{p^2}{2}\right) \\ &+ \frac{1}{8\bar{a}^3}\left(\frac{\bar{p}}{6\bar{a}}\right)^2\left(5h_{ab}h^{ab} - \frac{3h^2}{2}\right). \end{aligned} \tag{A.11b}$$

A.2 Derivation of graviton equation

The graviton equations are those for the phase space variables $h_I(k,t)$ and $p_I(k,t)$

for $I = 3, 4$ derived from the Hamiltonian (2.68):

$$\dot{h}_I = \frac{2}{\bar{a}}\left[\left(\frac{\bar{p}}{6\bar{a}}\right)h_I + \frac{p_I}{\bar{a}^2}\right], \tag{A.12a}$$

$$\dot{p}_I = \frac{\bar{a}^3}{2}\left[-\frac{k^2}{\bar{a}^2} - \frac{5}{2\bar{a}^2}\left(\frac{\bar{p}}{6\bar{a}}\right)^2 + V(\bar{\phi}) - \frac{\bar{p}_\phi^2}{2\bar{a}^6}\right]h_I - \frac{2}{\bar{a}}\left(\frac{\bar{p}}{6\bar{a}}\right)p_I. \tag{A.12b}$$

The first of these gives

$$p_I = \bar{a}^2\left[\frac{\bar{a}}{2}\dot{h}_I - \left(\frac{\bar{p}}{6\bar{a}}\right)h_I\right], \tag{A.13}$$

and

$$\ddot{h}_I = \frac{1}{3\bar{a}^2}\left(\dot{\bar{p}} - 2\bar{p}\bar{H}\right)h_I + \left(\frac{\bar{p}}{3\bar{a}^2}\right)\dot{h}_I - \frac{6\bar{H}}{\bar{a}^3}p_I + \frac{2}{\bar{a}^3}\dot{p}_I, \tag{A.14}$$

where $\bar{H} \equiv \dot{\bar{a}}/\bar{a} = -\bar{p}/12\bar{a}^2$ from the equations for the background. Substituting for p_I and $\dot{p}_I$ into the last equation gives

$$\ddot{h}_I = \left[\frac{1}{3\bar{a}^2}\left(\dot{\bar{p}} + \bar{p}\bar{H}\right) - \frac{k^2}{\bar{a}^2} + \frac{3}{2\bar{a}^2}\left(\frac{\bar{p}}{6\bar{a}}\right)^2 + V(\bar{\phi}) - \frac{\bar{p}_\phi^2}{2\bar{a}^6}\right]h_I - 3\bar{H}\dot{h}_I. \tag{A.15}$$

Finally using the background equation (2.23) for $\dot{\bar{p}}$ gives

$$\ddot{h}_I + 3\bar{H}\dot{h}_I + \left(\frac{k}{\bar{a}}\right)^2 h_I = 0. \tag{A.16}$$

A.3 Diffeomorphism constraint is first class

To show that the diffeomorphism constraint $\tilde{C}_\parallel$ (2.64) is first class we must show that

$$\frac{d\tilde{C}_\parallel}{dt} = \{\tilde{C}_\parallel, H^{S\phi}\} + \frac{\partial\tilde{C}_\parallel}{\partial t} = 0. \tag{A.17}$$

The first term is

$$\begin{aligned}\{\tilde{C}_{\parallel}, H^{S\phi}\} &= -2\bar{a}^2\left(\dot{p}_1+\sqrt{2}\dot{p}_2\right)+\left(\frac{\bar{p}}{6\bar{a}}\right)\left(\dot{h}_1-2\sqrt{2}\dot{h}_2\right)+\sqrt{3}\bar{p}_\phi\dot{\tilde{\phi}} \\ &= -\frac{\bar{p}}{3}\left(p_1+\sqrt{2}p_2\right)-\left[\frac{1}{4a}\left(\frac{\bar{p}}{6\bar{a}}\right)^2+\frac{1}{\bar{a}}\left(\frac{\bar{p}_\phi}{2\bar{a}}\right)^2-\frac{\bar{a}V(\bar{\phi})}{2}\right]\left(h_1-2\sqrt{2}h_2\right) \\ &\quad +\sqrt{3}\bar{a}^3V'(\bar{\phi})\tilde{\phi}, \end{aligned} \tag{A.18}$$

and the second term is

$$\frac{\partial\tilde{C}_{\parallel}}{\partial t} = -4\bar{a}\dot{\bar{a}}\left(p_1+\sqrt{2}p_2\right)+\left(\frac{\dot{\bar{p}}}{6\bar{a}}-\frac{\dot{\bar{a}}\bar{p}}{6\bar{a}^2}\right)\left(h_1-2\sqrt{2}h_2\right)+\sqrt{3}\dot{\bar{p}}_\phi\tilde{\phi}. \tag{A.19}$$

Substituting into this the equations for the background (2.23) and collecting terms gives

$$\frac{d\tilde{C}_{\parallel}}{dt} = 0. \tag{A.20}$$

Similar steps show that the same results holds for the transverse components of the linearized diffeomorphism constraint.

Appendix B

Ising-like models on Euclidean black holes

B.1 Unique, positive solution for $r(\rho)$ for the AdS black holes

Calculating $r(\rho)$ requires inverting

$$\rho(r) = \beta_0 \sqrt{F(r)} \tag{B.1}$$

which after discretization is equivalent to

$$n\epsilon = \beta_0 \sqrt{F(r_n)}. \tag{B.2}$$

Hereafter use r instead of r_n for neatness. For 4d Euclidean Schwarzschild AdS rearranging the equation above gives

$$a\, r^3 + b\, r + c = 0, \tag{B.3}$$

where

$$a = \frac{1}{L^2}, \quad b = 1 - \left(\frac{n\epsilon}{\beta_0}\right)^2 \quad \text{and} \quad c = -2M. \tag{B.4}$$

Hereafter use $f(r) = a\,r^3 + b\,r + c$ for simplicity whereby equation (B.3) becomes $f(r) = 0$. To ensure that for a given n there is an single, positive value for r it must be checked if $f(r)$ has a unique, positive root. This is indeed the case as it will be now be demonstrated.

It can be readily verified that $f(0) < 0$ and

$$\frac{df}{dr} = 3ar^2 + b. \tag{B.5}$$

Note that for $b > 0$, $\frac{df}{dr}|_{r\geq 0} > 0$ which indicates that the function increases for positive values of r and becomes zero for one such value; therefore a single, positive root is guaranteed. Conversely for $b < 0$:

$$\frac{df}{dr}\Big|_{r<\bar{r}} < 0, \quad \frac{df}{dr}\Big|_{r=\bar{r}} = 0, \quad \frac{df}{dr}\Big|_{r>\bar{r}} > 0, \quad \bar{r} = \sqrt{-\frac{b}{3a}}. \tag{B.6}$$

Therefore the function decreases till $r = \bar{r}$ after which it always increases. This also ensures a single, positive root.

This analysis applied to 5d Euclidean Schwarzschild AdS leads to a similar conclusion.

B.2 Spins on Euclidean Rindler background

Given that spins on a Euclidean black hole background undergo a second order phase transition as the metric parameter M is varied, it is natural to ask if this result is unique to Euclidean black hole backgrounds or if spins on any Euclidean background undergo a phase transition. For example if we use Minkowski spacetime,

derive its Euclidean version, consider a scalar field on this background and follow the steps presented in Section 3.4.1 to arrive at a spin model on this background, are we going to get a phase transition? The following heuristic argument supports an answer in the negative: consider the flat Euclidean background in d dimensions:

$$ds^2 = d\tau^2 + dx_1^2 + dx_2^2 + ... + dx_{d-1}^2; \tag{B.7}$$

this metric is homogeneous and parameter and singularity-free; due to the latter feature time compactification may be chosen arbitrarily; consequently varying the temperature will only change the upper limit of the Euclidean time coordinate. Consider now the action of a scalar field $\Phi(\tau, x_1)$ on this background and follow the steps from Section 3.4.1 to arrive at a 2d spin model on this background. Clearly changing the temperature only changes the number of rows in the model; since varying the temperature does not affect the couplings, a spin model on flat Euclidean background does not undergo a phase transition. This indicates that the existence of a phase transition depends on the type of background used.

Rindler spacetime describes how an observer with uniform acceleration a perceives Minkowski spacetime. For generality we will consider d spacetime dimensions and for simplicity we will assume that the observer is accelerating along one space direction which we will call x; the remaining $d-2$ space coordinates are named y_1, y_2, ... y_{d-2}. The Rindler metric we consider is

$$ds^2 = -(ax)^2 dt^2 + dx^2 + dy_1^2 + ... + dy_{d-2}^2, \tag{B.8}$$

where a is a constant, $t, y_1, ..., y_{d-2} \in \mathbb{R}$ and $x \in \mathbb{R}^+$. Rindler spacetime is flat and inhomogeneous; it also has a coordinate singularity at $x = 0$. Therefore there are some similarities between Rindler and Schwarzschild spacetimes; indeed under the

coordinate transformation $\mathcal{R} = a\,x^2/2$ the $t - \mathcal{R}$ part of Rindler spacetime is:

$$ds^2 = -\mathcal{F}dt^2 + \mathcal{F}^{-1}d\mathcal{R}^2, \quad \mathcal{F} = 2a\mathcal{R}. \tag{B.9}$$

In imaginary time $\tau = it$ the $\tau - x$ part of the metric (B.8)

$$ds^2 = (ax)^2\,d\tau^2 + dx^2 \tag{B.10}$$

represents flat space in polar coordinates where $a\tau$ is the angular coordinate. Periodically identifying $a\tau$ - whereby Euclidean time has periodicity $2\pi a^{-1}$ - removes the conical singularity at $x = 0$. Consequently the singularity-free Euclidean Rindler background is described by the metric (B.10) with coordinate ranges $\tau = [0, 2\pi a^{-1}]$ and $x \in \mathbb{R}^+$ and it has a natural temperature $T = \frac{a}{2\pi}$. Note that the natural temperature of this space is proportional to the metric parameter, unlike that of Euclidean Schwarzschild background which is inversely proportional to the black hole mass.

In this section spin models are constructed on a Euclidean Rindler background. It will be checked using Monte-Carlo simulations if spins on this background undergo a phase transition as the metric parameter is varied. The result, in addition to the findings for spin models on Euclidean black holes, may provide insight into the inquiry: what feature of the spin model makes a phase transition likely? For what follows, we choose $x \in [0, X]$ and $y_1, \ldots, y_{d-2} \in [0, Y]$ to ensure that the lattice and action are finite, as will be demonstrated shortly.

Consider a scalar field $\Phi \equiv \Phi(\tau, x)$; we choose this specification since the y coordinates do not contain background properties of interest. The Euclidean action of the

scalar field on Rindler background is

$$I^{(d)} = Y^{d-2}\left\{\frac{1}{2}\int\int d\tau dx\left[(ax)^{-1}\dot{\Phi}^2 + (ax)\,\Phi'^2 + (ax)\,\mu^2\Phi^2\right]\right\} \tag{B.11}$$

$$= Y^{d-2}\,I^{(2)}. \tag{B.12}$$

In the equations above $I^{(d)}$ is the action in d space dimensions, Y is the upper limit of the y_1, y_2 ... y_{d-2} integrals, and overdots and primes indicate partial derivatives with respect to τ and x respectively. In the case that the upper limit of the y integrals is set to 1, the d dimensional action is identical to the 2 dimensional action. Since physical properties of interest are in the $\tau - x$ plane we will set $Y = 1$.

The steps from section 3.4.1 are followed to arrive at the Euclidean action of spins on Rindler space:

$$\begin{aligned} I_E = \sum_{m,n=1}^{N_\beta,N_X}\Bigg\{ &- \Phi_{m,n}\left[\left(\frac{1}{ax_n}\right)\Phi_{m+1,n} + (ax_n)\,\Phi_{m,n+1}\right] \\ &+ {\Phi_{m,n}}^2\left[\frac{1}{ax_n} + \frac{a}{2}\,(x_n + x_{n-1}) + \frac{\mu^2\epsilon^2}{2}\,(ax_n)\right]\Bigg\} \end{aligned} \tag{B.13}$$

where

$$N_\beta = \frac{2\pi}{a\epsilon}, \qquad N_X = \frac{X}{\epsilon} \quad \text{and} \quad x_n = n\epsilon. \tag{B.14}$$

Notice that a appears differently in the Euclidean action from how the black hole mass appears in - for instance - the spin models on Euclidean Schwarzschild background (3.54).

For the simulations $X = 1$, $\epsilon = 10^{-2}$, $\mu = 0$ and periodic boundary conditions were used. Graphs of alignment vs. a are presented in Figure B.1 for the spin 1/2 and spin 1 models Euclidean Rindler backgrounds. These results are valid for $d \geq 2$ dimensions.

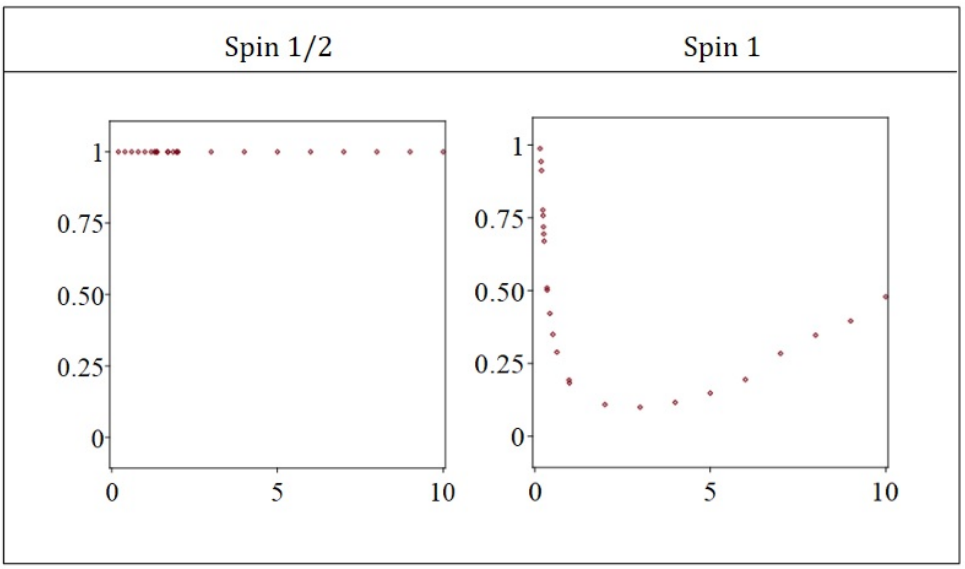

Figure B.1: Alignment as a function of metric parameter a for spin 1/2 and spin 1 models on a Euclidean Rindler background.

Two trends are obvious from Figure B.1. Firstly, changing the allowed excitations of the spins markedly influences their alignment as a is varied. The second trend is the transition from order to disorder to partial order as a is increased in the spin 1 model.

Both trends can be understood via a heuristic argument. To ensure applicability of this argument to both cases under consideration the allowed spin excitations (spin 1/2 or spin 1) will be not be committed to initially. Consider a starting lattice of aligned spins from which the group depicted in figure B.2 is selected.

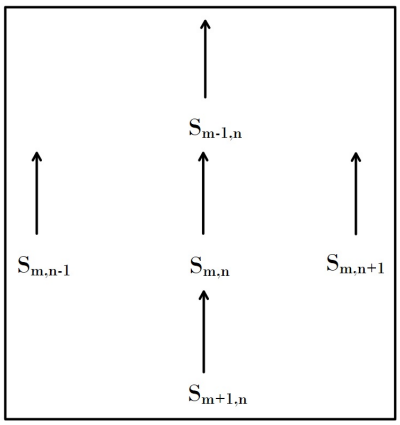

Figure B.2: A group of aligned spins.

It is reasonable to use the probability of changing the value of the central spin as a qualitative indicator of where one can expect order/disorder in the lattice. This probability requires the change in Euclidean action upon changing the value of the central spin; one can verify that

$$\Delta I_{1\to -1} = 4\left[\frac{1}{ax_n} + \frac{a}{2}\left(x_n + x_{n-1}\right)\right] \tag{B.15}$$

$$\Delta I_{1\to 0} = \left(\frac{1}{4}\right)\Delta I_{1\to -1} \tag{B.16}$$

$$\implies p_{1\to 0} > p_{1\to -1}. \tag{B.17}$$

Here the notation $b \to c$ indicates changing the value of the central spin from b to c. It is important to note that the self interactions cancel out in $\Delta I_{1\to -1}$ only.

In spin 1/2 models the central spin can only change value to -1 while in spin 1 models the central spin can also change its value to 0. This explains the the first feature. The second trend is due to how the metric parameter appears in (B.13): note that the vertical interactions are mediated by $1/a$, the horizontal ones by a and the point ones by a combination of a and $1/a$. This results in equally strong interactions in the extreme cases $a \to 0$ and $a \to \infty$ and weaker interactions in an intermediate region. Presented in figure B.3 is a graph of $p_{1\to 0}$ for the spin 1 model

for different a values.

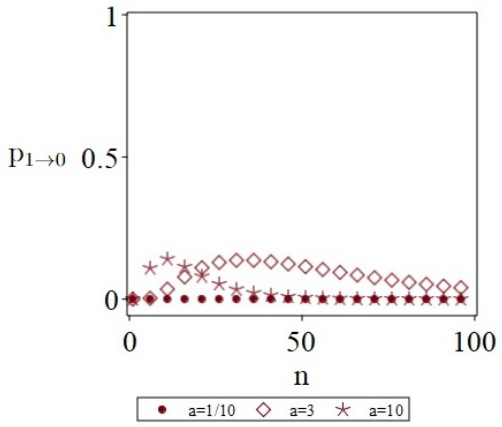

Figure B.3: For a spin 1 model on a Euclidean background, this graph shows $p_{1\to0}$ as a function of column number n for different a values.

For $a = 1/10$, $p_{1\to0} \approx 0$ which corresponds to order; at $a = 3$, $p_{1\to0} \approx 0.1$ for a majority of the lattice which indicates disorder; for $a = 10$, $p_{1\to0} \approx 0.1$ for a smaller portion of the lattice which results in lesser disorder than the $a = 3$ case. This confirms the observed trend in the alignment graph for the spin 1 model in figure B.1.

Studying spins on Euclidean Rindler backgrounds shows that phase transitions depend on the allowed excitations of spins and the background (specifically how the metric parameter appears in the Euclidean action of spins).

Appendix C

Publication rights

American Physical Society
Reuse and Permissions License

04-Jun-2023

This license agreement between the American Physical Society ("APS") and Mustafa Saeed ("You") consists of your license details and the terms and conditions provided by the American Physical Society and SciPris.

Licensed Content Information

License Number:	**RNP/23/JUN/067060**
License date:	04-Jun-2023
DOI:	10.1103/PhysRevD.102.124062
Title:	Cosmological perturbation theory with matter time
Author:	Viqar Husain and Mustafa Saeed
Publication:	Physical Review D
Publisher:	American Physical Society
Cost:	USD $ 0.00

Request Details

Does your reuse require significant modifications: No

Specify intended distribution locations:	Canada
Reuse Category:	Reuse in a thesis/dissertation
Requestor Type:	Author of requested content
Items for Reuse:	Whole Article
Format for Reuse:	Electronic

Information about New Publication:

University/Publisher:	University of New Brunswick
Title of dissertation/thesis:	Probing gravity-matter systems
Author(s):	Mustafa Saeed
Expected completion date:	Aug. 2023

License Requestor Information

Name:	Mustafa Saeed
Affiliation:	Individual
Email Id:	msaeed@unb.ca
Country:	Canada

American Physical Society
Reuse and Permissions License

TERMS AND CONDITIONS

The American Physical Society (APS) is pleased to grant the Requestor of this license a non-exclusive, non-transferable permission, limited to Electronic format, provided all criteria outlined below are followed.

1. You must also obtain permission from at least one of the lead authors for each separate work, if you haven't done so already. The author's name and affiliation can be found on the first page of the published Article.
2. For electronic format permissions, Requestor agrees to provide a hyperlink from the reprinted APS material using the source material's DOI on the web page where the work appears. The hyperlink should use the standard DOI resolution URL, http://dx.doi.org/{DOI}. The hyperlink may be embedded in the copyright credit line.
3. For print format permissions, Requestor agrees to print the required copyright credit line on the first page where the material appears: "Reprinted (abstract/excerpt/figure) with permission from [(FULL REFERENCE CITATION) as follows: Author's Names, APS Journal Title, Volume Number, Page Number and Year of Publication.] Copyright (YEAR) by the American Physical Society."
4. Permission granted in this license is for a one-time use and does not include permission for any future editions, updates, databases, formats or other matters. Permission must be sought for any additional use.
5. Use of the material does not and must not imply any endorsement by APS.
6. APS does not imply, purport or intend to grant permission to reuse materials to which it does not hold copyright. It is the requestor's sole responsibility to ensure the licensed material is original to APS and does not contain the copyright of another entity, and that the copyright notice of the figure, photograph, cover or table does not indicate it was reprinted by APS with permission from another source.
7. The permission granted herein is personal to the Requestor for the use specified and is not transferable or assignable without express written permission of APS. This license may not be amended except in writing by APS.
8. You may not alter, edit or modify the material in any manner.
9. You may translate the materials only when translation rights have been granted.
10. APS is not responsible for any errors or omissions due to translation.
11. You may not use the material for promotional, sales, advertising or marketing purposes.
12. The foregoing license shall not take effect unless and until APS or its agent, Aptara, receives payment in full in accordance with Aptara Billing and Payment Terms and Conditions, which are incorporated herein by reference.
13. Should the terms of this license be violated at any time, APS or Aptara may revoke the license with no refund to you and seek relief to the fullest extent of the laws of the USA. Official written notice will be made using the contact information provided with the permission request. Failure to receive such notice will not nullify revocation of the permission.
14. APS reserves all rights not specifically granted herein.
15. This document, including the Aptara Billing and Payment Terms and Conditions, shall be the entire agreement between the parties relating to the subject matter hereof.

Vita

Candidate's full name: Mustafa Saeed

Universities attended:

- 2019-present, PhD. Physics, University of New Brunswick, Fredericton, NB, Canada
- 2016-2019, MSc. Physics, University of New Brunswick, Fredericton, NB, Canada
- 2011-2015, BSc. Physics, Lahore University of Management Sciences, Lahore, Pakistan

Publications:
Viqar Husain and Mustafa Saeed. Cosmological perturbation theory with matter time. Phys. Rev. D, 102:124062, Dec 2020

Conference Presentations:

- Ising-like models on Euclidean black holes. Poster presentation at 2023 CAP Congress.
- Spin model on black hole space. Oral presentation at 2022 Canadian-Cuban-American-Mexican Graduate Student Physics Conference
- Cosmological perturbations with a matter clock. Oral presentation at 2021 CAP Congress
- Cosmological perturbation theory with matter time. Oral presentation at 2021 Canadian Student and Postdoc Conference on Gravity
- Cosmological perturbation theory in a new framework. Oral presentation at Atlantic General Relativity 2019